5-2024

Essays on Environmental and Natural Resource Economics

Annaliese R. Winton
awinton@g.clemson.edu

Essays on Environmental and Natural Resource Economics

A Dissertation
Presented to
the Graduate School of
Clemson University

In Partial Fulfillment
of the Requirements for the Degree
Doctor of Philosophy
Economics

---

by
Annaliese R. Winton
May 2024

Accepted by:
Dr. Scott L. Baier, Committee Co-Chair
Dr. Molly Espey, Committee Co-Chair
Dr. Devon Gorry
Dr. R. Aaron Hrozencik

Abstract

This dissertation explores how markets and producers respond to environmental risks that are becoming more severe due to climate change. It is comprised of two essays that empirically quantify the economic impacts of two water-related risks: storm surge flooding and groundwater depletion, which, respectively, can substantially affect coastal communities and agricultural production.

In the first chapter, I estimate the price differentials associated with single-family homes in hurricane evacuation zones in Miami-Dade County, Florida, using two near-miss hurricanes as a source of exogenous information. First, I develop a comprehensive data set of housing, neighborhood, and risk characteristics using geographic information system (GIS) software to merge spatial and administrative data. Unlike other counties, hurricane evacuation zones in Miami-Dade County extend significantly inland due to the county's widespread low elevation. Leveraging this unusual amount of non-coastal variation among hurricane evacuation zones, I estimate a hedonic property model within a difference-in-differences framework to investigate what effect, if any, two near-miss hurricanes had on property prices inside hurricane evacuation zones. Results show that home prices in hurricane evacuation zones declined by 2.9% to 13% after the first near-miss and further declined by 3.4% to 8.9% following the second near-miss hurricane of a higher intensity. As expected, these price reductions are largest for homes in the highest-risk evacuation zone.

This study is one of the first to show that markets internalize the risks associated with locating in a hurricane evacuation zone and provides new evidence that near-miss events can provide risk information that is internalized into market prices. Understanding

if and to what extent risk is priced into property markets is valuable, as housing markets are uniquely poised to facilitate adaptation in the sense that they both incorporate and convey new risk information. The capitalization of risks and new risk information can help to relocate future development away from risky areas and into safer areas. For a homeowner, these price changes can incentivize them to purchase disaster insurance or take other measures to protect their property from future damages.

The second chapter is the result of a joint project with co-authors R. Aaron Hrozencik and Taro Mieno. In this paper, we estimate the impacts of groundwater depletion as captured through declining well capacity, also referred to as well yield. Our study area is one of the most agriculturally productive regions of Colorado, the Republican River Basin, which largely overlies the rapidly depleting High Plains aquifer. Using a unique data set, we can incorporate both cross-sectional and temporal variation in well yields in our empirical models, enabling us to provide the first empirically-derived, causal estimates of the impact of well yield on irrigation behavior. Using a two-way fixed effects model, we examine the impact of well yield on total water use, which we then decompose into extensive (irrigated acreage) and intensive (water use per acre) margin adjustments. Our results provide evidence that declining well yields reduce total water use and show that producers are responding to declining groundwater stocks along both the intensive and extensive margins.

The common pool characteristics of aquifers lead to inefficiently high rates of groundwater extraction. The High Plains aquifer is one of many around the world experiencing depletion as pumping rates exceed natural recharge. Estimating the economic impacts of aquifer depletion is crucial as policymakers and groundwater management agencies must balance the benefits and costs of groundwater consumption when considering strategies to address depletion. Additionally, these results provide insight into how the costs and benefits of various groundwater conservation strategies may vary with well yield.

Dedication

To my parents.

Acknowledgments

I would first like to deeply thank each member of my advisory committee: Dr. Scott Baier, Dr. Molly Espey, Dr. Devon Gorry, and Dr. R. Aaron Hrozencik. Thank you each for your mentorship, guidance, and feedback, which has greatly contributed to my growth and development as an economist. I would also like to thank Dr. Jorge Luis García, Dr. Jonathan Leganza, Dr. Curtis Simon, Dr. Scott Templeton, and Dr. Christy Zhou as well as members of the Clemson Labor Economics Workshop and Clemson Public Economics Workshop for valuable comments and guidance. I am appreciative of the support from fellow graduate students in the John E. Walker Department of Economics during this journey. Thank you to the United States Department of Agriculture's Economic Research Service and The Farm Foundation for enriching learning experiences that had a profound impact on my professional development. I would also like to express my gratitude for the support and encouragement from my family and friends.

Table of Contents

List of Tables

List of Figures

Chapter 1

Risky Business: How Coastal Housing Markets Respond to Near-Miss Disasters

1.1 Introduction

Globally, economic losses from natural hazards have risen substantially over the past four decades, from $175 billion in the 1970s to over $1.3 trillion in the 2010s [Douris and Kim, 2021].[1] Tropical cyclones accounted for almost 40% of these damages. This increasing trend in global losses is largely attributed to increased exposure of people and assets to these disasters [Field et al., 2012]. In addition, climate change is projected to increase the severity, duration, frequency, and spatial extent of weather events such as droughts, wildfires, floods, and tropical cyclones [Lee et al., 2023]. Figure 1.1 highlights this trend in the context of the U.S., where the frequency and costs of billion-dollar weather events have risen substantially from 1980 to 2022.

Economic theory posits that efficient property markets will incorporate new risk information into their prices. Understanding the extent to which asset markets price changing

[1] Losses are adjusted to 2018 U.S. dollars.

climate risks has important implications for community planning, the stability of financial markets, and distributional wealth. If new information reflects increasing climate risks, then all else equal, we would expect homes in hazardous areas to experience a price reduction as this new information becomes known to market participants. This sends a signal to future buyers regarding the risk associated with the property and the expected costs of locating there. This price reduction would represent a real economic cost of climate change and negatively impact household wealth in the affected areas. Such price declines may also incentivize homeowners and communities to adopt mitigation measures such as elevating homes or installing storm shutters and can also help to refocus new development out of risky areas and into safer areas. Fiscal ramifications can arise as changes in property values affect local tax revenues. Therefore, understanding how property markets capitalize these changing climate risks is crucial for community planning and resilience.

This paper examines the extent to which real estate markets are pricing these increasing risks by utilizing the occurrence of natural disasters as exogenous information shocks. However, natural disasters can impact property values through two main channels: new information and physical damages. Disentangling price changes caused by new information from price changes caused by damages is challenging due to a lack of accurate and granular damage data. To overcome this challenge, I focus on near-miss disasters, defined as events that have a non-trivial probability of causing significant harm or damage but, by chance, do not [Dillon et al., 2011].

I explore this within the context of the deadliest and most destructive weather event in the U.S.: tropical cyclones, known as 'hurricanes' over the Atlantic Ocean. They average $22.2 billion in damages and about 50 deaths nationally [Smith, 2023, Rappaport, 2014].[2] Tropical cyclones are expected to increase in intensity and produce more precipitation and a higher magnitude of storm surge [Lee et al., 2023]. Globally, we are projected to experience a higher proportion of category 4 and 5 hurricanes, classified as having sustained wind speeds of 130 miles per hour or more [Masson-Delmotte et al., 2021]. The damage associated with

[2]This calculation is in 2022 U.S. dollars and based on billion-dollar events.

hurricanes of these categories is catastrophic and can leave affected areas uninhabitable for weeks to months [Taylor et al., 2010].

In this paper, I estimate how sale prices of single-family homes in hurricane evacuation zones (subsequently referred to as 'HEZs' or 'evacuation zones') respond to two near-miss hurricanes (subsequently referred to as 'near-misses') in Miami-Dade County (MDC), Florida. This region provides unique inland variation among these zones due to the county's widespread low elevation. Between 2005 and 2016, the county experienced an uncharacteristic period of calm from hurricanes as well as a remapping of their evacuation zones, which substantially increased the number of residents residing in an HEZ. In particular, there were only five tropical storms over these 11 years to come within 50 miles of MDC, and only two were hurricanes: Hurricane Katrina in 2005 and Hurricane Ernesto in 2006 [National Oceanic and Atmospheric Administration, n.d.a]. This set the stage for these near-misses to potentially provide new information regarding changing hurricane risks. I also investigate if these housing price responses are driven by the more general and widely studied flood risk, depicted by the Federal Emergency Management Agency's special flood hazard areas (SFHAs). Finally, I present suggestive evidence that these responses were due to changes in risk perceptions among home buyers and sellers rather than changes in flood insurance markets.

Hurricane evacuation zones are used along the East and Gulf coasts of the U.S. to inform evacuation decisions and depict storm surge risk. Storm surge is the deadliest component of a hurricane [Rappaport, 2014] and is defined as a rise in the water level that occurs when strong storms push water ashore [National Oceanic and Atmospheric Administration, n.d.c].[3] Floodwaters produced by storm surge can reach heights of up to 40 feet, equivalent to a three-story building, within a matter of minutes [Nott et al., 2014]. As of 2023, it is estimated that 7.8 million single-family homes and 260,000 multi-family homes in the U.S. are susceptible to flooding from hurricane-induced storm surge [CoreLogic,

[3]Storm surge was responsible for 49% of direct deaths from Atlantic hurricanes between 1963 and 2012, followed by rain accounting for 27%.

2023]. This makes up approximately 5.5% of the U.S. housing stock.[4] Therefore, knowing if the risks associated with these zones are priced into markets, and how that capitalization changes with new information, is important in assessing local economic implications and the stability of the financial sector [Martinez-Diaz and Keenan, 2020].

To estimate if near-miss hurricanes differentially affect property values in HEZs, I merge transaction data on single-family home sales from January 2014 through August 2017 with geospatial data from various sources. Using a difference-in-differences (DiD) design, I compare property prices of homes sold inside and outside HEZs before and after two near-miss hurricanes. The two near-misses are Tropical Storm (TS) Erika and Hurricane Matthew. Tropical Storm Erika occurred at the end of August 2015 and was forecasted to hit Florida, and potentially MDC, as a category one hurricane. This resulted in the Florida governor declaring a state of emergency. At the time, South Florida had not been hit by a hurricane in ten years, though historically, Southeastern Florida had been hit by a hurricane every five years on average.[5] The TS dissipated near Hispaniola and never caused damage to Florida. Hurricane Matthew occurred just over a year later, at the beginning of October 2016 [Pasch and Penny, 2016]. It was the strongest hurricane of the Atlantic season and was the 10^{th} costliest hurricane on record at the time [Stewart, 2017]. Although some forecasts placed Miami-Dade County inside the cone of projection, the category four hurricane ended up paralleling the eastern Florida coast and the county was largely spared from its destruction.

The key challenge with estimating the capitalization of coastal risks in property markets is adequately disentangling the coastal risk of interest from other correlated coastal risks and amenities. In this analysis, the coastal risk is the potential for storm surge flooding and being required to evacuate, which is delineated through HEZs. Other coastal amenities and risks, such as beach proximity, waterfront views, and erosion rates, are likely correlated with location in an HEZ because the potential for storm surge flooding, and thus the need

[4] Author's calculation using most recent data on quarterly housing units in the United States (Q2, 2023) obtained from the Federal Reserve Economic Data (Housing Inventory Estimate: Total Housing Units in the United States).

[5] Detailed information on return periods can be found at https://www.nhc.noaa.gov/climo/.

to evacuate, often diminishes as one moves inland. If these other correlated attributes are not accounted for, estimates of the price discount associated with location in an HEZ can be biased. For this reason, an ideal empirical setting could be an inland area where some homes are in an evacuation zone and some homes are not, abstracting from the coastal attributes that influence prices of homes that are directly on the water. However, HEZs in almost every coastal county are geographically restricted to areas along the coastline. Figure 1.2 shows that this is the case for much of Florida. Miami-Dade County is an exception, with its HEZs extending approximately 50 miles inland.[6] This offers a unique and substantial amount of non-coastal variation among evacuation zones.

Results from the DiD model show that the first near-miss hurricane reduced housing prices in HEZs by around 13% in the highest-risk evacuation zone and 2.9% in the lowest-risk evacuation zone. Evaluated at the mean sale price of the sample, this represents a $57,122 and a $12,742.60 price reduction, respectively. Price declines associated with Hurricane Matthew range from around 8.9% to 3.4%, depending on the evacuation zone. Holding with intuition, the magnitude of these price effects follows a gradient consistent with the level of risk, where the largest effects are in the most susceptible zones and the smallest effects are typically in the least susceptible zone. This illustrates the market awareness of the corresponding risk gradient. These results hold against an array of spatial fixed effects and various transformations of independent variables.

These price declines coincide with a notable increase in transactions of properties outside HEZs, suggesting that this effect may be driven by increased demand for safer properties. I investigate if this effect occurs separately from any price effect due to flood risk, as delineated through SFHAs, by restricting the sample of properties to those outside SFHAs. The results are consistent with the main results, highlighting that the risk depicted by HEZs is capitalized separately from the flood risk depicted by SFHAs.

Finally, I explore some of the mechanisms that could be underlying these results, namely changes in insurance rates or damages from Hurricane Matthew. I investigate the

[6] Author's calculation of county width using the Measure Distance tool in ArcGIS Pro 2.9.

flood insurance market in MDC to assess whether changes in national or local insurance rates may be driving these effects. The results are robust to insurance rate changes by Citizens Property Insurance Corporation, the state's non-profit insurer of last resort. While damages from Hurricane Matthew could potentially confound the price effects of the second near-miss, damages to the county were relatively minimal. Moreover, there was no physical damage from the first near-miss, so a price effect from TS Erika cannot be attributed to physical damages. Data on Google search trends during the study period show that searches for "hurricane preparation" and "hurricane evacuation zone" in the Miami-Ft. Lauderdale area were highest around the occurrence of these two near-misses. This suggests there may have been an increase in risk salience among residents following these two near-misses. Additionally, the results from the empirical analysis are consistent with changes in hurricane risk perceptions among market participants.

This study presents new evidence regarding the types of risk information provided by near-miss weather events. Other studies have documented a decrease in property values in hazard areas following disasters that were either classified as a near-miss or were proximate to damaged areas. These hazard areas include special flood hazard areas (SFHAs), also referred to as 'federal flood zones' or '100-year floodplains' [Hennighausen and Suter, 2020, Hallstrom and Smith, 2005, Bin and Landry, 2013, Kousky, 2010, Atreya and Ferreira, 2015], earthquake zones [Naoi et al., 2009, Gibbons et al., 2021], and areas exposed to wildfire risks [Loomis, 2004, Mueller et al., 2009]. Despite the fact that hurricanes are the deadliest and costliest weather event in the U.S.[7], it is not well known whether the risks associated with hurricanes are internalized in market prices. Existing work is limited and largely focuses on the wind risk component of a hurricane [Dumm et al., 2011, Zivin et al., 2023, Kim and Hammitt, 2022], whereas HEZs represent a flood-risk component of hurricanes (i.e., storm surge flooding). Only one study to date has examined the effect of a (near-miss) disaster on property prices in HEZs [Ortega and Taşpınar, 2018]. In fact, HEZs are essentially absent from the risk capitalization literature as a whole.

[7]Hurricanes have the highest average cost per event, based on billion-dollar events.

By exploring the effect of near-misses on property price differentials associated with HEZs, I provide one of the first estimates related to the market pricing of the risks associated with residing in an HEZ. This paper also provides the first estimate of the capitalization of HEZs in property prices, separately from the capitalization of flood risk as depicted by SFHAs. Existing literature examining the price effects of near-miss hurricanes focus on property price differentials in SFHAs. While Ortega and Taşpınar [2018] focus on HEZs, they use HEZs as a proxy for flood risk and do not separate or control for properties in SFHAs. However, SFHAs and HEZs differ in many ways that warrant separate analyses. The Federal Emergency Management Agency estimates that 40% of properties exposed to storm surge risk, the risk delineated by HEZs, are not in an SFHA [Hall, 2019]. This is reflected in Figure 1.3, which shows SFHAs and HEZs in Miami-Dade County. Specifically, HEZs delineate a particular type of flood risk, flooding from storm surge, which is not fully captured by SFHAs. For example, more than half of the properties that were flooded during Hurricane Sandy were outside an SFHA [Colvin, 2012]. Those residing in HEZs are also at risk of having to evacuate in the event of an approaching storm. Furthermore, whereas SFHAs come with flood insurance mandates, HEZs do not, nor do they come with disclosure requirements.

This work provides evidence that property markets are internalizing new risk information provided by both near, and distant, weather events. In particular, markets internalize unstudied, yet relevant, dimensions of risk. Through the signals sent via price changes in hazardous areas, markets can reduce new development in risky areas and incentivize individuals and communities to take protective measures. Well-functioning and efficient markets play a vital role in facilitating adaptation to increasing risks and mitigating future damages.

1.2 Related Literature

1.2.1 Environmental Risk and Housing Markets

In an efficient market where consumers have full information, property prices should reflect differences in observed and salient risks that are not fully transferable, such as those related to natural disasters. There is abundant literature examining the price impacts of various environmental risks in housing markets, including the risks associated with floods, erosion, sea level rise, nuclear energy, earthquakes, and wildfires. Flood risk, as delineated by SFHAs, has garnered the most attention. Special flood hazard areas are federally designated areas that will be inundated by the flood with at least a 1% annual chance of occurring. Properties in these areas have about a one in four chance of being flooded over the course of a 30-year mortgage. In many states, sellers of properties within an SFHA face disclosure requirements. As of 2022, 30 states required explicit disclosures by sellers regarding whether the property was located within an SFHA. The state of Florida does not have any disclosure requirements.[8] Miami-Dade County requires disclosure of an SFHA for improved real estate in unincorporated Metropolitan MDC [Miami-Dade County, 2015]. Nationally, flood insurance is required for homeowners residing within an SFHA who have a federally-backed mortgage. Properties in SFHAs typically sell for a discount relative to homes outside SFHAs [e.g., Bin et al., 2008b, Harrison et al., 2001]. However, there is considerable variability among the results within the literature [e.g., Beltrán et al., 2018], especially in coastal areas, likely due to the confounding of various unobserved coastal amenities [e.g., Bin et al., 2008a].

Similar studies related to hurricane risk are sparser and focus on the wind-risk component of a hurricane. Dumm et al. [2011] find that homes in Miami-Dade County built after the implementation of a stricter building code that increased hurricane resilience sold for around 10% percent more in the highest risk wind zone, which is subject to winds of 150 miles per hour or more.

[8] Information on recent coverage of disclosure requirements is provided by the Federal Emergency Management Agency, and can be accessed through https://www.fema.gov/.

To the best of my knowledge, Ortega and Taşpınar [2018] are the only researchers to provide capitalization estimates for HEZs within the economics literature. The capitalization of storm surge risk, which is the foundation for HEZs, was studied in Western Australia and delineated by the authors as areas at risk of four meters of storm surge [Rebecca et al., 2015]. However, no evidence of the anticipated price discounts was found, likely due to confounding coastal amenities, as noted by the authors. Outside of the economics literature, Morgan et al. [2023] use a difference-in-differences model to estimate the effect of an HEZ remapping on property values in Pinellas County, Florida. However, it is unclear if the identifying parallel trends assumption holds.

1.2.2 Hurricanes and Housing Prices

The hedonic literature related to hurricanes generally estimates the effect of hurricanes on housing prices or the the effect of hurricanes on property price differential for SFHAs. Hurricanes typically have a negative price effect on houses in SFHAs that ranges from around a 5% to 20% discount [e.g., Bin and Landry, 2013, Bakkensen et al., 2019]. However, this discount may be due solely to property damages.

Kim and Hammitt [2022] find that hurricanes result in price reductions which are larger for properties closer to the hurricane's path. The extent of the price reduction increases with the strength of the hurricane. Additionally, they find that homes more recently exposed to a hurricane sold for a discount compared to homes whose last hurricane experience was further in the past, suggesting that risks may be forgotten as more time elapses between hurricane occurrences.

Sometimes house prices increase following a hurricane [e.g., Zivin et al., 2023]. Rather than focusing on one major hurricane, Zivin et al. [2023] analyze the impact of all hurricanes that made landfall in Florida from 2000 to 2016 using a staggered difference-in-differences approach. They find that homes in Florida exposed to hurricane-strength wind speed experienced price increases that lasted for three years but peaked after two years at 10%. They also discover that transactions decreased for three years after a hurricane as

prices rose, indicative of a negative supply shock.

1.2.3 Market Responses to Near-Miss Hurricanes

This paper follows an extensive line of literature that exploits random variation in the timing of weather events, most commonly hurricanes or floods, to estimate changes in property price differentials between homes inside and outside hazard zones. It is often unclear the extent to which property price changes are due to physical damages or changes in risk salience or perceptions. To disentangle these effects, a growing avenue of research examines the effect of near-miss events on property prices. Specific studies utilizing this framework define near-misses differently depending on the context and study area, but it generally represents an area that came quite close to being detrimentally impacted by a hurricane [e.g., Hallstrom and Smith, 2005].

For example, properties in New York City that were within a mile of Hurricane Sandy's flooding, but were not themselves flooded, sold for a 6% to 7% discount [Cohen et al., 2021]. Hallstrom and Smith [2005] classify Hurricane Andrew as a near-miss hurricane for Lee County, Florida. Hurricane Andrew occurred in 1992 and made landfall in MDC, causing significant damage. Lee County was adjacent to MDC and was largely unharmed. Using a repeat sales model, they find that properties in SFHAs in Lee County sold for 19% less after near-miss Hurricane Andrew relative to homes outside SFHAs. Kousky [2010] finds that prices of riverfront properties fell by 6% to 10% following a major flood in St. Louis County, Missouri, despite only a small fraction of homes in the county incurring damage. Bin and Landry [2013] use a difference-in-differences model and find that properties in SFHAs sell for about 6% less following Hurricane Fran, and 9% less following Hurricane Floyd, in Pitt County, North Carolina relative to properties outside SFHAs. Both hurricanes resulted in minimal physical damages to the housing stock, suggesting the price changes were primarily due to new information provided to residents by the storms. While the information effects of near-miss hurricanes have previously been estimated, analyses are generally limited to price effects in SFHAs, which do not fully encompass the flood risk

component of hurricanes.

The closest work to this paper is that of Ortega and Taşpınar [2018]. They estimate the effect of Hurricane Sandy on property price differentials for HEZs. Using New York City property data in a difference-in-differences analysis, they find an 8% price decline for non-damaged properties in two of the three riskiest evacuation zones. Unlike in this paper, they use the HEZs as the only flood risk proxy and do not separately control for SFHAs, likely because of a substantial overlap between HEZs and SFHAs in the area. Exploring heterogeneity by SFHAs, this paper provides the first estimates on property price differentials for HEZs separately from federal flood zones.

Further, storm surge risk in MDC vastly differs from storm surge risk in New York City. In MDC, this risk extends significantly inland, yet even lower-risk properties can be relatively close to the coast. Additionally, a large proportion of the population, approximately two-thirds of the county, is located within an HEZ in MDC. A final element that differentiates this work from prior studies is that the first near-miss storm, Tropical Storm Erika, never developed into a hurricane as it approached Florida. This paper, therefore, evaluates two different information signals. The first is from a distant tropical storm that does not cause damage to the county, and the second, arguably stronger signal is from Hurricane Matthew, which causes significant damage to adjacent areas.

1.3 Background

1.3.1 Hurricane Evacuation Zones

In the U.S., HEZs are used along the East and Gulf coasts to aid evacuation communications and decisions and to depict areas at risk of storm surge flooding.[9] Many factors contribute to the magnitude of storm surges and these can be categorized into regional, local, and storm characteristics. Storm characteristics such as the size, strength, speed, and angle of approach all affect storm surge. The larger and stronger the hurricane, and the

[9]See Appendix A for a discussion on the creation of hurricane evacuation zones.

more perpendicular the approach, the higher the storm surge, all else equal. The time of day the storm approaches is another contributing factor. A storm approaching at high tide will cause a higher surge. Local features such as bays and estuaries and other features that impact where water flows will also affect surge heights. For example, barrier islands reduce storm surges on the mainland. More regional components that come into play include the concavity of the coastline and the width and slope of the continental shelf. Nonetheless, every coastal state along the East and Gulf coasts faces some degree of risk related to flooding from storm surges.

Hurricane evacuation maps were updated across Florida after an especially damaging series of hurricanes in 2004 and 2005. The state obtained funding from the Federal Emergency Management Agency to conduct regional evacuation studies in coordination with counties and produce updated and more accurate evacuation zones. In March 2013, the new maps for Miami-Dade County were implemented. This remapping nearly tripled the population residing within an evacuation zone. However, media coverage of the update appears to be limited. To provide time for the market to adjust, this analysis uses sales beginning in 2014.

Residents can find out which zone their property is located in through several ways. Maps of these zones appear in the Hurricane Readiness Guide, which is mailed to residents annually. Select bus stops within evacuation zones feature signage that reads 'EMERGENCY EVACUATION BUS PICKUP SITE'. Residents can also determine their zone by typing their address into a map feature accessible through the county's website.[10] However, there are no mandatory disclosures regarding HEZs when purchasing a home.

1.3.2 Overview of Near-Misses

In this study, I focus on two near-miss storms that occurred in 2015 and 2016 and are documented in Table 1.1. An unusual decade of calm prior to the near-misses, as well as a remapping of evacuation zones in 2013, set the stage for these near-misses to provide

[10]The webpage address is
https://mdc.maps.arcgis.com/apps/webappviewer/index.html?id=4919c85a439f40c68d7b3c81c3f44b58.

additional information to individuals regarding hurricane risk. When TS Erika placed MDC in a cone of projection for a category one hurricane in 2015, the county had not been directly impacted by a hurricane since Wilma in 2005.[11] Then in 2016, MDC prepared for the worst as category four Hurricane Matthew approached. Residents were largely spared as it paralleled the Florida coast, traveling northwards and eventually making landfall in South Carolina. While the county was in the cone of projection for both near-misses, the first storm (Erika) never reached hurricane status and dissipated long before approaching Florida. To the best of my knowledge, no other tropical storms were forecasted to hit MDC during the study period.[12]

1.3.3 Near Miss I: Tropical Storm Erika

Tropical Storm Erika developed west of the Lesser Antilles in late August 2015. It dropped 12 inches of rain on Dominica, caused 30 direct deaths, and left hundreds homeless [Pasch and Penny, 2016]. The tropical storm was forecasted to make landfall in MDC as a category one hurricane in August 2015, a forecast that lasted about 3.5 days until the storm dissipated [Miami-Dade County, 2017]. Figure 1.4 displays the forecasts for Erika from the top dynamical models. Guidance models with high bias resulted in "several official forecasts for Erika that showed the system as a hurricane near or over the Florida peninsula, prompting concern for the residents of that state," according to National Hurricane Center's report on Tropical Storm Erika [Pasch and Penny, 2016]. The Hurricane Weather Research Forecast model, which has been referred to as the "flagship" model for predicting intensity [National Oceanic and Atmospheric Administration, n.d.b], predicted Erika would near Ft. Lauderdale, Florida (about 20 miles north of Miami, FL) as a hurricane on August 31 [Pasch and Penny, 2016]. The governor of Florida declared a state of emergency, noting that "it's going to be coming clear across the state," and Miami-Dade County mayor Carlos Gimenez told residents to have "3 days of food and 3 days of water," [Chuck, 2015]. Dates of the

[11] In 2012, Hurricane Sandy remained substantially off the coast, but caused coastal erosion in MDC when it paralleled the coast as a category one hurricane.

[12] Author's determination based on the review of NOAA's tropical cyclone reports for the 2014 through 2017 Atlantic hurricane seasons. These reports can be found at https://www.nhc.noaa.gov/data/.

duration of the tropical storm are shown in Table 1.1.

1.3.4 Near Miss II: Hurricane Matthew

At the end of September 2016, MDC had another close call, this time with Hurricane Matthew, which made landfall four times and was the strongest storm of the 2016 Atlantic hurricane season [Armstrong, 2015]. It was the first Atlantic hurricane since 2007 to reach category five status. Miami-Dade County spent almost two days in the 5-day cone of projection for category five Hurricane Matthew. They were removed from the cone of projection for one day before coming back into a 3-day forecasted cone of projection for Hurricane Matthew as a major hurricane (category three or higher). Figure 1.5 shows numerous forecasts of the path of the storm.

On October 6, 2016, Hurricane Matthew traveled north-northwestward from the Bahamas after killing over 500 people and damaging hundreds of thousands of homes in Haiti [Stewart, 2017]. Residents made preparations and voluntary evacuations of low-lying areas were encouraged. The hurricane moved towards eastern Florida as a category four hurricane, as shown in Figure 1.6. Hurricane Matthew was the tenth most destructive U.S. hurricane at the time, resulting in 52 deaths, 3 million residential evacuations, and an estimated $10 billion of damages [Stewart, 2017]. From Florida to the Carolinas, there was widespread minor wind damage but significant structural damage due to a storm surge. In eastern Florida counties, hundreds to thousands of homes were damaged, beach erosion resulted in millions of dollars of damages, and saltwater intrusion affected buildings and facilities. The storm surge caused water levels to reach four feet above ground in St. Augustine in northeastern Florida. Hurricane watches were issued for parts of Broward County, which is just north of Miami-Dade County. However, Miami-Dade County was essentially spared. Matthew ended up paralleling the coast and the county was affected by its outer bands. The storm system did not make landfall until it reached South Carolina, and most of the damage to MDC was in the form of power outages and downed trees. Prior to Hurricane Matthew, no hurricanes had come within 150 nautical miles of the county in

over ten years.[13]

1.3.5 Suggestive Evidence of Information Shock

Both of these close calls may have provided information regarding hurricane risk. Figure 1.7 provides suggestive evidence of increased risk salience around the times of TS Erika and Hurricane Matthew, displaying the highest Google search intensities for "hurricane preparation" during these two events for the period between January 1, 2014 and August 30, 2017. Search intensity is measured relative to the highest intensity, which was October 2 through 8, 2016. The relative search intensity was the second highest between August 23 and 29, 2015, which was when Erika occurred and provides further support for viewing these two near-misses as information shocks.

Figure 1.7 also shows the relative search intensities for the term "hurricane evacuation zone", which was most searched during Hurricane Matthew. The next highest period of search intensity occurred September 13 through 19, 2015, which was two weeks after Erika. Searches that were listed as related searches, that is, searches that occurred along with 'hurricane evacuation zone' included 'storm surge' which had over a 5000% increase in search volume compared to the prior period. Google Trends notes that substantial growth like that is "probably because these topics are new and had few (if any) prior searches."

Additionally, new storm surge warning systems and graphics were implemented beginning in 2016 with Hurricane Hermine (August 28 - September 3) [Berg, 2017]. During this hurricane, the National Weather Service first used its Prototype Storm Surge Watch/Warning Graphic to depict areas with a possibility of life-threatening inundation (storm surge watch) and a danger of life-threatening inundation (storm surge warning). These same storm surge watch and warning graphics were used during Hurricane Matthew. Storm surge watches were issued for the upper half of Florida's east coast [Stewart, 2017]. Storm surge warnings indicating life-threatening conditions were issued for North Palm Beach (about 80 miles north of Miami) and areas northwards. Figure 1.8 shows these

[13] Author's determination based on information NOAA's Historical Hurricane Tracks.

watch and warning areas for Hurricane Matthew, with Miami-Dade County appearing just south of areas where these were issued.

1.4 Conceptual Framework

If housing markets are efficient and the near-miss events provide no new information, then in the absence of other confounding events, the effect of the near-miss on property values in HEZs relative to non-HEZs should be zero. This analysis relies on the hedonic property method, which arises from the theory that the price of land reflects the utility derived from the land and is equal to the net present value of the expected stream of rental income. The idea that we can estimate implicit prices of attributes using observed sales prices is widely known to have been formalized by Rosen in his 1974 paper [Rosen, 1974]. The model presents a competitive equilibrium in a market with differentiated products consisting of buyers and sellers that are maximizing agents. House prices depend on the characteristics of the home z_1,z_2,...,z_n and are reflected by the price schedule $P(z) = P(z_1, z_2, ..., z_n)$. Assuming the stock of homes is fixed in the short-run[14], prices are determined by demand, and the equilibrium price schedule arises from consumers, their preferences, and the variety of homes on the market [Palmquist, 2005]. Observed prices are equilibrium prices that reflect the tangency between a buyer's bid curve and a seller's offer curve.

Brookshire et al. [1985] show that in the context of low-probability, high-loss events, individual behavior is consistent with maximizing expected utility. Hallstrom and Smith [2005] and Kousky [2010] formulate expected utility models applied to hurricanes and floods, where there are two states of the world: one in which the event occurs and the other in which it does not. New information can impact either the subjective probability of occurrence, the expected amount of loss, or insurance rates, thus impacting price differentials for more exposed properties. The model employed here follows Kousky [2010] and incorporates the insurance component as done in Carbone et al. [2006].

[14]Based on one-year estimates from the American Community Survey, the supply of one-unit detached homes varied by less than one percent per year in MDC during the study period.

The consumer chooses a house of various attributes z_1,z_2,...,$z_n \in \mathbf{Z}$ and all other goods X to maximize utility subject to the budget constraint

$$Y = X + P(\rho(g), \mathbf{Z}, r) \tag{1.1}$$

where the price of X is normalized to one and a concave utility function is assumed. The price of a house P depends on the probability of a damage-producing hurricane occurring, ρ, which varies with the property's geographical location, g. The price also depends on a vector of other attributes, $\mathbf{Z}$, and the cost of flood insurance per dollar of coverage, r. There are two states of the world: the state in which a damage-producing hurricane occurs, denoted by H, and the state in which a damage-producing hurricane does not occur, denoted by NH.[15] Consumption of all other goods is given by

$$\begin{aligned} X_{NH} &= Y - P(\rho(g), \mathbf{Z}, r) \\ X_H &= Y - P(\rho(g), \mathbf{Z}, r) - L(g, \mathbf{Z}, r) \end{aligned} \tag{1.2}$$

where X depends on the state of the world. Consumption of the composite good X is equal to income less housing less monetary losses, L, when a hurricane occurs and is equal to income less housing when no hurricane occurs. Losses depend on the location of the house, g, the characteristics of the house $\mathbf{Z}$, and the cost of insurance, r. A hurricane occurs with probability ρ and does not occur with probability $(1 - \rho)$. Consumers choose a house with attributes Z and location g to maximize their expected utility over the two states of the world. The expected utility function is given by

$$EU = \rho(g)U_H(X_H, \mathbf{Z}, g) + (1 - \rho(g))U_{NH}(X_{NH}, \mathbf{Z}, g). \tag{1.3}$$

The first order conditions from maximizing expected utility subject to the budget

[15] This terminology is taken from Bin et al. [2008b]. It is possible that utility would not be affected in the event of a hurricane that does not produce damages.

constraint yields

$$\frac{\partial P}{\partial g} = \underbrace{\frac{\frac{\partial \rho}{\partial g}(U_H - U_{NH})}{\rho\frac{\partial U_H}{\partial X_H} + (1-\rho)\frac{\partial U_{NH}}{\partial X_{NH}}}}_{\frac{\partial \rho}{\partial g}\times\text{implicit price of risk}} - \underbrace{\frac{\rho\frac{\partial L}{\partial g}}{\rho\frac{\partial U_H}{\partial X_H} + (1-\rho)\frac{\partial U_{NH}}{\partial X_{NH}}}}_{\substack{\text{effect of location} \\ \text{on monetary losses}}} + \underbrace{\frac{\rho\frac{\partial U_H}{\partial g} + (1-\rho)\frac{\partial U_{NH}}{\partial g}}{\rho\frac{\partial U_H}{\partial X_H} + (1-\rho)\frac{\partial U_{NH}}{\partial X_{NH}}}}_{\substack{\text{direct effect of location} \\ \text{on utility}}}. \tag{1.4}$$

The first term on the right-hand side of Equation 1.4 represents the implicit price of the risk multiplied by the effect of location on the subjective probability of a hurricane. The second term reflects how losses vary with changes in location. The third term represents the direct impact of location on utility. This equality highlights the difficulty in disentangling the price effect of risk from other locational effects when risk is spatially varying, as is the case here, where hurricane risk is proxied by whether the property is located inside an HEZ. Changes in geographic location can affect prices through their impact on risk, monetary losses, and utility. Regarding losses, Kousky [2010] provides the example of a nearby access road flooding even if the property itself does not face the risk of flooding. Additionally, HEZs tend to be closer to the coast and therefore may be correlated with other coastal amenities that directly impact utility.

Carbone et al. [2006] show that an exogenous information shock provided by weather events can identify the risk discount. In this case, both the subjective probability of occurrence, ρ, and expected monetary losses L can be influenced by new information, I [Kousky, 2010]. Although new information could impact insurance markets, I argue that the price effect is through new information relayed to property owners and potential home buyers.[16] The expected utility function becomes

$$EU = \rho(g, I)U_H(X_H, \mathbf{Z}, g) + (1 - \rho(g, I))U_{NH}(X_{NH}, \mathbf{Z}, g), \tag{1.5}$$

and consumption in the hurricane-occurring state becomes

$$X_H = Y - P(\rho(g, I), \mathbf{Z}, r) - L(g, \mathbf{Z}, r, I). \tag{1.6}$$

[16] See Section 1.8.1 for a discussion on insurance rate changes during the study period.

Subsequently, the maximization of expected utility results in the equality

$$\frac{\partial P}{\partial I} = \underbrace{\frac{\frac{\partial \rho}{\partial I}(U_H - U_{NH})}{\rho\frac{\partial U_H}{\partial X_H} + (1-\rho)\frac{\partial U_{NH}}{\partial X_{NH}}}}_{\substack{\text{ex-ante} \\ \text{risk} \\ \text{discount}}} \underbrace{\times}_{\substack{\text{effect of} \\ \text{information on} \\ \text{subjective probability}}} - \underbrace{\frac{\rho\frac{\partial L}{\partial I}}{\rho\frac{\partial U_H}{\partial X_H} + (1-\rho)\frac{\partial U_{NH}}{\partial X_{NH}}}}_{\substack{\text{effect of information} \\ \text{on monetary losses}}}. \tag{1.7}$$

The first term on the right side of Equation 1.7 equals the ex-ante risk discount multiplied by the effect of information on the subjective probability of a hurricane occurring. The second right-side term reflects the effect of new information on losses. Thus, information shocks that lead to a change in property prices in HEZs could be due to changes in market participants' subjective probability, expected losses, or some combination of both. The larger the price effect of information, the larger the impact on market participants' risk perceptions. Suppose new information has no effect on subjective probability or expected losses. In that case, there should be no effect on property prices in HEZs unless through other channels, such as changes in insurance premiums.

1.5 Data and Variables

I use data on single-family home sales in Miami-Dade County from January 2014 through August 2017 to analyze the impact of these two near-miss hurricanes on property price differentials in HEZs. I restrict the study to this time frame for the following reasons. First, in March 2013 there was a remapping of the evacuation zones. In early September 2017, Hurricane Irma caused significant flooding in downtown Miami and as much as two to six feet of inundation in coastal areas [Cangialosi and Berg, 2021]. While individual sale prices are the preferred measure of value for hedonic studies [Bishop et al., 2020, Freeman III et al., 2014] and avoid the issue of measurement error that arises with assessed or self-reported values, there is selection into the sample as only certain homes sell each year. This is especially an issue if the constructed sample depends on proximity to the amenity where home sales outside some boundary are explicitly excluded [Taylor, 2013].

While sample selection is still a concern here, it is mitigated by the fact that the data contain the universe of housing transactions during the study period. Using Geographic Information System (GIS) software, I merge administrative property data with an array of spatial data from state and federal sources to account for variation in property prices due to neighborhood quality, amenity proximity, and environmental risk. The resulting data set used in the main analysis is a repeated cross-section containing 40,126 property-level observations.

Hedonic property models typically include the following three categories of property characteristics: structural characteristics, neighborhood features, and locational features [Taylor, 2013]. The measures of these features that should be utilized are those that are observed or perceived by buyers. When examining the effects of risk in a hedonic setting, it is important to use the subjective measure of risk. In this case, the objective and subjective measures of the risks associated with HEZs align because the delineations of these zones are publicly available from the county and are included in the Hurricane Readiness Guide mailed to residents every year.

1.5.1 Hurricane Evacuation Zones in Miami-Dade County

I obtained a GIS layer of HEZs from Miami-Dade County's Open Data Hub to identify properties within the boundaries of each evacuation zone. In MDC, there are five zones that correspond to each of the five hurricane categories, as previously shown in Figure 1.3. Evacuation decisions are determined by the individual storm and may not necessarily be required, or only a portion of the zone may be asked to evacuate. Though they were renamed in 2013 to 'storm surge planning zones,' I will refer to them as hurricane evacuation zones since they still depict hurricane-induced storm surge risk and inform evacuation decisions.[17] In MDC, location in an HEZ means you face the risk of either 1) being required to evacuate in the event of an approaching storm, 2) being inundated by at least 1.5 ft of water or being isolated, or both 1 and 2. Evacuation decisions will be determined based on each individual

[17] This coincided with the revision of the number of zones and their boundaries.

storm rather than entire zones. Therefore, it is best to think of one living in these zones as *potentially* having to evacuate in the event of a hurricane. Zone A corresponds to areas that face these risks in the event of a category one or higher hurricane. Zone E represents areas that face these risks only in the event of a category five hurricane. For effective communication, the evacuation zones are at the scale of a one-square-mile grid to correspond with the county's road system.[18] If any part of the square-mile grid could be inundated by at least 1.5 ft of storm surge, the entire square was coded as an evacuation zone. These zones are determined and maintained by the Miami-Dade County Office of Emergency Management in coordination with outside agencies such as the National Oceanic and Atmospheric Administration and the National Weather Service.[19]

1.5.2 Housing Characteristics

Property transaction records from Miami-Dade County are publicly available and were obtained from the Office of the Property Appraiser.[20] These represent the universe of sale transactions. Each transaction includes the sale date and amount as well as numerous structural characteristics, which are outlined in Table 1.2. Sale prices were deflated to 2014 dollars using the Consumer Price Index for All Urban Consumers. However, using a local Consumer Price Index produces similar results, as shown in Appendix J. The number of bedrooms, number of bathrooms, lot size, living space, garage space, and house age are included to control for their impacts on property price. Garage area was calculated by subtracting the living square footage from the measured square footage of the home. This captures the non-living area square footage of a home and includes attributes such as garages and covered patios. The data do not specify what attributes are included in the non-living for the property. The age of the house at the time of sale is calculated by subtracting the year the house was built from the year of sale.

[18] Source: Author's correspondence with Miami-Dade County's Protective Measures Planner at the Office of Emergency Management in April 2022.

[19] Answers to common questions regarding the evacuation zones in Miami-Dade County can be found at https://www.miamidade.gov/global/emergency/hurricane/storm-surge-zones.page.

[20] Data are available for purchase from https://bbs.miamidade.gov/.

I limit the analysis to arms-length transactions to exclude non-market transactions such as those between relatives. Minimal trimming is done, which includes dropping the lowest and highest percentile of inflation-adjusted prices, outliers, and homes whose age was less than zero at the time of sale. Details on the construction of the data set are provided in Appendix B. Properties were geocoded using Geographic Information System (GIS) software (ArcGIS Pro 2.9).

1.5.3 Neighborhood Quality

I proxy for neighborhood quality with an increasingly granular set of geographic fixed effects, including zip code, census tract, and square-mile grids of three, two, and one-mile (s). These spatial fixed effects capture time-invariant unobservables at different neighborhood levels, such as the income and gender composition of a neighborhood, to the extent that such traits do not vary throughout the study period. Time-varying neighborhood demographics are not included because of their endogeneity with sale prices. The zip code associated with each property's location is contained in the housing data. Census tract boundaries for 2014 were sourced from the U.S. Census Bureau's TIGER/Line shapefiles. While census tract fixed effects are often used in the hedonic literature [e.g., Bakkensen et al., 2019, Kousky, 2010], geographic size can vary widely between tracts, prohibiting some tracts from picking up localized factors. I create square-mile grids in ArcGIS Pro 2.9. Some researchers recommend such grids as an alternative to census tracts to capture localized time-invariant characteristics that may impact housing prices [Banzhaf, 2021].

1.5.4 Amenity Proximity

Data on property proximity to various amenities come from three sources. Data on park, lake, and golf course locations are from Miami-Dade County's Open Data Hub. Levee locations are from the National Flood Hazard Layer provided through the Federal Emergency Management Agency. I create an ocean proximity measure using the Composite Shoreline data set offered by the National Oceanic and Atmospheric Administration's Office

for Coastal Management. Since properties in evacuation zones tend to be closer to the coast, failing to control for coastal proximity could bias the estimated coefficients for evacuation zones. I also create a measure of distance to the nearest waterway, which includes, for example inlets, using the 2019 TIGER/Line Coastline Shapefile provided by the U.S. Census Bureau. The difference between these two coastal proximity measures is shown in Figure A1 of Appendix C.

1.5.5 Environmental Risk

Variables related to risk include an SFHA indicator and a variable to proxy for variation in flood insurance premiums. I use the National Flood Hazard Layer provided by the Federal Emergency Management Agency to identify homes in 100-year floodplains, known as 'special flood hazard areas', during the study period.[21] In the sample, 36% of properties are within the boundaries of an SFHA. To help control for changes in flood insurance premiums, I include the variable 'PREFIRM'. Properties built prior to the implementation of the first flood insurance rate maps, which delineate SFHAs, are eligible for rate subsidies [Federal Emergency Management Agency, 2022]. For MDC, the maps were first implemented on March 2, 1994.[22] Therefore, a property is coded as 'PREFIRM' if it was built before 1994 (housing data do not include the month the home was built). Updated flood insurance maps went into effect for the county on September 11, 2009. These maps are used in the National Flood Insurance Program to determine a home's flood zone and thus, flood insurance rates, which could potentially impact housing prices. The interaction of 'PREFIRM' and 'SFHA' captures some time-invariant heterogeneity in insurance rates across properties. The 'PREFIRM' dummy variable also captures variation in protective housing measures against hurricanes. The South Florida Building Code predated Florida's statewide building code that was implemented in 2001. The South Florida Building Code underwent significant updates after the devastating 1992 Hurricane Andrew, adding new re-

[21] The most recent revision to the SFHA boundaries was in September of 2009.

[22] Historic flood maps and other flood products can be found at FEMA's Map Service Center, accessible through https://msc.fema.gov/portal/home.

quirements to better protect against future hurricanes, including impact shutters, enhanced roof fastening, and truss bracing. These took effect for properties permitted after August 31, 1994.

Wind risk is controlled for to some extent by the coastal proximity measures and the number of stories. It is thought that peak one-minute winds decrease by an amount associated with one hurricane category on the Saffir-Simpson scale (i.e., from category three windspeed to category two windspeed) about half of a mile from the coast [Taylor et al., 2010]. Taller buildings are also more susceptible to wind damage. The inclusion of wind-borne debris regions was considered but omitted due to the limited variation among wind zones for the sales in the sample period.

1.5.6 Descriptive Statistics

Table 1.3 shows the number of sales by event period for each HEZ. Approximately 30% of sales occurred before TS Erika, 43% occurred after TS Erika but before Hurricane Matthew, and 26% occurred after TS Erika and Hurricane Matthew. Table 1.4 displays the means and standard deviations of the full sample and each zone. The sample contains 40,126 sales, with an average sale price of $439,348 in 2014 dollars. Bedrooms range from 1 to 12, and bathrooms range from 1 to 11. The average lot size is about a quarter of an acre. The newest house is brand new, built in the year it was sold, and the oldest house is 114 years old. The average house age is 47 years. The number of stories and structures ranges from 1 to 4, with an average of one story and one structure. The majority of properties, 76%, are in HEZs. Homes outside evacuation zones are mainly located 5 to 15 miles from the coast. This likely, at least in part, explains why homes in higher-risk evacuation zones have higher average sales prices than homes in lower-risk zones or non-evacuation zones. Properties in Zone A are much more likely to be coastal properties and are, on average, less than a mile from the coast. Average coastal proximity decreases from Zone B to Zone E, and properties outside evacuation zones have the furthest average distance from the ocean, about 9 miles. Additionally, homes in higher-risk zones are, on average, larger, newer, and

have more bedrooms and bathrooms. There is also heterogeneity among the proportion of properties within an SFHA. For example, in Zone A, 50% of properties are in an SFHA but only 20% in Zone E are. 72% of homes in an SFHA are in an HEZ. However, only 34% of the properties in an HEZ are also in an SFHA. This highlights the independence of the measures and types of flood risk depicted by the two hazard zones (HEZs and SFHAs).

As shown in Figure 1.9, before Tropical Storm Erika, log sale prices are trending upwards in the non-evacuation zone and all the evacuation zones, except for Zone A, whose log sale price remains flat. This differing trend could be explained by the high proportion of coastal homes in Zone A. In Zone A, the average distance to the coast is .8 miles. Properties in Zone A also tend to be larger and newer and have a higher number of bedrooms and bathrooms when comparing mean attributes with other evacuation zones. Interestingly, home prices outside evacuation zones experience a greater price appreciation around the beginning of 2016 relative to homes inside evacuation zones.

The sale price and number of transactions follow a seasonal pattern, dipping in the first quarter of each year for properties inside and outside HEZs. While transactions remain relatively stable across zones, transactions in properties outside HEZs increase, particularly after TS Erika.

1.6 Empirical Methods

To estimate the causal impact of the near-miss hurricanes on sale prices, I use a difference-in-differences research design, which relies on variation over time and across groups to estimate the average treatment effect on the treated. In this context, the difference-in-differences estimator compares the log sale prices in HEZs with those outside HEZs before and after the near-miss hurricane, Erika.

The DiD design is one of the most commonly used empirical methods to estimate treatment effects within a hedonic context [Parmeter and Pope, 2013]. It is beneficial for hedonic methods because many characteristics that affect housing prices are not controlled

for by the researcher or even explicitly measured, such as neighborhood noise levels. Furthermore, hedonic models are often utilized in a spatial context, such as looking at the effect on prices of homes close to an airport versus far away, where there are likely numerous differences between these two groups of homes. Importantly, DiD allows for homes in the two groups to be systematically different as long as the trends in price growth for each group would have remained constant, in expectation, in the absence of the treatment [Angrist and Pischke, 2009].

Log prices are commonly used in the hedonic literature, supporting the assumption of indivisibility in the theoretical framework, namely that because attribute bundles cannot be perfectly repackaged (i.e., a two-bedroom house cannot be repackaged as two one-bedroom houses), the relationship between prices and attributes will be non-linear [Rosen, 1974, Freeman III et al., 2014]. Additionally, it is likely that the dollar effect of an additional bedroom for a $100,000 home would be different from that of an additional bedroom for a $1,000,000 home. Non-linear price functions, such as semi-log and Box-Cox transformations, overcome this issue. While Box-Cox transformations allow for more flexibility, their interpretation is not as straightforward. Following similar studies [Bin and Landry, 2013, Atreya et al., 2013, Bin and Polasky, 2004], I use a variant of the log-log model for the main specification, with logged distance measures and quadratic forms of continuous structural characteristics to capture the diminishing effects on prices as levels of the attribute increase. Additionally, these studies found that these transformations of the independent variables had the best fit. Table A1 in Appendix C presents the results when using different functional forms. The estimated coefficients remain similar in magnitude and statistical significance across specifications.

I begin the empirical analysis by examining the effect of the near-misses on sale prices in HEZs, aggregating sales in all HEZs to serve as a single treated group, which I refer to as the aggregate treated group. While this provides an average effect on sales across HEZs, the price effect likely varies across evacuation zones since some zones are considered to be at greater risk than others. For this reason, I also estimate models in which the treated

group is an individual HEZ (I refer to these as disaggregate treated groups) to understand how the price effect differs across zones. An alternative to five different models in which each treated group consists of one of the five HEZs is to estimate a model for the entire sample using a categorical variable to allow for different estimated effects across HEZs. Results from this pooled model are similar in significance and magnitude to those from the models with disaggregate treated groups and are available in Table A3 of Appendix G.

1.6.1 Evidence of Parallel Trends Assumption

The key identifying assumption is referred to as the parallel trends assumption. It requires that the log sales prices in evacuation zones would have evolved the same as those in non-evacuation zones had the near-misses not occurred. In other words,

$$E[Y_t^0|Post] - E[Y_t^0|Pre] = E[Y_c^0|Post] - E[Y_c^0|Pre],$$

where $Post$ (Pre) is the time-period after (before) the near-miss and t and c denote the treatment and control groups, respectively. Y^0 indicates the value of the outcome variable when treatment does not occur.

I examine the validity of the parallel trends assumption in the following ways. First, Figure 1.9 provides suggestive evidence of the similar evolution between the control and treatment groups in the periods prior to the treatment event. It shows that log sale prices in and outside HEZs were trending similarly prior to Tropical Storm Erika. However, these price trends alone do not hold constant the numerous attributes that influence housing prices, many of which will be controlled for in the main specification. To assess the validity of the parallel trends assumption conditional on covariates, I present the requisite event study plots in Figure 1.10 and Figure 1.11 to elicit pre- and post-treatment patterns after controlling for other influences on price [Cunningham, 2021]. Coefficients are reported in Table A4 and Table A5 of Appendix H.

Figure 1.10 and Figure 1.11 are estimated by Equation 1.8 for the aggregate treated

group which consists of all evacuation zones (Figure 1.10), and the disaggregate treated groups where a separate model is estimated for each zone (Figure 1.11), with all the models using non-evacuation zones as the control group.

Interpreting the lead coefficients to assess the validity of the parallel trends assumption requires the assumption of no anticipation. This assumption is plausible given the random paths of tropical storms and hurricanes and the relative infrequency of storms that MDC and Florida had experienced in the time leading up to the treatment events. The event study plots are modelled by the ordinary least squares regression

$$\begin{aligned} ln(P)_{i,t} =& \alpha + \beta_1 EVACZONE_i + \beta_2 \upsilon_t \\ &+ \sum_{\tau=Q12014}^{Q12015} \gamma_\tau lead_\tau EVACZONE_i + \sum_{\tau=Q32015}^{Q32017} \gamma_\tau lag_\tau EVACZONE_i \\ &+ \beta_3 X_i + \phi_i + \epsilon_{i,t}, \end{aligned} \tag{1.8}$$

with the natural logarithm of sale price as the dependent variable. The coefficient estimating the differences between HEZ and non-HEZ in each quarter relative to the quarter before TS Erika is denoted by γ_τ. Quarter fixed effects are denoted by υ_t and capture the evolution of log sale prices in the non-HEZ group. A vector of housing and locational covariates, X_i, is included and contains the following attributes described in Table 1.2: bedrooms, bathrooms, lot size, living area, garage area, stories, structure, and age. I include quadratic forms of the continuous housing characteristics (lot size, living area, garage area, age), and logged geodesic distance measures of ocean, lake, golf, park, and levee. Additionally, X_i includes a dummy variable for if the property is located in an SFHA and a proxy for insurance rates. I proxy for flood insurance rates by interacting the pre-FIRM indicator with the SFHA indicator. The covariate vector X_i also includes indicators for whether the property is a waterfront or lakefront property, or located near a golf course. However, there are no waterfront properties in Zone E and outside evacuation zones, so the waterfront indicator is omitted from models with Zone E as the treated group.

Zip code fixed effects are used in the main analysis and are denoted by ϕ_i. These fixed effects capture time-invariant unobserved heterogeneity across postal areas. Though smaller geographic regions will capture more localized characteristics and help to reduce bias, there is little variation among evacuation zones at these finer spatial scales. The full sample contains 75 zip codes, enabling the fixed effects to account for a portion of geographic heterogeneity while still providing adequate identifying variation.

The coefficients of interest that provide support for the parallel trends assumption are the γ's associated with the leading quarters (Q12014 through Q12015), which are reported in Table A4 and Table A5 of Appendix H. These coefficients provide evidence for the parallel trends assumption for all treatment groups. However, two lead coefficients are statistically different from zero for the model in which Zone A is the treated group.

The event study plots provide further evidence that the DiD design is appropriate and also show that sale prices in HEZs drop within a quarter or two after the near-miss storms. This delayed effect is likely due to the time it takes from when an offer is made on the house to when the house is actually sold. In MDC, the median time a home was on the market was 95 days in January 2017.[23]

1.6.2 Main Specification

I use a difference-in-differences design to estimate the average treatment effect on the treated for the full post-event period. Using the ordinary least squares method, I estimate the regression

$$\begin{aligned} ln(P)_{i,t} =& \alpha + \beta_1 EVACZONE_i + \beta_2 ERIKA_t + \beta_3 MATTHEW_t \\ &+ \beta_4 EVACZONE_i \times ERIKA_t \\ &+ \beta_5 EVACZONE_i \times MATTHEW_t \\ &+ \beta_6 X_i + \phi_i + \tau_t + \delta_t + \epsilon_{i,t}, \end{aligned} \tag{1.9}$$

[23]This is based on residential data downloaded from www.realtor.com.

where the main coefficient of interest, β_4, shows the causal impact of TS Erika on property prices in HEZs. The coefficient β_5 shows how prices in HEZs change after Matthew. The indicator variable $EVACZONE$ equals one if the sale was in an evacuation zone. The indicator variable $ERIKA$ ($MATTHEW$) equals one if the sale occurred after TS Erika (Hurricane Matthew) and zero if the sale took place prior to TS Erika (Hurricane Matthew). The covariate vector, X_i, contains the attributes described in Section 1.6.1. Zip code fixed effects, ϕ_i, are included to account for any time-invariant unobserved characteristics that vary across postal areas. Year fixed effects and quarter-of-year fixed effects are denoted by τ_t and δ_t, respectively, and account for time trends common to all observations. Bertrand et al. [2004] show that due to serial correlation, conventional standard errors often overstate the standard deviations of the difference-in-differences estimator, leading to an overestimation of t-statistics and over-rejection of the null hypotheses. One way to remedy this is to allow for correlation within a group over time when the number of groups is large (around 50). Therefore, I cluster standard errors at the census tract level to allow for correlation among unobservables over time within a census tract. The full sample contains 412 census tracts. Results are robust to alternative specifications of the dependent variable (as shown in Table A1 of Appendix C) and alternative spatial fixed effects (as shown in Table A2 of Appendix D).

1.7 Results

1.7.1 Main Results

Table 1.5 and Table 1.6 present the results from the main DiD analysis specified in Equation 1.9 for the aggregate treated group comprising all zones (Table 1.5) and the disaggregate treated groups (Table 1.6). The main analysis utilizes zip code fixed effects since variation in HEZs at finer geographic scales is not always sufficient for estimation. The first row in each table displays the estimated coefficients on the interaction term of Erika and HEZ indicators, β_4. These coefficients are the average treatment effect on the treated of

Tropical Storm Erika on sale prices in each evacuation zone relative to non-evacuation zones. The percentage change in sale prices for homes in HEZs following TS Erika is calculated by solving $(e^{\beta_4} - 1) \times 100$. Similarly, the percentage change in sale prices for homes in HEZs following Hurricane Matthew is calculated by solving $(e^{\beta_5} - 1) \times 100$.

Table 1.5 shows the base specification with no control variables in column 1. Columns 2 through 5 add covariates, year fixed effects, quarter-of-year fixed effects, and zip code fixed effects, respectively. The preferred specification is presented in column 5 and highlights the importance of controlling for zip code fixed effects, which reduces the magnitude of the price effects on HEZs from TS Erika and Hurricane Matthew. Tropical Storm Erika decreased property prices in HEZs by about 3.9% and this is statistically significant at the 1% level. Property prices in HEZs were associated with a further 4% decline following Hurricane Matthew, also significant at the 1% level.

Each column in Table 1.6 shows one of five models where each treated group is a different HEZ (Zone A, B, C, D, or E). Beginning with TS Erika, the results show a price decline for sales in Zone A relative to non-HEZs of about 13%. Sale prices in Zone C fell by 4.2% and prices in Zone D decreased by about 3.6% after TS Erika relative to non-evacuation zones. These estimates are statistically significant at the 5% level. Sale prices in Zone E fell by 2.9% relative to non-evacuation zones following TS Erika. The estimated effect of TS Erika is statistically significant for all zones aside from Zone B, which still showed a negative price effect. Estimated effects for Zone A are significant at the 1% level. Estimated effects for Zones C and D are statistically significant at the 5 percent threshold, and the effects for Zone E are significant at the 10 percent level.

After Hurricane Matthew, sale prices in Zone A fell by 8.9%. Zone B prices dropped by 5.3% and Zone C prices fell by 4.9%. Estimates for Zone A, B, and C are statistically significant at the 1 percent level. Sale prices in Zone D and E decreased by 3.4% and 2.5%, though the coefficient for Zone E is not statistically significant. Almost all the coefficients for the covariates are statistically significant and have the expected signs.

The results displayed in Table 1.6 along with the event study plots in Figure 1.11

show that the effects of Erika differed across zones and were generally of larger magnitude in higher-risk zones. Property prices in evacuation zones fell after TS Erika relative to properties outside of evacuation zones. However, there is about a one-quarter lag in the decrease from the time of the near-miss, which I attribute to the lag that occurs from the time an offer is placed to the time of sale. This reduction does not immediately rebound; rather, prices drop even further after the occurrence of Hurricane Matthew. The further price drop is relatively similar in size to the price decline after TS Erika, suggesting markets responded similarly to these two quite different storms. For each of the models, I cannot reject the null hypothesis that the estimated effects of Erika and Matthew are equal.

The results presented here support prior studies that found property price differentials in hazard areas respond to near-miss events, particularly near-miss hurricanes. Furthermore, the magnitudes of these effects align with previous findings, which range from around 2 to 20 percent [e.g., Hallstrom and Smith, 2005, Kousky, 2010]. Absent other contributing factors, the results show that the near-misses impacted risk perceptions among market participants by increasing either their subjective probability of being impacted by a hurricane or increasing the expected monetary losses associated with a hurricane.

1.7.2 Heterogeneity Across Special Flood Hazard Areas

One of the primary goals of this paper is to understand if the effect of prices in HEZs is separate from any SFHA effect or capitalization. To investigate if the price effects in HEZs are due to SFHAs, I re-estimate the event study and difference-in-differences model for two subsamples: one that contains only properties inside SFHAs (n=14,513) and one that contains only properties outside SFHAs (n=25,613). Finding an effect on HEZs in the subsample of properties outside of SFHAs would verify that SFHAs are not driving this result and that there is an independent and separate effect on HEZs.

A slightly higher proportion of sales were in HEZs for the subsample of properties outside of SFHAs (78%) than for the subsample of properties inside SFHAs (72%). Trends and events study plots for the two subsamples are shown in Appendix E and provide evidence

of the parallel trends assumptions, as the error bars span zero for almost all of the point estimates prior to TS Erika. The event study plots of the aggregate treated group (all HEZs) show an effect on prices in HEZs regardless of SFHA. However, fewer post-Erika coefficients are statistically significant in the SFHA-only subsample. The growth rate in prices decreases following TS Erika for homes in evacuation zones relative to homes outside evacuation zones, and this is more consistent across HEZs in the subsample of properties outside SFHAs. For the subsample of properties inside SFHAs, the price effect is most pronounced for properties in Zone A. Results from the DiD models for the subsets of properties outside and inside SFHAs are displayed in Table 1.7 and Table 1.8.

For the subsample of homes outside SFHAs, I find effects similar to the main analysis. Prices in HEZs decrease notably in the first quarter of 2016, which begins four months post-Erika and coincides with the lag between offer and date of sale. Breaking this up by each evacuation zone, Figure A4 shows evidence of the parallel trends assumption for all models and decreases in the point estimates after TS Erika. The DiD coefficients presented in Table 1.7 are similar in magnitude to the full sample, with slightly larger effects in Zones C, D, and E. Most of the coefficients are statistically significant, and all are negative, as expected. These results provide evidence that there is an HEZ capitalization that is fully independent of any price effect due to being located in an SFHA.

The results from the subsample of homes in SFHAs paint a less clear picture. The sample size is also smaller, which contributes to the imprecision of the estimates. The non-SFHA sample has 25,613 sales. The SFHA sample has 14,513 sales. Despite this, there appears to be a price drop in HEZs three quarters after TS Erika, an apparent rebound, and another drop in the quarter following Hurricane Matthew. However, the 95% confidence intervals overlap, and many of the DiD estimates shown in Table 1.8 are not statistically significant. Two estimates even have a positive but not statistically significant coefficient.

There are still parallel trends for the SFHA subsample (see Appendix E) when the treated group is comprised of sales in Zone A. Properties in Zone A experience price declines similar in magnitude to the full sample and non-SFHA subsample, and these esti-

mated effects are significant at the 1% level. The statistical insignificance and unexpected coefficient signs in other models of the subsample could be due to sample size. However, it could also be possible that people in SFHAs are not updating their risk beliefs like residents outside SFHAs are. This could be because communities in SFHAs take mitigating actions to protect homes and buildings against flooding, which not only protects homes but also reduces insurance premiums. It could be that those in an SFHA are not learning as much from the near-miss if they already have updated knowledge of their flood risk. It could also be that many homes in SFHAs are required to purchase federal flood insurance, so many homeowners transfer a large part of the flood risk onto the insurance companies. All of these results highlight that storm surge risk is differentiated from other types of flood risk in residential markets.

1.8 Mechanisms

In order to assess if the effect of the near-misses on property values is indeed due to a change in risk perceptions amongst market participants, it is necessary to evaluate the likelihood of other channels that could have caused prices to decrease in evacuation zones after the near-misses.

1.8.1 Insurance Rates

If insurance companies respond to the near-miss by changing their rates, then the difference-in-differences coefficients may be capturing an increase in insurance costs rather than changes in risk perceptions among market participants. In this paper, I contend that insurance rates do not respond to the near-misses. I proceed by discussing the three main flood insurance markets: federal, state, and local. Federal flood insurance is provided by the National Flood Insurance Program (NFIP). The largest state provider of flood insurance in Florida is Citizens Property Insurance. Typical homeowner's insurance does not provide coverage for flooding.

The NFIP is the largest residential flood insurance provider in the United States, issuing over 90% of flood insurance policies. In 2018, NFIP policies accounted for 91% of flood insurance policies in Florida [Kousky et al., 2018]. This federal insurance covers up to $100,000 of contents damage and up to $250,000 of building damage for single-family homes. The rate-setting scheme for the NFIP is updated yearly, and rates are set at a national scale. Therefore, rates in Florida will be determined the same way as rates in all other parts of the country. Due to both the timing of rate changes and the geographic scale of rate setting, federal rates would not have responded to these two near-miss storms, and moreover, not in a way that would differentiate between HEZs and non-HEZs. This is because the rates are complexly determined based on several factors, such as if the home is located in a flood zone, if the home was built before the last flood insurance rate map update (i.e., PRE-FIRM), whether the property has a basement, and the base flood elevation of the home.[24] While I do not have data on all of the inputs, my results capture some variation in flood insurance rates because I include the interaction term $SFHA \times PREFIRM$ as a covariate in the empirical models.

Citizen's Property Insurance, the state's subsidized insurance company, offers flood insurance and their rates notably changed in February 2016, with around a 10% increase in rates for coastal properties. In MDC, coastal properties were defined as east of Route 1. I argue this does not confound the results for the following two reasons. First, the rate increases are proposed on an annual basis and must be approved by the state of Florida. Though the rate increases took effect after TS Erika and coincide with the timing of price declines in HEZs, they were discussed, approved, and announced in mid- to late-2015. As an additional test, I restrict the analysis to properties located more than 5 miles from the coast (based on the 'DIST_OCEAN' variable) as a proximate boundary of Route 1. I still find similar effects of the near-misses in this restricted sample that was not subject to the significant rate increases. These results are presented in Table A6 and Table A7 of

[24]Detailed rate structures are available from FEMA on their Flood Insurance Manuals Archive: 2005 - 2021 webpage, which can be accessed at https://www.fema.gov/flood-insurance/work-with-nfip/manuals/archive.

Appendix I. Although Table A7 shows positive and statistically significant coefficients on the interaction term for TS Erika for models where the treatment group is Zone B or Zone C, these models do not include zip code fixed effects due to a lack of spatial variation. The models with treatment groups Zone D and Zone E do include zip code fixed effects and show a negative and statistically significant impact on property prices in evacuation zones after TS Erika.

1.8.2 Hurricane Matthew Damages

Atreya and Ferreira [2015] show that failing to adequately control for property damages can impact a researcher's ability to isolate the information effect of a flood. As the result of Hurricane Matthew, MDC experienced minor beach erosion and tropical storm-force wind gusts that resulted in primarily downed tree limbs and power outages. On October 6, the county experienced a tropical depression and high surf. Damage estimates vary. The Storm Events Database from NOAA's National Centers for Environmental Information estimated property damages of $1.2 million. There were 369 claims from homeowners, 122 claims associated with dwellings, and 11 federal flood claims. Over half of the homeowner claims (55%), 48% of the dwelling claims, and 90% of the federal flood claims were reported as closed without payment as of March 2017 [Florida Office of Insurance Regulation, 2017].

Even so, the results show clear and robust evidence that near-miss TS Erika reduced property values in HEZs, and that reduction was not confounded by any physical damages. Both of these close calls may have provided information regarding hurricane risk.

1.9 Conclusion

Following a decade-long period of unusual calm, MDC experienced two near-miss hurricanes just after an update of their hurricane evacuation zones and just before being impacted by a hurricane that caused widespread damage. This long period when no hurricanes approached Florida, combined with the increasing risks conveyed to residents through

an expansion of the hurricane evacuation zones, set the stage for possible learning and belief updates regarding hurricane risk. I posit that two near-miss hurricanes provided new information to residents regarding hurricane risk, as evidenced by the increase in property price differentials between homes inside and outside evacuation zones.

This study is among the first to estimate property price differentials associated with HEZs. Specifically, I provide the first estimates on the price effect of HEZs independently of SFHAs. I find that homes in HEZs experienced a decrease in price relative to homes outside HEZs following a near-miss tropical storm projected to impact the state as a category one hurricane in 2015 and a further price decline after the category four Hurricane Matthew paralleled the Florida coast in 2016.

Future research could examine the effect of near-misses on prices in non-evacuation zones. It is possible that the storms affected both the properties in HEZs and those outside HEZs, in which case non-HEZs are not the most suitable control group. One could find a comparable coastal county that was not subject to the near-misses that MDC faced to use as a control group to learn how non-HEZs were affected by the near-miss relative to how HEZs were affected.

Another avenue of extension involves further exploring the mechanisms that cause the observed price effects. While I provide suggestive evidence of a potential increase in salience, without significant institutional background it is difficult to rule out other influences with certainty. Though federal flood insurance rates are set annually at the national level, it is possible that local flood or homeowner's insurance companies responded to the near-misses and that an increase in insurance costs drove down prices in HEZs.

As increasingly severe weather events become more frequent, understanding through what channels and to what extent residents obtain risk information is crucial for adaptation planning. This is especially important for areas that face potentially catastrophic damage and where risk disclosure is not mandatory, as is the case for HEZs in Florida. This paper shows that markets respond to information along risk dimensions in a way that internalizes these risks in property prices. Furthermore, this price change is likely due to a change

in consumer perceptions regarding risk. Future policy approaches may consider leveraging near-miss weather events as an opportunity to increase risk awareness, knowledge, and mitigation measures. However, these results also provide evidence of the ability of markets to internalize changing climate risks even in the absence of government interventions.

Figure 1.1: Frequency of Billion-Dollar Weather Events in the U.S. from 1980 to 2022

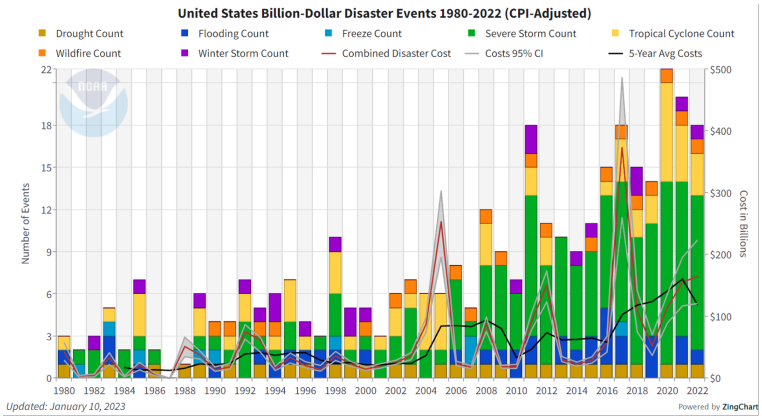

Notes: Costs are adjusted to 2022 U.S. dollars.
Source: National Oceanic and Atmospheric Adminstration National Centers for Environmental Information

Figure 1.2: Hurricane Evacuation Zones in Florida

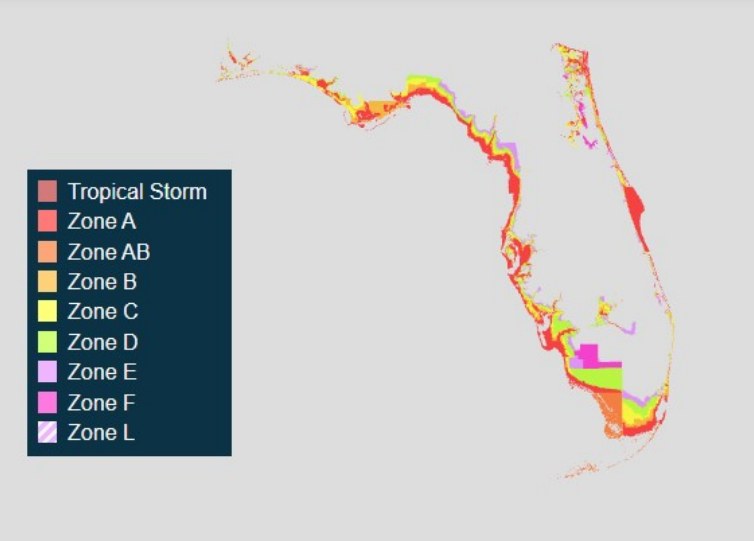

Notes: Zone definitions vary by county.
Source: Florida Public Radio Emergency Network

Figure 1.3: Maps of Special Flood Hazard Areas (left) and Hurricane Evacuation Zones (right) for Miami-Dade County, Florida

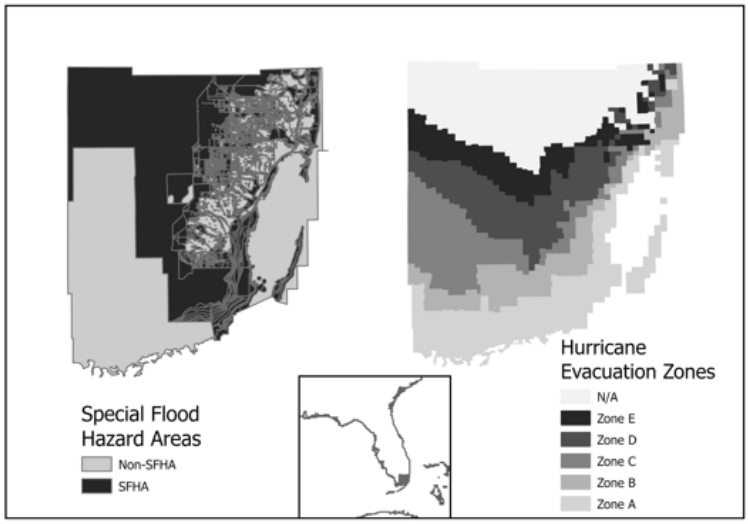

Figure 1.4: Forecasts of Tropical Storm Erika

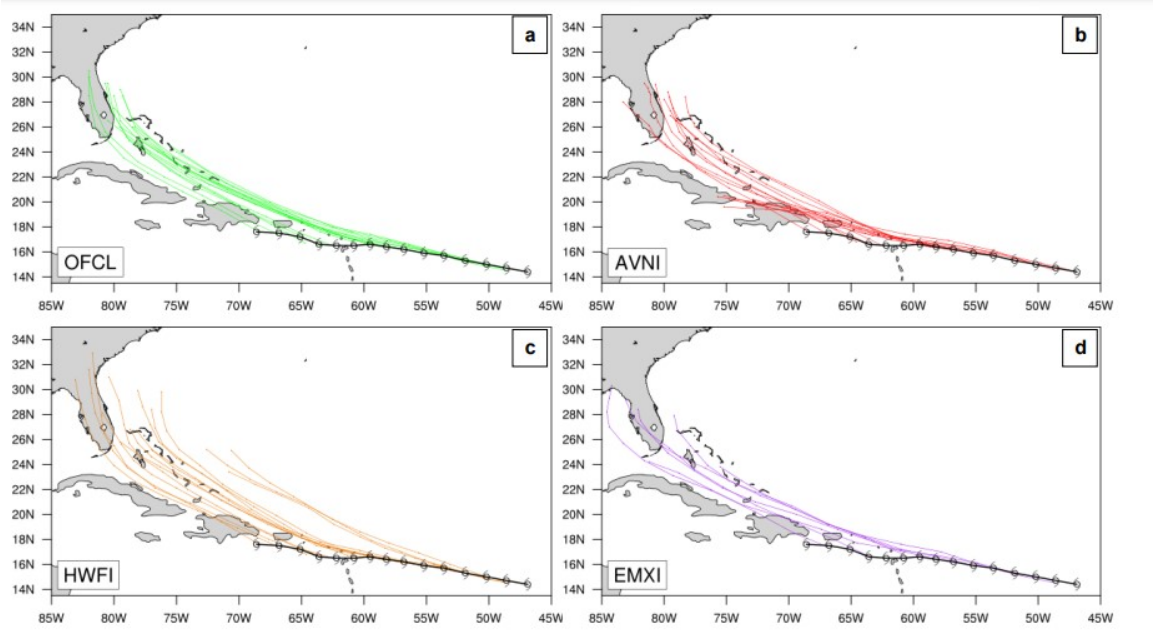

Figure 4. Five-day forecast track plots of the (a) NHC official forecasts (OFCL), (b) GFSI, (c) HWFI, and (d) EMXI for the forecast cycles from 0000 UTC 25 August to 1200 UTC 28 August 2015 for Tropical Storm Erika. The best track of Erika is indicated by the black lines with six-hourly tropical cyclone positions.

Notes: These forecasts are approximately five days prior to potential landfall in Florida.
Source: National Hurricane Center Tropical Cyclone Report

Figure 1.5: Forecasts of Hurricane Matthew

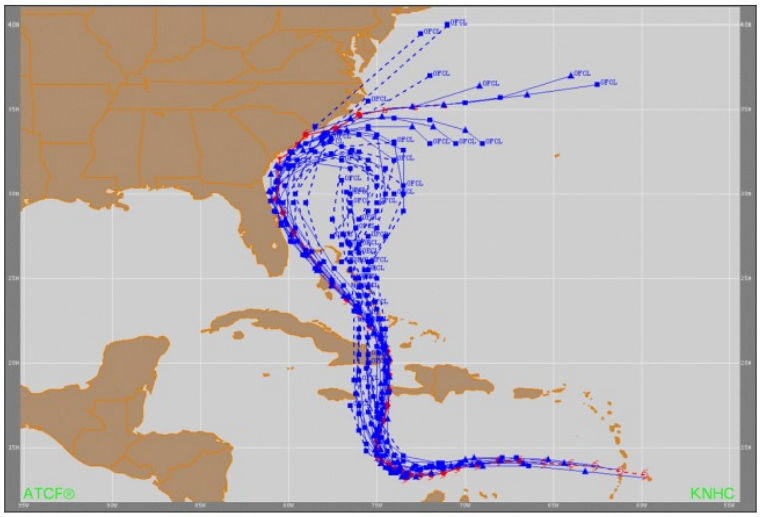

Source: National Hurricane Center Tropical Cyclone Report

Figure 1.6: Hurricane Matthew's Track

Source: National Weather Service

Figure 1.7: "Hurricane Preparation" (top) and "Hurricane Evacuation Zone" (bottom) Google Search Intensity for Miami-Ft. Lauderdale, Florida

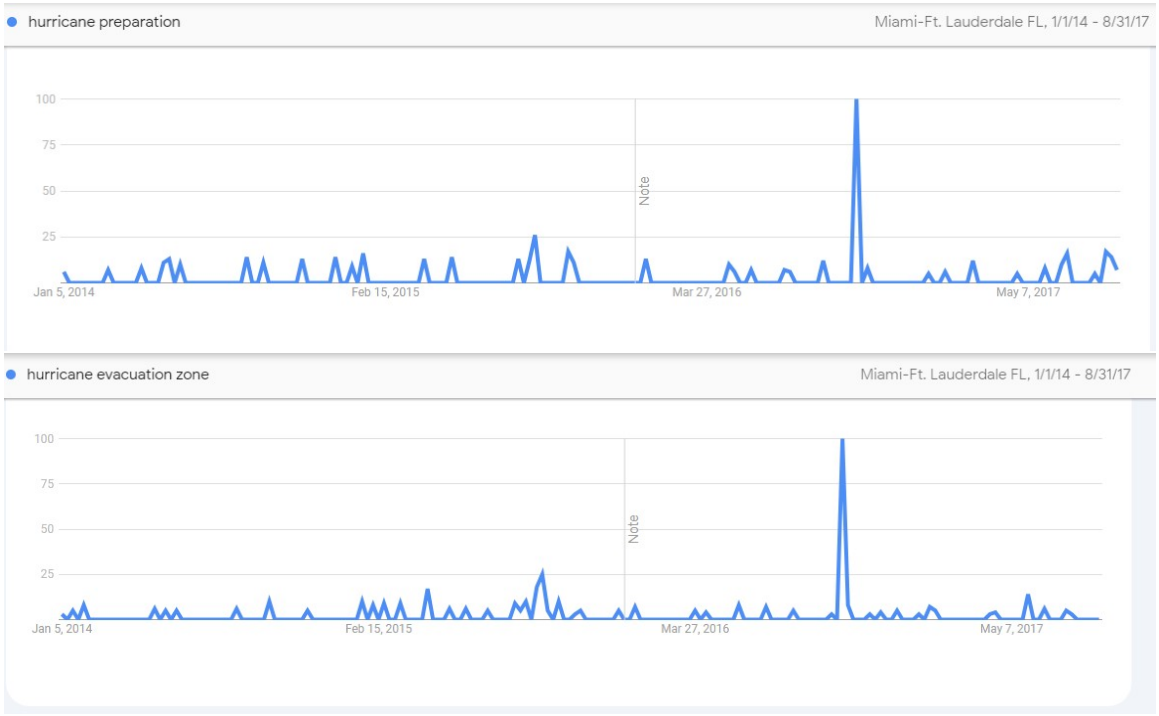

Notes: Google search trends in Miami-Ft. Lauderdale, FL from January 1, 2014 through August 31, 2017 for the mentioned terms. The y-axis denotes search interest and ranges from 0 to 100, with 100 representing the time of highest search intensity. All values are relative to the highest search intensity during the covered period.

Figure 1.8: Storm Surge Watches (gray) and Warnings (magenta)

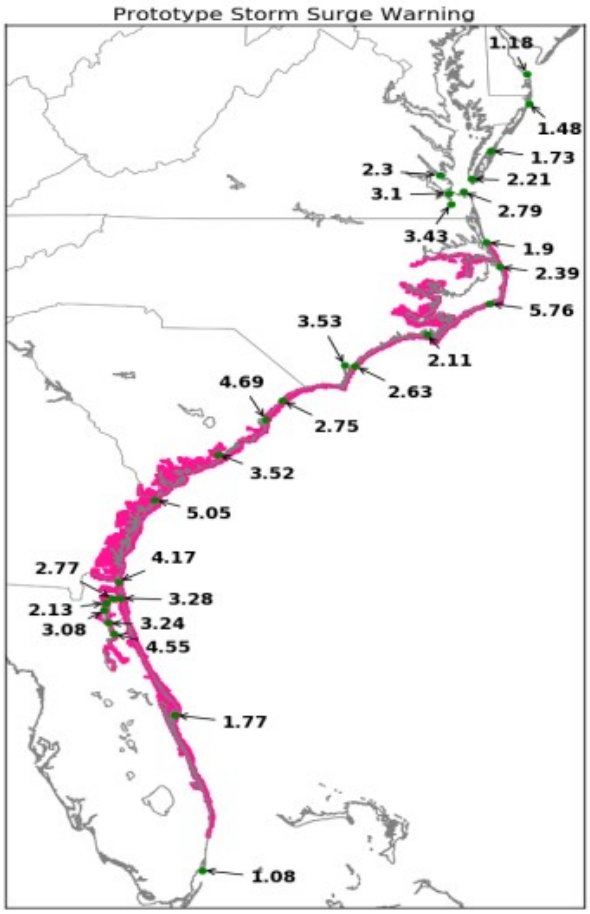

Notes: This figure displays areas depicted in the Prototype Storm Surge Warning system for Hurricane Matthew. Storm surge warnings represent the danger of life-threatening inundation (or isolation), where the inundation threshold is three feet. Storm surge watches convey the possibility for life-threatening inundation (or isolation). Numbers correspond to maximum water levels above mean higher high water (in ft.) recorded by the National Ocean Service. More information on this system can be found at https://www.nhc.noaa.gov/experimental/surgewarning/.
Source: National Hurricane Center Tropical Cyclone Report

Figure 1.9: Quarterly Sale Price (left) and Transaction Volumes (right)

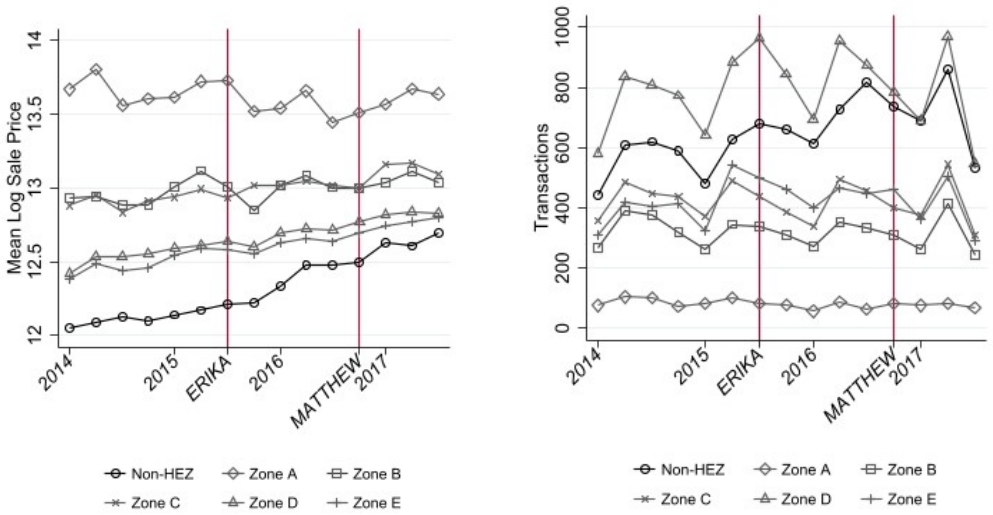

Figure 1.10: Effect of Near-Miss Hurricane on Sale Prices in Hurricane Evacuation Zones

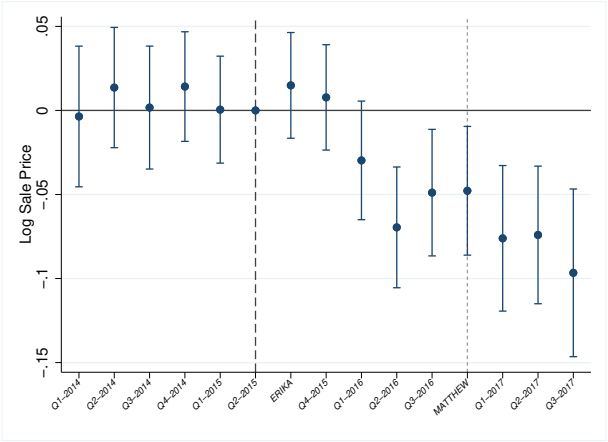

Notes: Average treatment effect on the treated of near-miss on log sale prices of properties located inside hurricane evacuation zones. The dependent variable is the log sale price in 2014 U.S. dollars. Point estimates correspond to the γ_τ's in equation Equation 1.8. Estimates are relative to the quarter prior to Tropical Storm Erika's occurrence (Q2-2015), denoted by the thicker dashed line. The thinner dashed line indicates the occurrence of Hurricane Matthew. Error bars represent the 95% confidence interval with standard errors clustered at the census tract level. The treated group comprises all sales occurring within a hurricane evacuation zone.

Figure 1.11: Effect of Near-Miss Hurricane on Sale Prices, By Hurricane Evacuation Zone

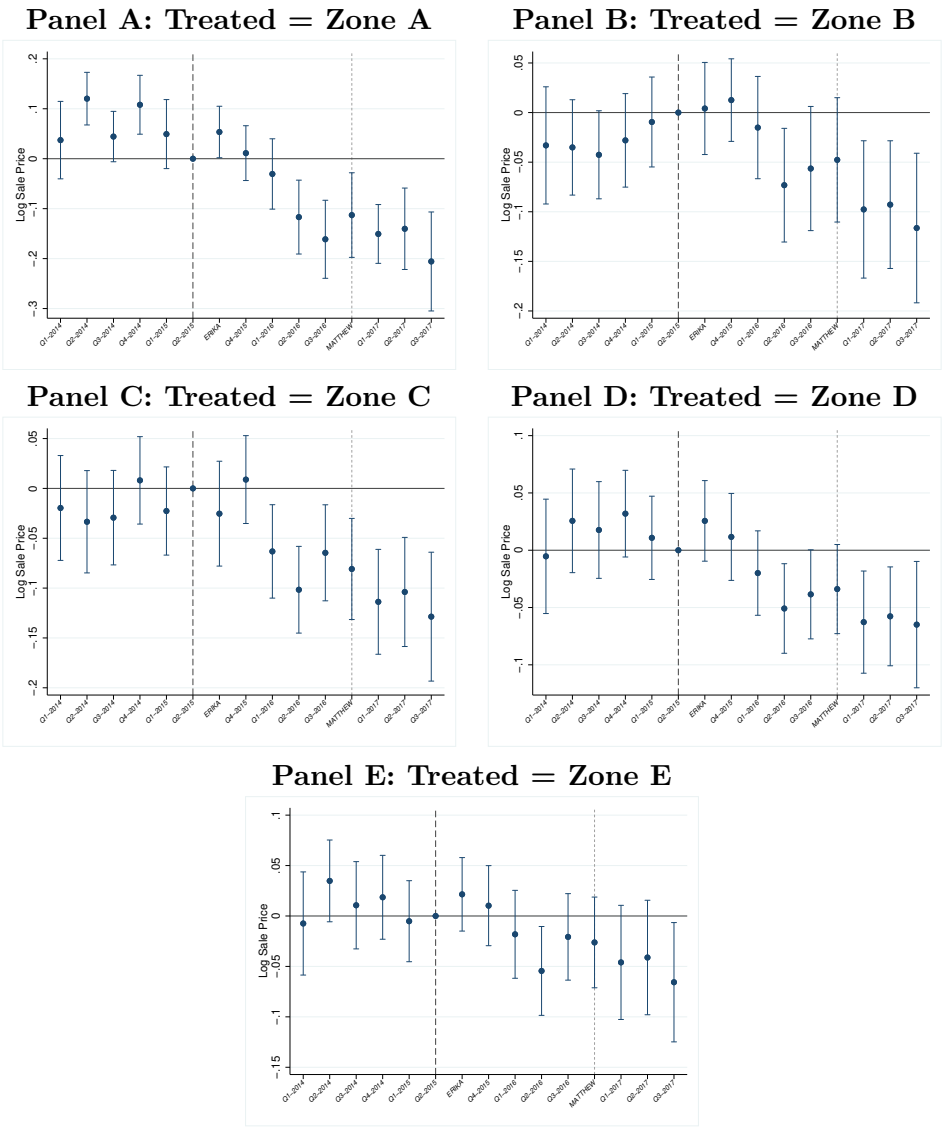

Notes: Average treatment effect on the treated of near-miss on log sale prices of properties located inside hurricane evacuation zones, by hurricane evacuation zone. The treated group differs across panels. The untreated group in all panels comprises all sales outside hurricane evacuation zones. The dependent variable is the log sale price in 2014 U.S. dollars. Point estimates correspond to the γ_τ's in equation Equation 1.8, restricted to sales in the treated and untreated groups. Estimates are relative to the quarter prior to Tropical Storm Erika's occurrence (Q2-2015), denoted by the thicker dashed line. The thinner dashed line indicates the occurrence of Hurricane Matthew. Error bars represent the 95% confidence interval with standard errors clustered at the census tract level.

Table 1.1: Dates and Forecasts of Near-Miss Storms

Near-Misses	Actual Date	County Warnings
Tropical Storm Erika	Aug. 24-28, 2015	Inside category 1 cone of projection
Hurricane Matthew	Sept. 28 - Oct. 9, 2016	Inside 5-day category 5 cone; 3-day category 3+ cone

Notes: This table presents the near-miss storms, their dates, and the corresponding warnings for Miami-Dade County, Florida. The dates listed in the table comprise the date of the event itself, not the date of the warning. Dates are from the National Hurricane Center's Tropical Cyclone Reports [Pasch and Penny, 2016, Stewart, 2017].

Table 1.2: Variable Names and Descriptions

Variable	Definition
PRICE	Sales price, thousands (2014 dollars)
Near-Miss Hurricanes	
EVACZONE	In any hurricane evacution zone (=1)
ERIKA	Sold after August 2015 (=1)
MATTHEW	Sold after September 2016 (=1)
Housing Characteristics	
BEDROOM	Number of bedrooms (categorical: 1, 2, 3, 4, 5, 6+)
BATHROOM	Number of bathrooms (categorical: 1, 2, 3, 4, 5, 6+)
LOT_SIZE	Total lot size (hundreds of sq. ft.)
LIVING_AREA	Total livable area (hundreds of sq. ft.)
GARAGE_AREA	Measured area- Living area (hundreds of sq. ft.)
STORIES	Number of stories (categorical: 1, 2+)
STRUCTURES	Number of structures (e.g., guest house, shed) (categorical: 1, 2+)
HOUSE_AGE	Age of house at time of sale (years)
Amenity Proximity	
DIST_OCEAN	Distance to ocean (miles)
DIST_WATER	Distance to waterway (miles)
DIST_LAKE	Distance to nearest lake (miles)
DIST_GOLF	Distance to nearest golf course (miles)
DIST_PARK	Distance to nearest park (miles)
DIST_LEVEE	Distance to nearest levee (miles)
WATERFRONT	Less than .03 miles from waterway (=1)
LAKEFRONT	Less than .03 miles from lake (=1)
GOLFFRONT	Less than .03 miles from golf course (=1
Risk Characteristics	
SFHA	In Special Flood Hazard Area (=1)
PREFIRM	House built before 1994 (=1)

Table 1.3: Sales By Time and Hurricane Evacuation Zone

Zone	Pre-Erika	Post-Erika (Pre-Matthew)	Post-Matthew (& Post-Erika)
Zone A	591	309	307
Zone B	2,176	1,384	1,229
Zone C	2,877	1,819	1,625
Zone D	5,155	3,688	2,987
Zone E	2,746	1,936	1,617
Non-HEZ	3,828	3,034	2,818
Total	17,373	12,170	10,583

Notes: This table displays the number of sales by hurricane evacuation zone for the periods before the first near-miss hurricane, after the first near-miss hurricane, and after both near-miss hurricanes.

Table 1.4: Means and Standard Deviations of Housing and Neighborhood Attributes

	Full Sample	Non-HEZ	Zone A	Zone B	Zone C	Zone D	Zone E
PRICE	439.4	274.4	1181.0	644.3	623.8	362.6	354.1
	(452.2)	(196.9)	(967.7)	(653.2)	(587.6)	(230.7)	(247.6)
Housing Characteristics							
BEDROOM	3.282	3.195	3.712	3.401	3.357	3.322	3.096
	(0.865)	(0.789)	(1.086)	(0.854)	(0.988)	(0.814)	(0.840)
BATHROOM	2.204	2.010	3.076	2.436	2.401	2.164	2.039
	(1.038)	(0.954)	(1.532)	(1.019)	(1.246)	(0.897)	(0.916)
LOTSIZE	102.7	74.65	121.0	93.64	124.5	127.6	80.79
	(116.4)	(42.75)	(72.85)	(53.64)	(118.0)	(165.6)	(106.8)
LIVING_AREA	19.41	16.92	28.16	21.10	22.01	19.43	17.65
	(8.899)	(7.052)	(13.21)	(9.045)	(11.37)	(7.949)	(6.911)
GARAGE_AREA	4.520	3.283	7.386	4.694	5.497	5.150	3.577
	(4.215)	(3.162)	(6.084)	(3.996)	(5.039)	(4.427)	(3.122)
STORIES	1.133	1.128	1.331	1.215	1.123	1.084	1.142
	(0.346)	(0.337)	(0.532)	(0.424)	(0.331)	(0.280)	(0.351)
STRUCTURES	1.109	1.112	1.066	1.073	1.109	1.118	1.127
	(0.328)	(0.328)	(0.259)	(0.268)	(0.325)	(0.346)	(0.347)
HOUSE_AGE	46.83	45.81	42.28	47.27	50.15	43.64	51.61
	(22.61)	(23.08)	(23.79)	(24.61)	(21.14)	(19.88)	(24.90)
Amenity Proximity							
DIST_OCEAN	5.729	8.950	0.781	2.388	3.444	6.228	5.624
	(3.394)	(2.965)	(0.521)	(1.703)	(1.653)	(2.205)	(3.299)
DIST_WATER	3.888	5.938	0.482	1.647	1.892	4.644	3.677
	(3.081)	(3.104)	(0.415)	(1.647)	(2.037)	(2.586)	(3.037)
DIST_LAKE	0.593	0.443	1.160	0.658	0.574	0.512	0.839
	(0.531)	(0.335)	(1.217)	(0.587)	(0.360)	(0.348)	(0.739)
DIST_GOLF	1.895	1.995	2.018	2.102	1.628	2.039	1.558
	(1.207)	(0.912)	(0.722)	(1.551)	(1.307)	(1.304)	(0.946)
DIST_PARK	0.415	0.419	0.348	0.398	0.373	0.458	0.398
	(0.278)	(0.264)	(0.189)	(0.282)	(0.219)	(0.292)	(0.321)
DIST_LEVEE	6.925	9.322	3.660	5.907	6.140	6.501	6.229
	(4.242)	(3.314)	(3.153)	(4.622)	(4.842)	(3.572)	(4.360)
WATERFRONT	0.0175	0	0.0804	0.0576	0.0516	0.000338	0
	(0.131)	(0)	(0.272)	(0.233)	(0.221)	(0.0184)	(0)
LAKEFRONT	0.0277	0.0430	0.0257	0.0182	0.00981	0.0234	0.0378
	(0.164)	(0.203)	(0.158)	(0.134)	(0.0986)	(0.151)	(0.191)
GOLFFRONT	0.00768	0.00496	0.00331	0.0148	0.0106	0.00710	0.00540
	(0.0873)	(0.0702)	(0.0575)	(0.121)	(0.102)	(0.0840)	(0.0733)
Risk Characteristics							
SFHA	0.362	0.421	0.497	0.604	0.331	0.303	0.200
	(0.480)	(0.494)	(0.500)	(0.489)	(0.471)	(0.460)	(0.400)
PREFIRM	0.819	0.811	0.774	0.816	0.867	0.810	0.813
	(0.385)	(0.392)	(0.419)	(0.387)	(0.340)	(0.392)	(0.390)
N	40126	9680	1207	4789	6321	11830	6299

Notes: For descriptive purposes, this table presents summary statistics based on the total number of bedrooms, bathrooms, stories, and structures, though these are categorized for the analysis as shown in Table 1.2.

Table 1.5: Impact of Near-Miss on Sale Prices (Aggregate Treated Group: All Evacuation Zones)

	(1) ln(P)	(2) ln(P)	(3) ln(P)	(4) ln(P)	(5) ln(P)
ERIKA × EVACZONE	-0.176***	-0.0768***	-0.0746***	-0.0747***	-0.0386***
	(0.0562)	(0.0197)	(0.0196)	(0.0195)	(0.0136)
MATTHEW × EVACZONE	-0.103***	-0.0613***	-0.0636***	-0.0645***	-0.0390***
	(0.0294)	(0.0169)	(0.0169)	(0.0169)	(0.0144)
EVACZONE	0.613***	0.0477	0.0471	0.0470	0.0398
	(0.0750)	(0.0450)	(0.0452)	(0.0452)	(0.0446)
ERIKA	0.249***	0.199***	0.0731***	0.0465**	0.0240*
	(0.0539)	(0.0172)	(0.0175)	(0.0186)	(0.0127)
MATTHEW	0.224***	0.163***	0.0789***	0.0531***	0.0292*
	(0.0272)	(0.0150)	(0.0153)	(0.0190)	(0.0150)
Constant	12.13***	11.58***	11.54***	11.51***	11.99***
	(0.0552)	(0.131)	(0.131)	(0.131)	(0.110)
All Covariates		✓	✓	✓	✓
Year FE			✓	✓	✓
Quarter-of-Year FE				✓	✓
Zip Code FE					✓
N	40126	40126	40126	40126	40126
R^2	0.105	0.739	0.742	0.743	0.872

Notes: This table displays the key estimates from Equation 1.9, where the treated group consists of all sales inside hurricane evacuation zones. The dependent variable is the natural logarithm of the sale price in 2014 U.S. dollars. Standard errors are in parentheses and clustered at the census tract, with 412 total clusters.
* p<0.10, ** p<0.05, *** p<0.010

Table 1.6: Impact of Near-Miss on Sale Prices in Hurricane Evacuation Zones

	(1) Treated= Zone A	(2) Treated= Zone B	(3) Treated= Zone C	(4) Treated= Zone D	(5) Treated= Zone E
ERIKA × HEZ	-0.122***	-0.0158	-0.0416**	-0.0356**	-0.0282*
	(0.0263)	(0.0242)	(0.0170)	(0.0140)	(0.0158)
MATTHEW × HEZ	-0.0854***	-0.0514***	-0.0479***	-0.0333**	-0.0249
	(0.0207)	(0.0193)	(0.0172)	(0.0136)	(0.0178)
EVACZONE	0.0725	0.380	0.141	0.0716	-0.0613
	(0.0630)	(0.279)	(0.107)	(0.0624)	(0.0517)
ERIKA	0.0110	-0.00490	-0.00162	0.0172	0.0146
	(0.0129)	(0.0129)	(0.0132)	(0.0118)	(0.0115)
MATTHEW	0.0200	0.0143	0.00384	0.0254*	0.0266*
	(0.0156)	(0.0164)	(0.0159)	(0.0144)	(0.0145)
Constant	12.05***	11.98***	12.19***	11.91***	12.46***
	(0.184)	(0.189)	(0.144)	(0.170)	(0.265)
All Covariates	✓	✓	✓	✓	✓
Year FE	✓	✓	✓	✓	✓
Quarter-of-Year FE	✓	✓	✓	✓	✓
Zip Code FE	✓	✓	✓	✓	✓
N	10887	14469	16001	21510	15979
R^2	0.898	0.893	0.890	0.823	0.839

Notes: This table displays the estimates from Equation 1.9, where the models (1) through (5) have different treated groups, Zones A through E, respectively. The untreated group in each model comprises sales outside hurricane evacuation zones. The dependent variable is the natural logarithm of the sale price in 2014 U.S. dollars. Standard errors are in parentheses and clustered at the census tract. There are 129, 181, 183, 235, and 201 clusters in models (1) through (5), respectively.
* p<0.10, ** p<0.05, *** p<0.010

Table 1.7: Robustness: Impact of Near-Miss on Sale Prices in Hurricane Evacuation Zones (Restricted Sample: All Properties Outside Special Flood Hazard Areas)

	(1) Treated= Zone A	(2) Treated= Zone B	(3) Treated= Zone C	(4) Treated= Zone D	(5) Treated= Zone E
ERIKA × EVACZONE	-0.109***	-0.0349	-0.0654***	-0.0598***	-0.0371*
	(0.0357)	(0.0305)	(0.0207)	(0.0160)	(0.0190)
MATTHEW × EVACZONE	-0.0887***	-0.0413*	-0.0452**	-0.0497***	-0.0522***
	(0.0293)	(0.0219)	(0.0192)	(0.0154)	(0.0188)
EVACZONE	0.0289	0.132	0.0600	0.0375	-0.0786
	(0.0691)	(0.179)	(0.0936)	(0.0657)	(0.0607)
ERIKA	-0.00440	-0.00877	-0.00545	0.0227*	0.0141
	(0.0155)	(0.0149)	(0.0158)	(0.0134)	(0.0135)
MATTHEW	0.0156	0.0104	0.0110	0.0405**	0.0352*
	(0.0225)	(0.0216)	(0.0211)	(0.0176)	(0.0191)
Constant	12.29***	12.28***	12.32***	12.00***	12.76***
	(0.343)	(0.280)	(0.160)	(0.200)	(0.303)
All Covariates	✓	✓	✓	✓	✓
Year FE	✓	✓	✓	✓	✓
Quarter-of-Year FE	✓	✓	✓	✓	✓
Zip Code FE	✓	✓	✓	✓	✓
N	6209	7498	9828	13844	10642
R^2	0.840	0.848	0.885	0.816	0.823

Notes: This table displays the estimates from Equation 1.9, where the models (1) through (5) have different treated groups, Zones A through E, respectively and the sample is restricted to sales which occurred outside special flood hazard areas. The untreated group in each model comprises sales outside hurricane evacuation zones. The dependent variable is the natural logarithm of the sale price in 2014 U.S. dollars. Standard errors are in parentheses and clustered at the census tract. There are 107, 132, 154, 209, and 171 clusters in models (1) through (5), respectively.
* p<0.10, ** p<0.05, *** p<0.010

Table 1.8: Robustness: Impact of Near-Miss on Sale Prices in Hurricane Evacuation Zones (Restricted Sample: All Properties Inside Special Flood Hazard Areas)

	(1) Treated= Zone A	(2) Treated= Zone B	(3) Treated= Zone C	(4) Treated= Zone D	(5) Treated= Zone E
ERIKA × EVACZONE	-0.109***	0.00719	-0.0122	-0.00935	-0.0435**
	(0.0395)	(0.0274)	(0.0208)	(0.0193)	(0.0213)
MATTHEW × EVACZONE	-0.0975***	-0.0485*	-0.0664***	-0.0182	0.0309
	(0.0296)	(0.0258)	(0.0246)	(0.0192)	(0.0367)
EVACZONE	0.107	1.303***	0.728***	0.115**	-0.0166
	(0.0972)	(0.133)	(0.139)	(0.0520)	(0.0372)
ERIKA	0.0331*	-0.00435	0.0162	0.0234	0.0355*
	(0.0197)	(0.0199)	(0.0208)	(0.0193)	(0.0191)
MATTHEW	0.0138	0.00515	-0.00111	0.00793	0.0295*
	(0.0165)	(0.0211)	(0.0203)	(0.0182)	(0.0171)
Constant	11.60***	11.60***	11.78***	12.09***	10.94***
	(0.149)	(0.192)	(0.209)	(0.275)	(0.403)
All Covariates	✓	✓	✓	✓	✓
Year FE	✓	✓	✓	✓	✓
Quarter-of-Year FE	✓	✓	✓	✓	✓
Zip Code FE	✓	✓	✓	✓	✓
N	4678	6971	6173	7666	5337
R^2	0.948	0.922	0.912	0.858	0.895

Notes: This table displays the estimates from Equation 1.9, where the models (1) through (5) have different treated groups, Zones A through E, respectively and the sample is restricted to sales which occurred inside special flood hazard areas. The untreated group in each model comprises sales outside hurricane evacuation zones. The dependent variable is the natural logarithm of the sale price in 2014 U.S. dollars. There are 94, 141, 132, 177, and 142 clusters in models (1) through (5), respectively.
* p<0.10, ** p<0.05, *** p<0.010

Chapter 2

Estimating the Impacts of Groundwater Depletion on Irrigation Decisions in the Republican River Basin of Colorado

2.1 Introduction

Groundwater is a crucial resource for agriculture, supplying over 40% of water used for irrigation [Siebert et al., 2010]. The expansion of groundwater pumping has enabled large-scale agricultural production in arid regions and provided a vital buffer against drought. However, groundwater pumping at rates that exceed natural recharge is depleting aquifers in many of the world's most agriculturally productive regions [Famiglietti, 2014]. Economics literature has estimated the value of groundwater stocks and costs of depletion [e.g., Fenichel et al., 2016, García Suárez et al., 2019, Sampson et al., 2019, Perez-Quesada

et al., 2024], which are useful for implementation and acceptance of groundwater management policies. Aquifer depletion threatens the sustainability of groundwater-fed agriculture through two main channels: pumping costs and well yield (also referred to as well capacity). However, well yield has been largely absent from the economics literature, despite recent research suggesting it is an important determinant of groundwater demand. In this paper we address this research gap by providing the first causal estimates of well yield on irrigation decisions in the Republican River Basin of eastern Colorado. Using time-varying data on well yields, we are able to interpret our estimates as impacts of groundwater depletion on total water use, irrigated acreage, and water use per acre, as captured through changes in well yields.

Aquifer depletion affects groundwater-fed agricultural production through two main mechanisms: depth to water and well yield. As aquifer thickness declines, depth to the water table increases, increasing pumping costs as more energy is required to lift water greater vertical distances. Well yields, which represent a physical constraint on the flow rate of irrigation application, are also reduced. While it is possible in some cases that total seasonal groundwater consumption could be maintained in the presence of reduced well yields, lower well yields can affect the ability of farmers to meet crop water demands during crucial stages of the growth process, reducing crop yields and profitability [Foster et al., 2014].

The economic literature on groundwater demand has widely focused on depth to water, which affects groundwater use through its impact on pumping costs [Gonzalez-Alvarez et al., 2006, Hendricks and Peterson, 2012, Moore et al., 1994]. However, much less is known about the relationship between irrigation decisions and well yield, which recent research has suggested may be an arguably more important determinant of irrigation decisions, as it places an upper bound on the maximum rate at which water can be pumped out of a well over a sustained period of time [Foster et al., 2014, Hrozencik et al., 2017, Foster et al., 2017]. This is also suggested by our main sample in Figure 2.1, which displays the strikingly different relationships well yield and depth to water have with water use. In our

main sample, depth to water accounts for less than 2% of the variation in total water use, whereas well yield accounts for 50%.

In this study, we provide the first causal estimate of the impact of well yields on irrigation behavior by utilizing a unique time-varying data set that allows us to exploit both cross-sectional and temporal variation in well yields. Our study area is the Colorado portion of the Republican River Basin, which is one of the most agriculturally productive regions in the state. The uniqueness of our data set is the result of a reporting requirement for high-capacity irrigation wells that require well pump tests to be conducted. We combine well yield data with groundwater use and crop data at the well-level, in addition to weather controls, water prices, and depth to water. Incorporating time and well fixed effects, we estimate a two-way fixed effects model analyzing the impact of well yield on total water use, water use per acre (intensive margin), and irrigated acreage (extensive margin). We find a well-yield water use elasticity of .21 for total water use and .20 for water use per acre. We find the elasticity of well yield with respect to irrigated acreage to be .05, suggesting that producers are responding to declining well yields along both the intensive and extensive margins.

This work contribute to three strands of literature. First, we expand the literature that analyzes the impact of well yield on agriculture by providing the first empirical, causal estimates. Through numerical simulations, recent studies have shown that well yields can affect irrigated area [Foster et al., 2015b, 2014, Rad et al., 2020], water use [Foster et al., 2015a, 2014, Rad et al., 2020], agricultural profits [Foster et al., 2015a, 2014, Rad et al., 2020, Hrozencik et al., 2017], the productivity of water [Hrozencik et al., 2017, Foster et al., 2017], and the ability of farmers to respond to droughts [Foster et al., 2015a, 2017].

Foster et al. [2015b] use data on static well yields from the Nebrasksa Department of Natural Resources, which they believed to be the only data set in the world on water use also containing well yields. They find in both their fitted relationships and numerical simulations that irrigated area declines substantially beyond some well yield threshold of around 5000 m3/day, which translates to about 920 gallons per minute.

Foster et al. [2014] find nonlinear relationships between farmer irrigation decisions and groundwater availability resulting from simulations of corn production in the Texas High Plains region, accounting for both weather variability and changes in well yield. Their simulations reveal that for low seasonal water supplies, higher well yields would have little impact on optimal irrigation decisions because farmers will still face a binding seasonal water supply. However, at moderate or high seasonal groundwater supplies, well yield matters more for irrigation behavior. In particular, they find that even if total seasonal groundwater supply is held constant, there are rapid reductions in irrigated area and intensity below a well yield of around 1000 gallons per minute. They note that optimal irrigated area is reduced with lower well yields so that farmers can maintain soil moisture targets and per-acre yields as well as lower fixed costs of production.

Other work has simulated how declining well yields affect crop yields and profits [Lamm et al., 2007, O'brien et al., 2001]. For example, O'brien et al. [2001] find a positive association between simulated crop yields and flow rates in western Kansas that follows a non-linear form. They find a concave relationship between crop yields and well yields for both center pivot systems and furrow surface systems.

However, empirical estimates of well yield impacts are widely absent since well yield data are significantly limited, especially time-varying measures. Furthermore, there is a lack of data on well yield at the crop-parcel level [Foster et al., 2015b]. Utilizing our time-varying data, we are able to causally estimate the effect of well yield on irrigation behavior along both the intensive and extensive margin, incorporating crop-parcel data at the well-level.

This work also contributes to the economic literature on groundwater demand. Groundwater demand elasticity studies have proxied for water prices using different measures, as explicit water prices often do not exist and the only costs farmers incur is typically the cost of extraction. Studies have utilized energy prices [Pfeiffer and Lin, 2014], total energy expenditures [Ogg and Gollehon, 1989], and estimated pumping costs using depth to water estimates [Gonzalez-Alvarez et al., 2006, Hendricks and Peterson, 2012] as the variable of interest for groundwater demand analysis. The consensus in the literature is

that groundwater demand for irrigation is price inelastic [Pfeiffer and Lin, 2014, Ogg and Gollehon, 1989, Hendricks and Peterson, 2012, Moore et al., 1994] and is on average 0.48 [Scheierling et al., 2006]. However, most of these studies do not control for well yield, which is correlated with pumping costs, resulting in biased price elasticity estimates of as much as 50% [Mieno et al., 2021]. In particular, failing to account for well yield likely biases estimates such that the responses to pumping costs are overstated. This suggests that higher pumping costs that arise from groundwater depletion will have a limited impact on groundwater use. We contribute to this literature by presenting specifications that include and exclude well yields, while controlling for depth to water, and find that the inclusion of well yield reduces the magnitude of the coefficient on depth to water similar to that of Mieno et al. [2021]. In doing so, we provide additional evidence that failing to control for well yield can lead to biased estimates of groundwater use price elasticities, a finding with important implications for the effectiveness of price-based conservation strategies.

Finally, our analysis extends prior work that estimates the costs of groundwater depletion by focusing on the impacts of well yields, a lesser explored mechanism through which groundwater depletion impacts agricultural producers. Recent literature has explored how groundwater depletion affects agriculture by estimating the effect of saturated thickness on the proportion of irrigated acreage [Mieno et al., 2024, Perez-Quesada et al., 2024]. Perez-Quesada et al. [2024] use predevelopment saturated thickness to instrument for saturated thickness, and find that declines in saturated thickness reduced irrigated acreage and irrigated rental rates in the High Plains aquifer. Though similar to Mieno et al. [2024], the magnitude of these effects varies across high and low levels of saturated thickness. Mieno et al. [2024] find that corn and soybean yields respond in a non-linear manner to declines in aquifer thickness under conditions of high water deficit. In particular, the reduction of yields is smaller when initial saturated thickness is greater and the reduction of yields is driven by a reduction of irrigated acreage. While these studies provide important insight on the economic and agricultural impacts of groundwater depletion, they do not differentiate between the channels through which these effects occur.

By controlling for depth to water, we are able to separately estimate the margin of cost associated with aquifer depletion that occurs through changes in well yields. Well yields vary cross-sectionally due to heterogeneity in local aquifer and well pump characteristics. Well yields vary temporally as a result of changes in groundwater levels. Moreover, well yields will experience greater reductions with groundwater level declines when the initial level of saturated thickness, is lower. This variation enables us to identify the marginal impact of well yields on irrigator decisions while controlling for well and year fixed effects. Using static well yield data would only enable us to estimate the marginal impact of a change in well yield due to current local aquifer conditions or well pump characteristics. Leveraging a unique time-varying data set of well yields allows us to isolate the marginal impact of a change in well yield due to groundwater depletion. In this sense, our estimated marginal impacts of well yield on irrigator decisions reflect an economic impact of aquifer depletion through one of two main mechanisms.

Our empirical results show that declining well yields have an economically and statistically significant negative impact on water use and irrigated acreage. We find evidence that producers are already responding to declining well yields along both the intensive and extensive margins. This study shows that groundwater depletion is affecting irrigated agriculture through a channel other than pumping costs. This raises additional concerns about the sustainability of groundwater-fed agriculture and the rural communities that it often supports. Our results also have implications for the effectiveness of groundwater conservation policies as well as the distributional costs of these policies, highlighting the importance of accounting for well yield in cost-benefit and groundwater demand analyses.

This paper proceeds with a description of our study area and a discussion of the hydrology of groundwater irrigation to describe how well yields are determined. We then present our empirical specification and address the endogeneity concerns related to the feedback between groundwater pumping and well yields. Next, we explain the samples used in the empirical analysis, data sources, and variables. Finally, we provide our results and discuss their implications and avenues for future research.

2.2 Background

2.2.1 Study Area

In this study, we focus on the Colorado portion of the Republican River Basin (RRB). The RRB itself spans 15.9 million acres across eastern Colorado, northern Kansas, and southwestern Nebraska as shown in Figure 2.3 [McGuire, 2017a]. The majority of this land (87%) overlies the High Plains aquifer (HPA), which is the largest aquifer in the U.S. and supplies 30% of national groundwater used for irrigation [McGuire, 2017a, Maupin and Barber, 2005].

Areas across the HPA began experiencing water level declines as early as the 1950s following the expansion of irrigation, which is the primary source of groundwater discharge in the region [McGuire, 2017a]. The introduction of the center pivot irrigation system in the 1960s further contributed to the expansion of irrigated acreage that occurred in the latter half of the century [Robson and Banta, 1995]. Portions of the RRB had begun experiencing water level declines by the mid 1960s and by 2002, water levels in some areas had declined by more than 50 ft. [McGuire, 2017a].

The Colorado portion of the RRB spans all or parts of seven counties: Sedgwick, Phillips, Logan, Washington, Yuma, Kit Carson, and Lincoln. The economy is largely agriculturally-based, with corn and alfalfa comprising the main irrigated crops [Thorvaldson et al., 2005]. As a result, reductions in irrigated acreage are likely to be more impactful than in other areas where the economic base is more comprised of non-agricultural activity [Thorvaldson et al., 2006]. As of 2012, there were 477,530 irrigated acres in the Colorado portion of the basin, of which over 99.9% overlaid the HPA. Much of the irrigated area is in Phillips, Yuma, and Kit Carson county which is where about 88% of the wells in our analysis are located [McGuire, 2017a].

Irrigation in the Colorado RRB overwhelmingly relies on groundwater. Of the over 45,000 annual crop parcels in the irrigation data, only 16 of those were irrigated with surface water. As with other parts of RRB and HPA, some areas of the Colorado RRB have

experienced water level declines of 10-20 ft. from 1980-1995, 5 to 15 ft. from 1995-2000, 15 to 25 ft. from 2000 to 2005, and 15 to 25 ft. from 2005 to 2009. In 2009, saturated thickness was estimated to range from less than 50 ft. to upwards of 200 ft. [McGuire et al., 2012c]. Well yields used in our analysis, as well as in the Colorado RRB more broadly, vary greatly, from less than 100 gallons per minute to well over 1900 gallons per minute [Hrozencik et al., 2017].

2.2.2 Hydrology of Groundwater Irrigation

Demand for agricultural groundwater is influenced by pumping costs, weather conditions, crop choice and price, soil attributes, and well yield [Gonzalez-Alvarez et al., 2006, Kreins et al., 2015, Pfeiffer and Lin, 2014, Mieno et al., 2021]. In this section, we discuss the hydrogeological parameters that influence irrigator decision-making: well yield, which constrains daily irrigation rates and depth to water, which increases marginal extraction costs.

Figure 2.2 displays a simple graphical representation of a well. Well yield is typically measured in gallons per minute and is affected by well and local aquifer characteristics [Bentall, 1964, Kristine Uhlman and Artiola, 2011]. Water is pumped through the well screen located at the base of the well, causing the water level in the vicinity of the well to fall, which is referred to as drawdown. This creates a cone of depression around the well, which can last for months after pumping as water levels are restored [Buddemeier, 2000].

Well yield is impacted by hydraulic conductivity and storativity. Hydraulic conductivity measures how quickly groundwater can flow through the aquifer. Hydraulic conductivity depends on the viscosity of the fluid, the type of sediment and its distribution, and is therefore constant over time absent land subsidence [Davie and Quinn, 2019]. Storativity refers to how much water can be released from the aquifer to take the place of water being pumped out the well. It is equal to the product of specific storage and saturated thickness. Specific storage is the amount of water held within some unit volume of porous material [Fetter, 2018]. Saturated thickness is the vertical height of the aquifer.

Well yields are increasing with saturated thickness, hydraulic conductivity, and specific storage. Importantly, saturated thickness, hydraulic conductivity, and specific storage can vary significantly throughout an aquifer, resulting in different potential well yields at various locations throughout the aquifer [Buchanan et al., 2001]. Well yields also vary over time as water levels change, which occurs when there is an imbalance between withdrawals and recharge. When groundwater is pumped from the aquifer at rates that exceed natural recharge, water levels decline, causing a decrease in saturated thickness which reduces well yields. However, the extent of the reduction in well yield will largely depend on the pre-development level of saturated thickness at the well, as minimum initial levels of saturated thickness are required to enable and maintain pumping [Hecox et al., 2002]. Even in instances where there is an adequate volume of groundwater in storage to irrigate land, sustained pumping cannot occur if the saturated thickness at the location of the well is such that the water level falls below the pump intake [Buddemeier, 2000]. It has been suggested that around 30 ft. of saturated thickness is needed for irrigation pumping, though this will vary locally [Buddemeier, 2000].

Finally, declines in saturated thickness also increase the depth to water, and subsequently the marginal cost of extraction as more energy is required to lift water to the surface. Therefore, changes in well yield and depth to water for a given well are correlated over time as both are impacted by changes in current saturated thickness.

2.3 Empirical Model

In this section we introduce the econometric models used to estimate the impact of well yield on irrigation decisions. We then describe the endogeneity concern arising from the reverse causality between well yield and irrigation decisions, and discuss how it impacts our interpretation of well yield coefficients.

For each outcome variable, we specify both a linear functional form and a constant elasticity functional form. The preferred specification for estimating the linear impact of

well yield (gal./min.) on irrigation decisions for well i in year t is given by:

$$y_{i,t} = \alpha + \beta\omega_{i,t} + \gamma Z_{i,t} + \upsilon_i + \tau_t + \mu_t + \epsilon_{i,t}, \tag{2.1}$$

and our preferred specification for estimating the constant elasticity of well yield with respect to irrigation decisions is

$$log(y_{i,t}) = \alpha + \beta log(\omega_{i,t}) + \gamma Z_{i,t} + \upsilon_i + \tau_t + \mu_t + \epsilon_{i,t}, \tag{2.2}$$

Our three outcome variables are total annual groundwater use (acre-ft.), irrigated acreage, and water use per acre (ft.). We control for key factors impacting irrigation decisions with a vector of covariates, $Z_{i,t}$, well-level fixed effects, υ_i, year fixed effects, τ_t, and test-month fixed effects, μ_t. Well-level fixed effects control for time-invariant well-level factors that influence irrigation decisions, including soil type, managerial ability, well construction and pump characteristics, and local aquifer characteristics. Year fixed effects control for time-varying factors common to all observations that impact irrigation decisions and may be correlated with well yield, such as input and output prices. The test-month fixed effect corresponds to the month the well test was conducted and is included to account for variation in well yields that are due to the timing of the test relative to the growing season, as local water levels can take months to recover after groundwater pumping [Buddemeier, 2000]. The covariates included in $Z_{i,t}$ depend on the sample and outcome variable. To control for the influence of water price, depth to water is included as a covariate in the full sample, whereas marginal cost is used in the restricted sample. In all models, the type of crop is controlled for as water demand varies across crops. When modelling total groundwater use, we also control for temperature, precipitation, and irrigated acreage. In our model of water use per acre we omit irrigated acreage as a control variable, since our outcome variable equals total water use divided by irrigated acreage. When modelling irrigated acreage, we omit temperature and precipitation controls since acreage decisions are made prior to the growing season before weather conditions have been realized. $\epsilon_{i,t}$ is an idiosyncratic error term. Standard

errors are clustered at the well-level in all models to allow for correlation in unobservables at the well-level over time.

Our coefficient of interest is β, which captures the effect of a one gallon per minute increase in well yield on water use and acreage decisions. Within-well changes in yield are a direct result of changes in saturated thickness. Therefore, under the inclusion of a well-level fixed effect, decreases in well yield are due to groundwater depletion. Thus, a two-way fixed effects model allows us to estimate the impact of groundwater depletion on irrigation decisions through the channel of well yield. The identifying assumption is that well yield is as good as randomly assigned, conditional on covariates and fixed effects. This is plausible as our well-level fixed effects capture local time-invariant aquifer and pump characteristics that affect well yield as well as managerial traits that may lead some producers to use more or less water when other factors are fixed. Interpreting the well yield coefficients as causal requires that the treatment effect be additive and constant [Angrist and Pischke, 2009]. However, the treatment effect will likely vary across initial levels of well yield. Previous research has indicated 'switching points', beyond which declines in well yield significantly impact water use or acreage [e.g., Rad et al., 2020]. Even if the treatment effect is not constant, the average treatment effect can still be identified using fixed effects estimation as long as the coefficient on well yield is independent of idosyncratic deviations in yield [Wooldridge, 2005]. This is a reasonable condition for our analysis because the extent to which decreases in groundwater levels affect well yields depends primarily on the well's initial level of saturated thickness. Importantly, this condition still allows the well-level treatment effect to be correlated with time-invariant well characteristics that lead to higher or lower yield on average, including predevelopment and initial saturated thickness.

2.3.1 Identification Concern: Reverse Causality

A key challenge to identification is the potential endogeneity that arises due to the feedback between groundwater extraction and groundwater depletion. Higher well yields are expected to increase water use, however, more water use reduces saturated thickness, and

subsequently well yields. In this case, our estimated coefficient could be downwardly biased, understating the true effect of well yield on water use. Therefore, we interpret the coefficient on well yield as a lower bound of the causal effect. Yet, even with this potential negative bias, our empirical models still identify statistically and economically significant effects of well yield on water use. In the remainder of this section, we discuss three factors that may mitigate the extent of this bias: the exogeneity of predevelopment saturated thickness, the limited feedback effect of private water use, and the myopic behavior of producers.

First, for a given well, the extent to which groundwater depletion reduces well yield depends primarily on the initial level of saturated thickness, which is highly correlated with the exogenous predevelopment saturated thickness[1]. Predevelopment saturated thickness refers to the saturated thickness that existed prior to major impacts from human development. This correlation is shown in the right panel of Figure 2.4. This figure plots the observed relationship between predevelopment saturated thickness and 2015 saturated thickness for wells in our main sample, using data publicly available on HydroShare from [Haacker et al., 2023]. The R-squared from regressing 2015 saturated thickness on predevelopment saturated thickness is 0.91.

To sustain a particular pumping rate, or well yield, the drawdown must not be such that the water level falls below the well intake screen causing the well to run dry. For a given pumping rate and duration, drawdown depends on the radius of the well and the local aquifer characteristics of saturated thickness, hydraulic conductivity, and specific yield. Hydraulic conductivity and specific storage are constant over time [Davie and Quinn, 2019]. For an unconfined aquifer, as is most of the High Plains aquifer, groundwater pumping reduces saturated thickness, causing a concern about reverse causality in our empirical model. The estimated drawdown equation is then corrected to account for reduced saturated thickness at the well due to groundwater pumping. Specifically, the corrected drawdown is a function of the uncorrected drawdown and the initial level of saturated thickness Brookfield [2016]. The corrected drawdown is decreasing with initial saturated thickness, showing

[1]For more detail on the exogeneity of predevelopment saturated thickness refer to Perez-Quesada et al. [2024].

that changes in drawdown due to local groundwater pumping are largely dependent on initial saturated thickness, which is highly correlated with the exogenous predevelopment saturated thickness. Figure 2.4 highlights the positive correlation between average well yield and predevelopment saturated thickness.

Another factor that may reduce the bias introduced by reverse causality is the extent of the feedback effect at the well-level. According to Hornbeck and Keskin [2014], despite the variation in the speed of groundwater flows throughout the High Plains aquifer, nowhere would farmers internalize a notable portion of their private water consumption, suggesting that any endogeneity concerns introduced between the feedback of private water use and well yields at the individual level would be minimal (although water withdrawals at a broader scale will be impactful to water levels).

Finally, prior literature has shown that farmers do not dynamically optimize their water use decisions [Guilfoos et al., 2013], so we can reasonably expect that farmers are not adjusting their current groundwater consumption to affect their future well yield.

2.4 Data

We use two main samples of well-level observations to estimate the impact of well yield on irrigation decisions. All samples include well yield, annual groundwater use, acreage, crop, temperature, and precipitation variables for the period spanning 2015 through 2021. Our main sample includes a depth to water variable to proxy for groundwater pumping costs, whereas our restricted sample includes a marginal water price variable.

The groundwater use data we utilize only allow us to observe annual water use at the well-level. This presents a challenge as many parcels are irrigated with more than one well and we cannot observe the proportion of irrigation associated with each well. Additionally, one well often irrigates multiple parcels and we cannot observe how annual water use at the well-level is allocated across parcels. Therefore, we restrict our sample to include parcels that are irrigated by only one well and that well must not irrigate more than one parcel in

a given year. This assists us in accurately estimating the impact of well yield on water use and irrigated acreage. A detailed description on the construction of the data set is provided in Appendix K.

The main sample used in our analysis is an unbalanced panel of 7,081 observations containing 1,632 individual irrigation wells. Of these wells, about 47% experienced declines in well yield over time (n=768), 33% experienced increases in yield (n=545), and 20% did not experience any change in yield (n=319). The largest increase in well yield was 803 gallons per minute and the greatest decline was 398.6 gallons per minute. However, the differences in yield over time for a given well may be impacted by the timing of the well pump test, which we control for in our empirical models. An individual well appears in the sample between one and seven times, and 4.34 times on average. The irrigation wells span the seven counties within the Colorado RRB with the majority of wells located in the easternmost counties of Yuma, Kit Carson, and Phillips as shown in Figure 2.5.

Annual groundwater data are publicly available through the state of Colorado from Colorado's Decision Support System. These data contain measures of well yield, the test pump date, and annual groundwater use at the well-level. Effective 2009, all active high-capacity irrigating wells in our study area must be equipped with a totalizing flow meter or an alternative measuring method deemed acceptable, namely the power conversion coefficient method, to conduct well pump tests.[2] Well pump tests are typically required on a biennial or triennial basis, depending on the type of test conducted.[3] Based on this, we extrapolate well yields up to three years beyond their test date. Figure 2.6 illustrates the range of well yields in our main sample by displaying the distribution of yields for all observations.

As shown in Figure 2.6 and Table 2.1, well yields range from less than 10 gallons per minute to almost 3,000 gallons per minute, with a mean of 750. A well yield of 250 gallons per minute could generally irrigate around 40 acres [Robson and Banta, 1995].

[2]See Colorado Department of Natural Resources; 2CCR 402-16.

[3]Power conversion coefficient tests conducted between October 16 and June 14 must be redone between the following June 15 and August 14 (CDNR; 2CCR 402-16).

Figure 2.7 displays the temporal variation in well yields for the growing and non-growing seasons, to highlight some of the within-well variation in yields on which our estimation relies. We illustrate this with two samples, based on whether well pump tests were conducted during the growing or non-growing season. The growing season spans June, July, and August and the non-growing season is from September through May. We create the growing season (non-growing season) sample by restricting it to observations with well pump tests conducted during the growing season (non-growing season). Then, for each unique well in the sample, we subtract the most recent well yield from the first well yield. The figure shows that many wells experienced changes in yield over time even when tests were conducted only during the growing or non-growing season. 35% (25.5%) of wells with tests conducted during the growing (non-growing) season experienced temporal declines in yield. Well yield increases are also present and reflect the heterogeneity in aquifer conditions throughout the region. Still, many wells experienced no notable changes in yields for both the growing season and non-growing season samples. This stability could occur if well yields were constant over time for certain wells or if a well only appeared once in the sample.

Well yield and annual groundwater use data are merged together based on a unique well-identifier. Annual water use from November 1 through October 31 is reported in acre-feet with a mean of 200. Dividing annual water use by acreage produces our intensive margin measure of water use per acre, measured in feet. On average, a parcel irrigates 1.5 ft. per acre, but this varies significantly from less than one inch to over seven feet.

Temperature and precipitation data are obtained from PRISM Climate Group and are restricted to the growing season months of June, July, and August as they will affect crop water demands. The precipitation variables measures cumulative precipitation in inches throughout the growing season and averages just 7.9 inches, emphasizing the region's reliance on irrigation. Our temperature variable represents the average daily growing season temperature, which ranges from 70 to 76 degrees fahrenheit.

Crop data are also acquired from Colorado's Decision Support Systems and contain information on irrigated parcels and their associated wells, acreage, and crop type. Each

parcel contains only one crop type. The average parcel size is 137 acres which falls within the range of a typical center pivot's coverage. In Colorado, the average size for a center pivot is 123 acres [Bauder, 2004]. The overwhelming majority of parcels in our sample utilize sprinkler systems (99.48%), which in the Colorado High Plains region are predominantly center pivots [Barta et al., 2004]. 50% of parcels are between 124 and 135 acres, suggesting that most producers utilize the full range of a center pivot for a given crop. The primary crop in the region is corn, accounting for 81% of the sample, followed by alfalfa making up 6.5%, both of which are water intensive crops [Schneekloth and Andales, 2017]. Other crops include dry beans, potatoes, snap beans, small grains, sorghum, sunflower, vegetables (unspecified), and fall and spring wheat.

We estimate depth to groundwater for each well-year observation using the interpolation methods documented in Appendix L. Depth to water ranges from 14 to 326 ft., with a mean of 173. The average change in depth to water for a given well over time is a reduction of 1.07 ft[4]. Depth to water increased for 616 wells (38%) and decreased for 866 wells (53%). However, many wells did not experience any notable changes in depth to water, as displayed in Figure 2.8 which plots the distribution of depth to water changes. Depth to water measures the depth to the water table and reflects the variation in energy requirements for pumping a unit-volume of water for a given well, holding the pump efficiency and irrigation system constant. However, this does not control for differences in marginal energy prices across users, which depend on well pump horsepower and kilowatt hours of demand [Hrozencik et al., 2022]. Well pump horsepower will be captured with the well fixed effect assuming pumps are not replaced during the study period.

Since a decreasing block rate price structure is utilized across the study area, the depth to water variable will not fully capture variation in water prices. Even if depth to water is equal for two wells, marginal electricity prices may not be. The two primary electricity providers to irrigators in the region set marginal price thresholds based on kilowatt hours demanded and well pump horsepower [Hrozencik et al., 2022]. To fully control for

[4]This is calculated by subtracting the first depth to water measure from the most recent depth to water measure for a given well.

water price, we use marginal water price data from Hrozencik et al. [2022] which also include average price data. Marginal water price is measured in dollars per acre inch of water use. Average water price is measured in dollars per kilowatt hour (kWh). These data are only available for the portion of our wells using power conversion coefficient tests, which measure the electricity required to pump one unit of groundwater. This restricted sample contains 1,668 observations.

2.5 Empirical Results

Here we present our estimates from the econometric model described in Section 2.4, obtained by regressing our outcomes of interest on well yield. We begin by modelling total groundwater use as a function of well yield and proceed by examining the mechanisms that could be driving that effect: irrigated acreage and water use per acre, to learn if producers are responding to well yield changes along the extensive or intensive margin. We present results from our main sample as well as our restricted sample. The restricted sample includes marginal electricity prices which reduces potential bias that may be present when price variation is not completely controlled for. However, only a subset of our main sample has data on marginal electricity prices, so this sample size is significantly reduced. Additionally, there is the concern of reverse causality as producers may alter water use to try to reach a price threshold and incur lower marginal water prices. Finally, we provide results using binned samples of well yields to explore potential nonlinearities of the impacts of well yield.

2.5.1 Total Water Use

First, we present our estimates of the model analyzing total water use before decomposing this effect into extensive (irrigated acreage) and intensive (water application per acre) margin adjustments. Table 2.3 presents the results from our estimating equations in Section 2.3 for the main sample. The specification in column (1) highlights the majority

of groundwater demand studies, which do not control for well yield. The coefficient on depth to water is expected to be negative, as an increase in pumping costs from increased depth to water would be expected to reduce total water use. The depth to water coefficient is negative in the first two specifications. However, the inclusion of the well yield variable in column (2) reduces the magnitude of the depth to water coefficient by nearly 70%. Mieno et al. [2021] find up to a 50% reduction in price elasticities when well yield is omitted. However, neither of these specifications incorporate the well-level fixed effect. Still, they provide insight into the importance of accounting for well yield in groundwater demand estimation. In column (2), the well yield variable is capturing temporal and cross-sectional variation in well yield. The well yield coefficient is about .14 in column (2) but falls to .087 in column (3) with the inclusion of well-level fixed effects, which are capturing time-invariant cross-sectional variation in well yields. In column (3), the well yield variable is capturing within-well changes in yield, which are due to changes in groundwater levels. Importantly, the well-level fixed effects are also accounting for other factors that may influence total water use, such as soil type and managerial factors. Column (3) shows that a decrease in well yield of one gallon per minute reduces total water use by .0877 acre-ft. per year and this is statistically significant at the 1% level. In more meaningful terms, a 100 gallon per minute decrease in well yield reduces total water use by 8.77 acre-ft which represents 4.4% of average water use. Interestingly, the depth to water coefficient becomes positive with the inclusion of the well-level fixed effect, potentially picking up the effect of some time-varying, well-level unobservable, such as marginal electricity prices. Therefore, we compare our results to the specifications using the restricted sample where we are able to explicitly control for marginal electricity prices at the well-level.

The estimates from the restricted sample are shown in Table 2.4. The coefficients on well yield for the preferred specifications (column (3)) in both the main and restricted sample models are similar: 0.087 in the main sample and 0.098 in the restricted sample. Columns (4) present the constant elasticity functional form with only well yield coefficient in the main sample being statistically significant (at the 10% level). In the main sample,

a one percent decrease in well yield leads to a 0.2 percent decrease in total water use. In the restricted sample, the decrease in water use becomes .12 percent, albeit not statistically significant.

Figure 2.8 shows results from seven samples where each sample is restricted to a range of well yields, as shown in Table 2.2. The specification for all seven samples is that of column (3) from Table 2.3. Precision is reduced, especially for the lowest bin of well yields (0-200 gallons per minute) which contain only 182 observations. Prior work that has modelled water use as a function of well yield has found that water use remains stable until some well yield threshold is reached, below which water use declines [e.g., Rad et al., 2020, Foster et al., 2015b]. However, the point estimates for well yield are largest for well yields between 0 and 200 gallons per minute, and 1000-1200 gallons per minute. The point estimates are closer to zero in the mid-range of well yields, and increase at the upper and lower ends.

2.5.2 Irrigated Acreage

When irrigated acreage is the dependent variable, we are capturing producer adjustments to varying well yields along the extensive margin, which can easily be made by the producer by changing the arc of coverage on their center pivot system.

The results of the analysis using the main sample are reported in Table 2.5. We exclude weather controls, as acreage decisions are decided prior to the growing season. Without the inclusion of well fixed effects in column (2), our model explains 56% of the seasonal variation in irrigated acreage. Once we include well fixed effects, our model explains almost all (98%) of the variation in irrigated acreage and significantly reduces the magnitude of the well yield coefficient. Focusing on column (3) which includes well-level fixed effects, a decline in well yield leads to a reduction of irrigated acreage, showing that producers are adjusting to decreasing well yield along the extensive margin. A 100 gallon per minute decrease in well yield decreases irrigated area for a given crop by 1.32 acres, which represents about 1% of acreage for the average parcel. This is statistically significant at the 1% level.

The magnitude of this effect is slightly smaller for the restricted sample, shown in Table 2.6. The preferred specification for the restricted sample shows that a 100 gallon per minute decline in well yield reduces irrigated area by 0.8 acres. This coefficient is statistically significant at the 5% level. In the restricted model, we control for average price rather than marginal price. Due to the decreasing block rate structure of electricity prices, marginal water prices will depend on water use. The acreage decisions are made prior to the growing season when producers do not know how much water they will use and therefore do not know what the water price will be at the margin.

Figure 2.9 shows the results from the binned samples following the specification from column (3) in Table 2.5. Rad et al. [2020] find a reduction in profit-maximizing irrigated acreage below well yields of around 500 gallons per minute for irrigated corn production in southwest Nebraska. Our point estimates show a relatively small effect on irrigated acreage beginning in the 400-600 gallon per minute range, consistent with Rad et al. [2020]. However, the coefficient is notably larger for yields between 0 and 200 gallons per minute, suggesting that declines in well yields that occur at already low levels of yield will have the largest reduction on irrigated acreage. The point estimates are near zero for well yields above 600 gallons per minute, perhaps because producers are responding to reduced well yields along the intensive margin at these ranges. This plot suggests that reductions in irrigated acreage in our study area may begin when well yields decline below 600 gallons per minute and become larger in magnitude at very low well yields.

2.5.3 Water Use Per Acre

Having evidence that at least some of the reduction in water use is due to an extensive margin adjustment, we now turn our attention to analyzing the impact of well yield on water use per acre (intensive margin). In Table 2.7 we present results from the main sample. The dependent variable in columns (1) through (3) is water use per acre which equals total annual water use divided by irrigated acreage. Temperature and precipitation coefficients have the expected signs. Again, including well yield reduces the magnitude on

the depth to water coefficient as we move from column (1) to column (2). Column (3) shows that a 100 gallon per minute decline in well yield reduces water use by 0.05 ft, or about .6 inches. This represents about 3.3% of average water use per acre. This estimate is statistically significant at the 1% level and is similar in magnitude to the coefficient from the restricted sample, shown in Table 2.8. Column (4) in Table 2.7 shows that a one percent decrease in well yield reduces water use per acre by .16%, significant at the 10% level.

Figure 2.10 shows a similar pattern to the effects of well yield on total water use. Point estimates appear to increase over the 600 to 1200 gallon per minute range of well yields. Effects on acreage were near zero over this same range of well yields in Figure 2.9, further suggesting that producers adjust along the intensive margin to declines from higher initial well yields and adjust along the extensive margin to declines at lower well yields, less than 600 gallons per minute. This finding would be consistent with other studies which have found intensive margin adjustments to occur at higher well yields and extensive margin adjustments to be increasingly optimal as well yields decline below some threshold [e.g., Foster et al., 2014, Rad et al., 2020, Baumhardt et al., 2009].

2.6 Conclusion

This paper empirically estimates the causal effect of well yields on irrigation behavior, first focusing on total water use and then decomposing that effect into extensive and intensive margin adjustments. We are able to do this by leveraging a unique data set that provides time-varying well yields which we merge with well-level groundwater and irrigation data. This data enables us to estimate a two-way fixed effects model including a well-level fixed effect which captures time-invariant well-level unobservables. Within-well variation in yield is the result of changes in groundwater levels, and so we can interpret our causal impact of well yield on irrigation behavior as an economic impact of groundwater depletion.

Given the reverse causality between groundwater use and well yield, we interpret our estimates as a lower bound on the causal effect of well yields on irrigation behavior. Despite

this, we still find economically and statistically significant results. We find that a 100 gallon per minute decline in well yield reduces the average annual groundwater use by 4.4$, the average irrigated parcel size by about 1%, and the average of water use per acre by 3.3%. Our results are robust to a restricted sample that controls explicitly for marginal water prices in the study region. These results show that well yield is an important determinant of agricultural groundwater demand and that producers are responding to declining well yields along both the intensive and extensive margins, as predicted by prior numerical simulations. Our point estimates from binned samples suggest that intensive margin adjustments may occur at higher well yield ranges and extensive margin adjustments may occur at lower well yield ranges. This behavior would be consistent with the profit-maximizing behavior demonstrated by prior studies and would impact the effectiveness of various groundwater policies.

Our results have important implications for the sustainability of groundwater-fed agriculture and the implementation of policies to address aquifer depletion. The impacts of well yield estimated in this study suggest that future groundwater depletion could substantially reduce the proportion of irrigated land and total irrigated crop production in groundwater-dependent regions and convey the implicit value in preserving aquifer thickness. Our findings also provide insight regarding how the effectiveness of groundwater policies may vary with well yields. For example, the negative effect we find of decreasing well yields on total water use supports prior work suggesting that quantity restrictions of water use will likely be non-binding for low-yielding wells [Hrozencik et al., 2017].

While we provide the first causal evidence of the impact of well yield on irrigation behavior, including intensive and extensive margin adjustments, our study does not account for other avenues through which producers may respond to declining well yields. For example, we do not account for crop switching or transitions to dryland farming. We also assume that irrigation management practices remain constant over the study period, whereas in the future it is possible that producers in the region may begin implementing more efficient irrigation systems. Finally, future research should further explore the non-linearities, allowing

for more flexible functional forms and empirically estimating the 'switching point' of well yields that has been noted in prior literature.

Figure 2.1: Water Use Relationships

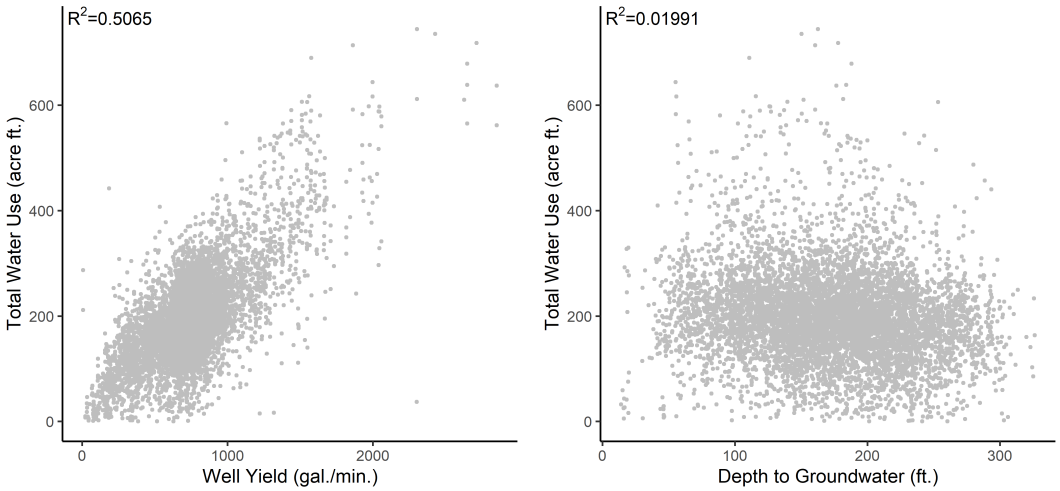

Notes: This figure displays the relationship between water use and well yield (left) and water use and depth to water (right). The R-squared values are obtained by regressing total water use on well yield (n=7124) or depth to water (n=7080) using data from the main sample.

Figure 2.2: Aquifer Description

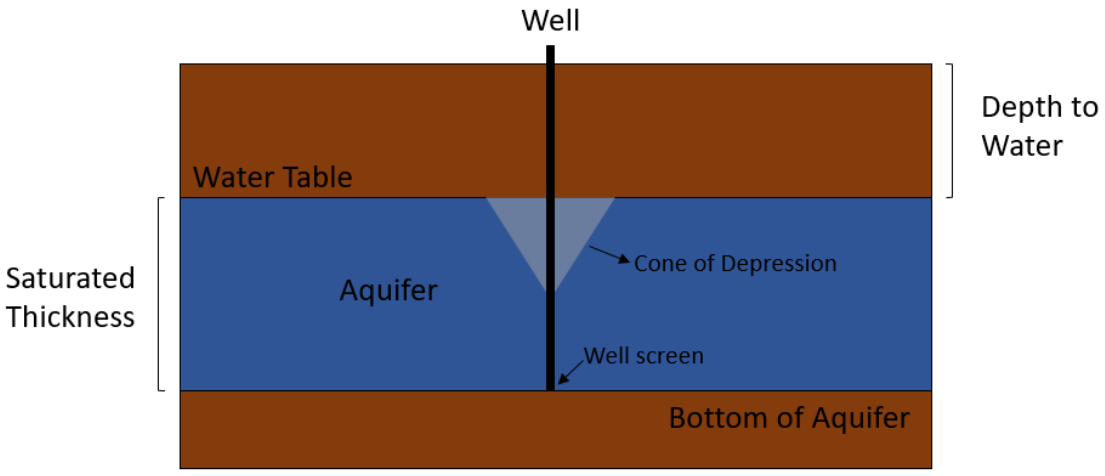

Figure 2.3: Republican River Basin

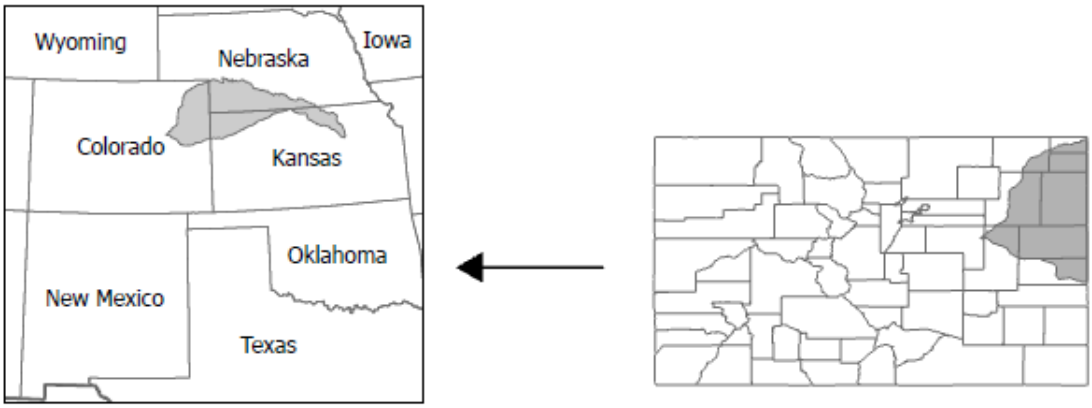

Figure 2.4: Predevelopment Saturated Thickness Relationships

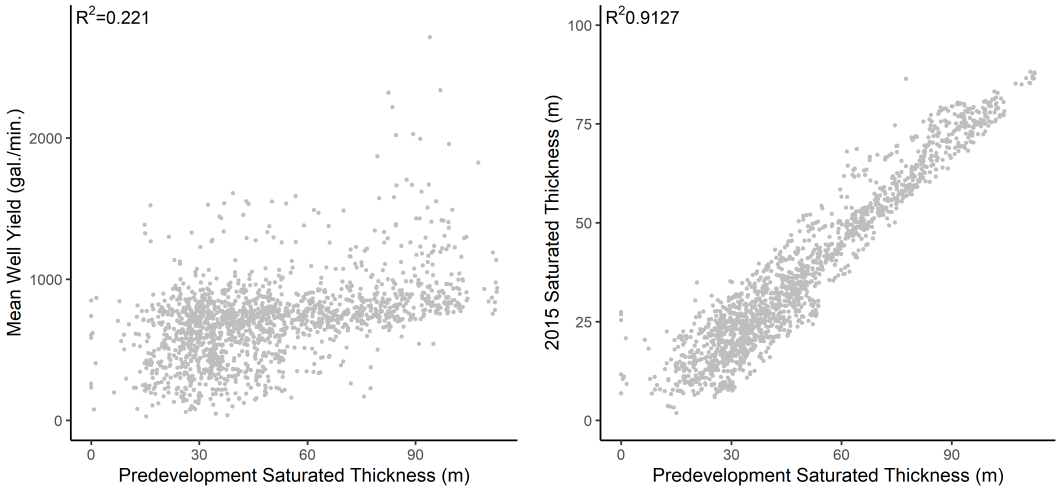

Notes: The left figure displays the relationship between the mean well yield for each unique well in our sample and its predevelopment saturated thickness. The right figure displays the relationshp between 2015 saturated thickness and predevelopment saturated thickness for unique wells in our sample. Saturated thickness data was obtained from Haacker et al. [2023]. Raster values were extracted to well locations using ArcGIS Pro 2.9. In this figure, predevelopment saturated thickness refers to the estimated saturated thickness in 1935.

Figure 2.5: Spatial Distribution of Irrigation Wells

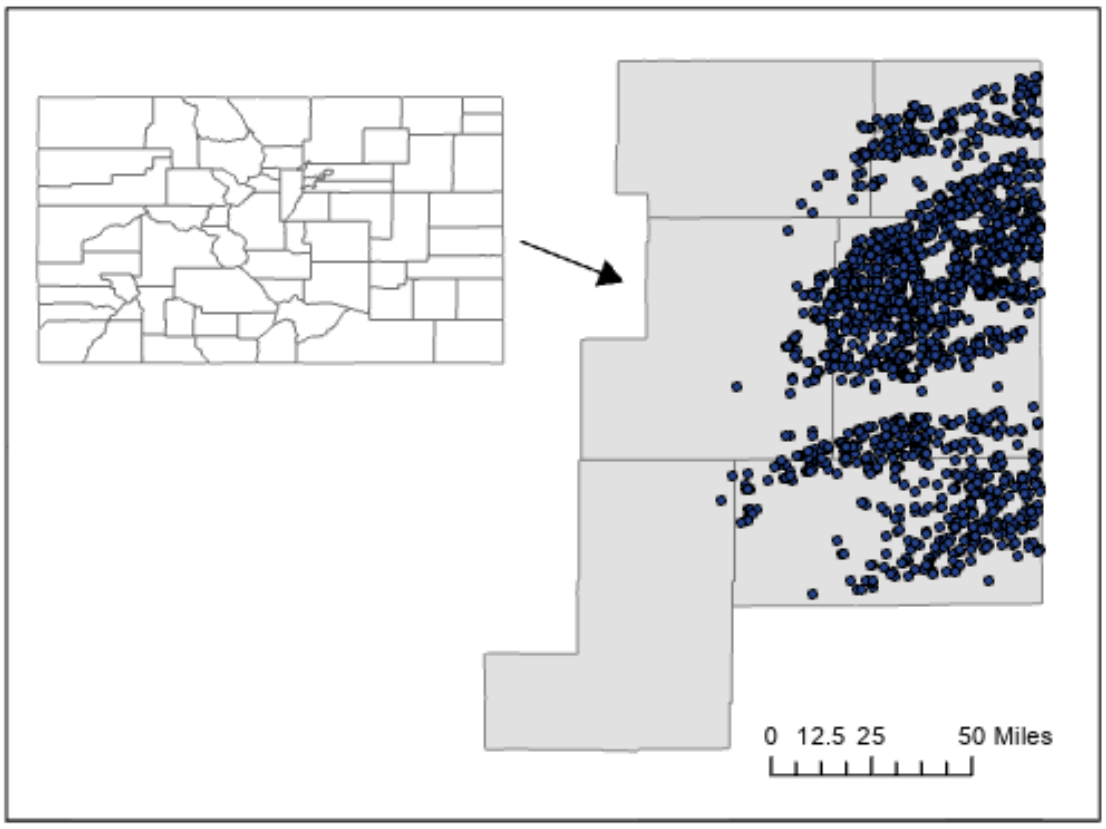

Figure 2.6: Distribution of Well Yields

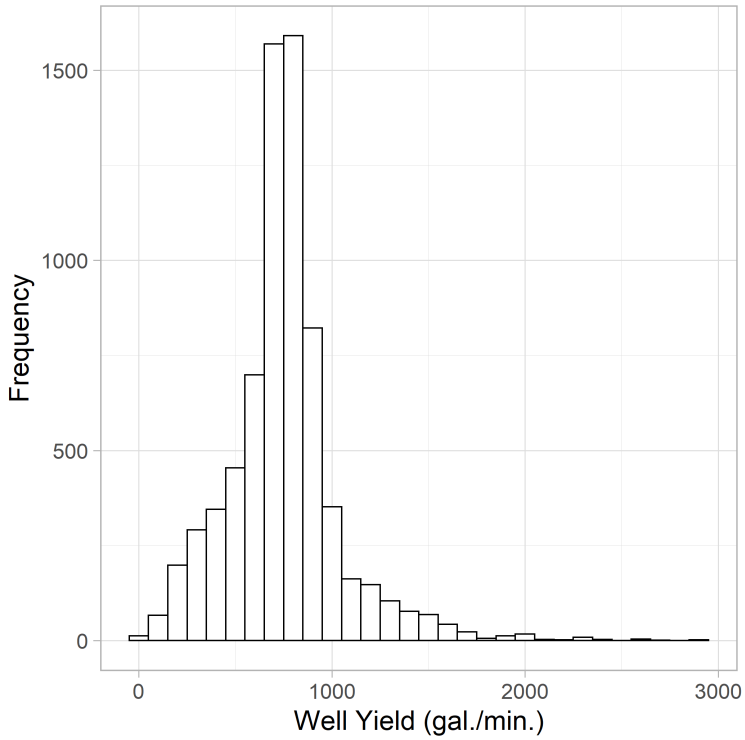

Notes: This figure displays the distribution of well yields (gal./min.) for the main sample (n=7,081).

Figure 2.7: Well Yield Changes By Season

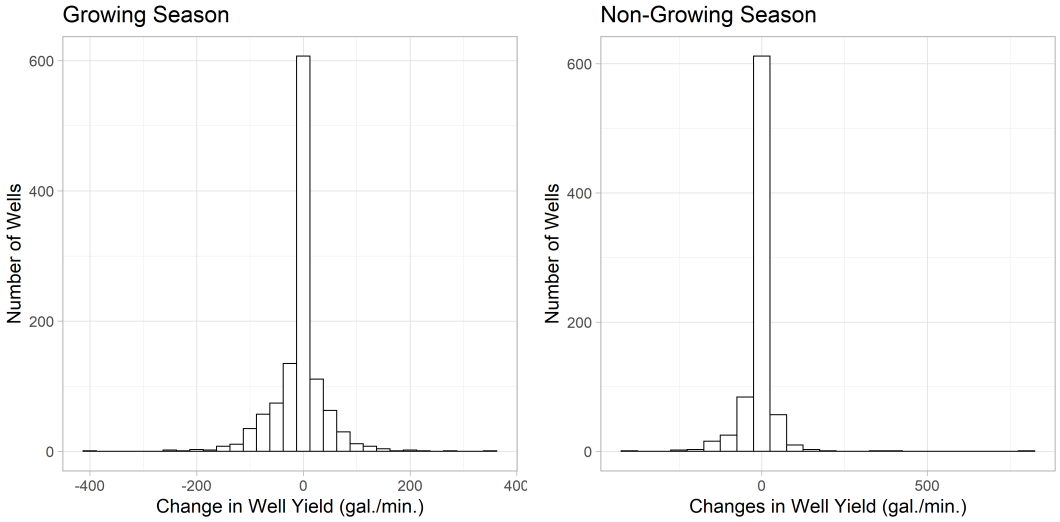

Notes: Well yield changes are calculated by first restricting the sample to observations where well tests were conducted during (left) or outside (right) the growing season. Then the first available well yield was subtracted from the most recent well yield to calculate changes in capacity. For tests conducted during the growing season, 35% (412/1170) of the wells experienced declines, 38% (442/1170) experienced no changes, and 27% (316/1170) experienced increases. For tests conducted outside of the growing season, 26% (210/817) of the wells experienced declines, 57% (465/817) experienced no changes, and 17% (142/817) experienced increases.

Figure 2.8: Impact of Binned Well Yields on Total Water Use

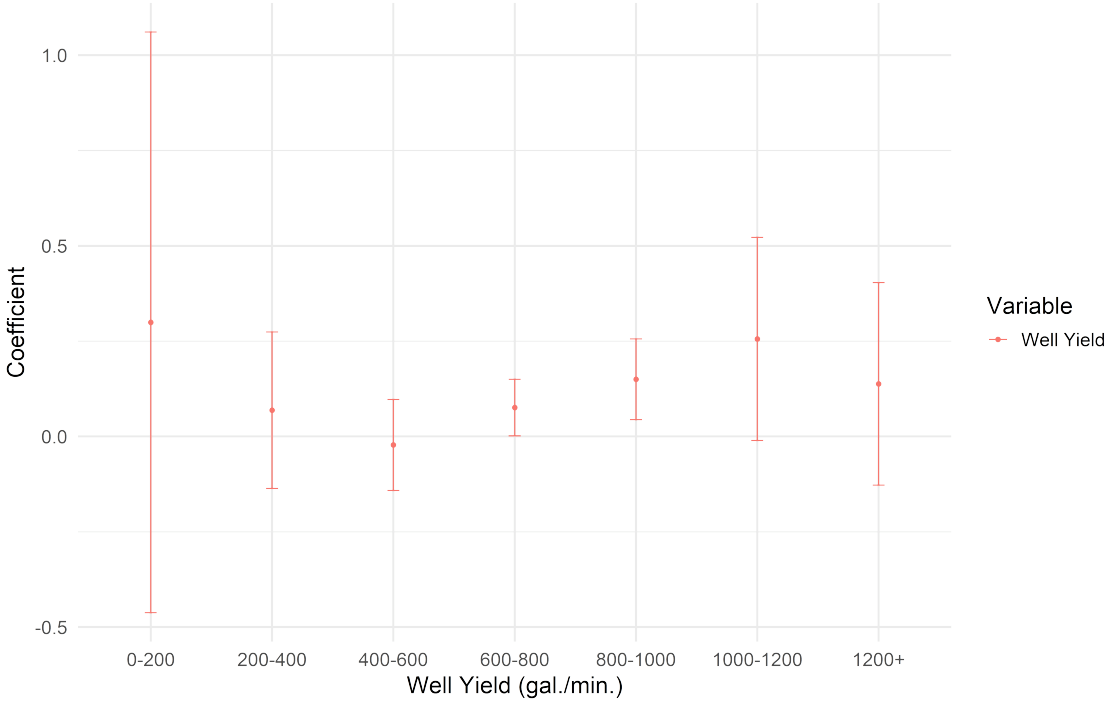

Notes: This plots models of restricted samples corresponding to values of well yields as labeled on the x-axis. Estimates correspond to the column (3) specification in Table 2.3 for each model.

Figure 2.9: Impact of Binned Well Yields on Irrigated Acreage

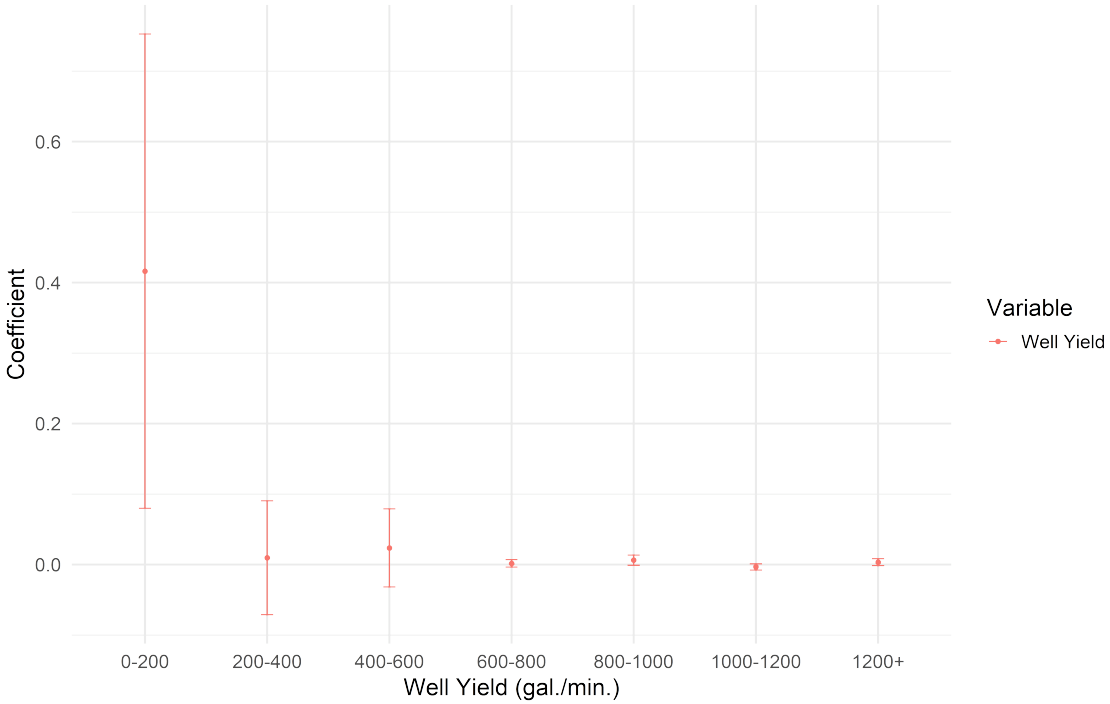

Notes: This plots models of restricted samples corresponding to values of well yields as labeled on the x-axis. Estimates correspond to the column (3) specification in Table 2.5 for each model.

Figure 2.10: Impact of Binned Well Yields on Water Use Per Acre

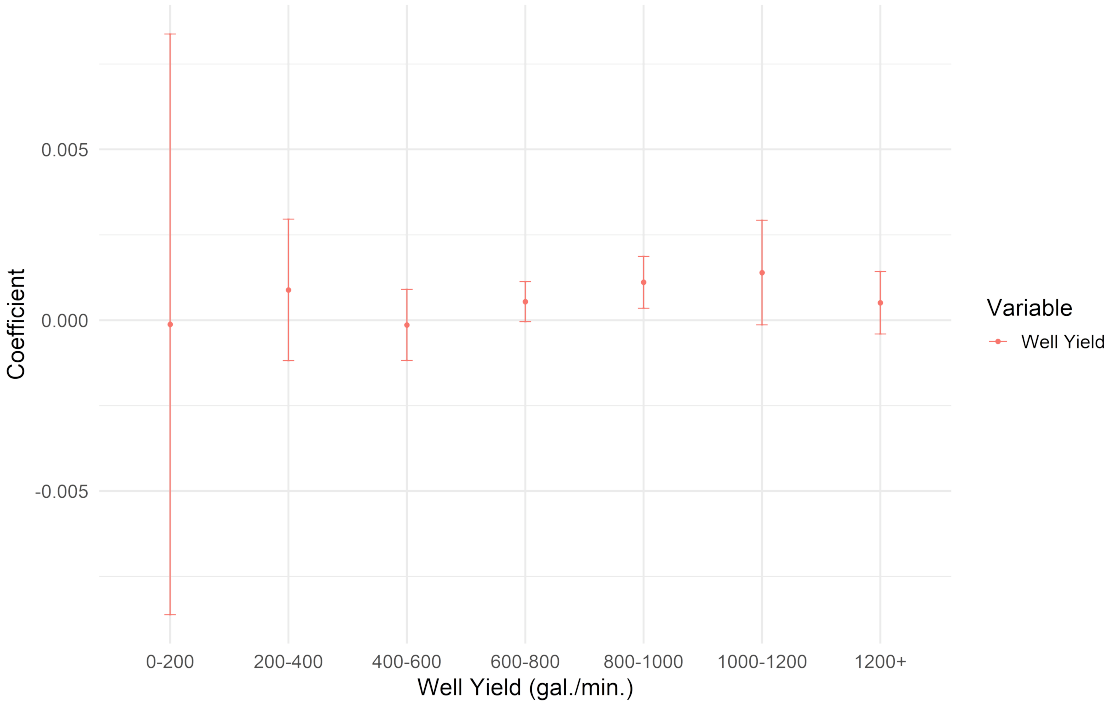

Notes: This plots models of restricted samples corresponding to values of well yields as labeled on the x-axis. Estimates correspond to the column (3) specification in Table 2.7 for each model.

Table 2.1: Summary Statistics (Main Sample)

Variable	N	Mean	Std. Dev.	Min	Pctl. 25	Pctl. 75	Max
Yield (gal./min.)	7081	750	291	7.8	619	856	2852
Water Use (acre/ft.)	7081	200	90	0.071	148	240	1054
Water Use Per Acre (ft.)	7081	1.5	0.51	0.00058	1.1	1.7	7.2
Acreage	7081	137	41	7	124	135	533
Temp (°F)	7081	73	1	70	72	73	76
Precip (inches)	7081	7.9	2.5	1.7	6	9.6	14
Depth to Water (ft.)	7081	173	56	14	134	213	326

Table 2.2: Number of Observations for Binned Samples

Well Yield Range (gal./min.)	Obs.
0-200	182
200-400	554
400-600	902
600-800	2879
800-1000	1771
100-1200	352
1200+	437

Notes: This table shows the sample size for the restricted samples based on well yield. These samples are used to estimate the coefficients displayed in Figure 2.8, Figure 2.9, and Figure 2.10.

Table 2.3: Impact of Well Yield on Total Water Use (Main Sample)

Dependent Variables:	Total Water Use			Log(Total Water Use)
Model:	(1)	(2)	(3)	(4)
Variables				
Yield (gal./min.)		0.1359***	0.0877***	
		(0.0063)	(0.0199)	
Log(Yield)				0.2018*
				(0.1137)
Depth to Water (ft.)	-0.1828***	-0.0585***	0.2755***	0.0013***
	(0.0230)	(0.0186)	(0.0524)	(0.0003)
Temp (°F)	3.540	7.695***	10.40***	0.0721***
	(2.465)	(1.911)	(2.068)	(0.0171)
Precip (inches)	-3.636***	-4.815***	-5.105***	-0.0272***
	(0.4083)	(0.3637)	(0.3411)	(0.0028)
Acreage	1.442***	0.7533***	0.2145*	0.0032**
	(0.0585)	(0.0671)	(0.1214)	(0.0012)
Fixed-effects				
Crop Type	Yes	Yes	Yes	Yes
Year	Yes	Yes	Yes	Yes
Test Month		Yes	Yes	Yes
Well			Yes	Yes
Fit statistics				
Observations	7,081	7,081	7,081	7,081
R^2	0.57087	0.65219	0.85010	0.76550
Within R^2	0.50772	0.59720	0.06100	0.03407

Notes: Well-level clustered standard errors in parentheses.
* p<0.10, ** p<0.05, *** p<0.010

Table 2.4: Impact of Well Yield on Total Water Use (Restricted Sample)

Dependent Variables:	Total Water Use			Log(Total Water Use)
Model:	(1)	(2)	(3)	(4)
Variables				
Yield (gal./min.)		0.0684***	0.0983**	
		(0.0106)	(0.0407)	
Log(Yield)				0.1273
				(0.1536)
MC ($/acre-inch)	-18.54***	-15.64***	-31.69***	-0.2776***
	(1.604)	(1.756)	(4.234)	(0.0354)
Temp (°F)	4.437	2.577	21.26***	0.1335***
	(4.018)	(4.038)	(3.711)	(0.0224)
Precip (inches)	-2.341***	-1.828**	-2.718***	-0.0112**
	(0.8193)	(0.8054)	(0.7894)	(0.0044)
Acreage	1.478***	1.103***	0.3073***	0.0024**
	(0.0626)	(0.0945)	(0.1132)	(0.0009)
Fixed-effects				
Crop Type	Yes	Yes	Yes	Yes
Year	Yes	Yes	Yes	Yes
Test Month		Yes	Yes	Yes
Well			Yes	Yes
Fit statistics				
Observations	1,668	1,668	1,668	1,668
R^2	0.66171	0.68061	0.89993	0.88101
Within R^2	0.62494	0.64188	0.16178	0.26386

Notes: Well-level clustered standard errors in parentheses.
* p<0.10, ** p<0.05, *** p<0.010

Table 2.5: Impact of Well Yield on Irrigated Acreage (Main Sample)

Dependent Variables:		Acreage		Log(Acreage)
Model:	(1)	(2)	(3)	(4)
Variables				
Yield (gal./min.)		0.1081***	0.0132***	
		(0.0076)	(0.0035)	
Log(Yield)				0.0504*
				(0.0296)
Depth to Water (ft.)	-0.0333*	0.0779***	0.0053	9.67×10^{-5}*
	(0.0184)	(0.0138)	(0.0057)	(5.61×10^{-5})
Fixed-effects				
Crop Type	Yes	Yes	Yes	Yes
Year	Yes	Yes	Yes	Yes
Test Month		Yes	Yes	Yes
Well			Yes	Yes
Fit statistics				
Observations	7,081	7,081	7,081	7,081
R^2	0.02023	0.56307	0.98009	0.94112
Within R^2	0.00209	0.55064	0.00635	0.00480

Notes: Well-level clustered standard errors in parentheses.
* p<0.10, ** p<0.05, *** p<0.010

Table 2.6: Impact of Well Yield on Irrigated Acreage (Restricted Sample)

Dependent Variables:		Acreage		Log(Acreage)
Model:	(1)	(2)	(3)	(4)
Variables				
Yield (gal./min.)		0.1119***	0.0080**	
		(0.0062)	(0.0040)	
Log(Yield)				0.0317
				(0.0295)
Average Price ($/kWh)	-385.8**	-661.8***	-53.07	-0.5903
	(150.5)	(99.48)	(37.65)	(0.4370)
Fixed-effects				
Crop Type	Yes	Yes	Yes	Yes
Year	Yes	Yes	Yes	Yes
Test Month		Yes	Yes	Yes
Well			Yes	Yes
Fit statistics				
Observations	1,668	1,668	1,668	1,668
R^2	0.01880	0.64879	0.98982	0.97566
Within R^2	0.00719	0.64103	0.00878	0.01016

Notes: Well-level clustered standard errors in parentheses.
* p<0.10, ** p<0.05, *** p<0.010

Table 2.7: Impact of Well Yield on Water Use Per Acre (Main Sample)

Dependent Variables:	Water Use Per Acre			Log(Water Use Per Acre)
Model:	(1)	(2)	(3)	(4)
Variables				
Yield (gal./min.)		0.0004***	0.0005***	
		(4.8×10^{-5})	(0.0001)	
Log(Yield)				0.1674*
				(0.0969)
Depth to Water (ft.)	-0.0013***	-0.0008***	0.0016***	0.0013***
	(0.0002)	(0.0002)	(0.0003)	(0.0003)
Temp (°F)	0.0207	0.0405**	0.0725***	0.0691***
	(0.0193)	(0.0171)	(0.0150)	(0.0172)
Precip (inches)	-0.0268***	-0.0325***	-0.0382***	-0.0278***
	(0.0030)	(0.0029)	(0.0025)	(0.0028)
Fixed-effects				
Crop Type	Yes	Yes	Yes	Yes
Year	Yes	Yes	Yes	Yes
Test Month		Yes	Yes	Yes
Well			Yes	Yes
Fit statistics				
Observations	7,081	7,081	7,081	7,081
R^2	0.20826	0.27457	0.73086	0.67721
Within R^2	0.03700	0.10885	0.05396	0.02807

Notes: Well-level clustered standard errors in parentheses.
* p<0.10, ** p<0.05, *** p<0.010

Table 2.8: Impact of Well Yield on Water Use Per Acre (Restricted Sample)

Dependent Variables:	Water Use Per Acre			Log(Water Use Per Acre)
Model:	(1)	(2)	(3)	(4)
Variables				
Yield (gal./min.)		0.0002***	0.0006*	
		(4.45×10^{-5})	(0.0003)	
Log(Yield)				0.1240
				(0.1501)
MC ($/acre-inch)	-0.1335***	-0.1252***	-0.2331***	-0.2677***
	(0.0112)	(0.0117)	(0.0309)	(0.0363)
Temp (°F)	0.0366	0.0268	0.1681***	0.1385***
	(0.0274)	(0.0279)	(0.0262)	(0.0224)
Precip (inches)	-0.0184***	-0.0168***	-0.0191***	-0.0102**
	(0.0056)	(0.0056)	(0.0053)	(0.0044)
Fixed-effects				
Crop Type	Yes	Yes	Yes	Yes
Year	Yes	Yes	Yes	Yes
Test Month		Yes	Yes	Yes
Well			Yes	Yes
Fit statistics				
Observations	1,668	1,668	1,668	1,668
R^2	0.31313	0.33033	0.80106	0.81608
Within R^2	0.16670	0.17552	0.17332	0.24194

Notes: Well-level clustered standard errors in parentheses.
* p<0.10, ** p<0.05, *** p<0.010

Appendices

Appendix A Creation of Hurricane Evacuation Zones

Potential storm surge flooding is mapped by the National Hurricane Center, which uses the hydrodynamic Sea, Lake, and Overland Surge from Hurricanes Model, referred to as the SLOSH model. The decades-old SLOSH model is a computer model that runs thousands of hurricane simulations. These simulated hurricanes vary in attributes that affect storm surge, such as storm intensity, speed, angle of approach, landfall location, and initial water level. Data from this model "serve as the foundation to create the national hurricane evacuation zones," [Zachry et al., 2015].

The simulations are used to calculate storm surges under various scenarios. Two storm surge products are created from the SLOSH: MEOWs and MOMS. The first product, MEOWs, stands for 'maximum envelopes of water' and shows the maximum storm surge produced from around 10,000 to 60,000 simulations. The second product, MOMs, stands for 'maximum of maximums' and is created by compiling all the MEOWs and separating by hurricane category and initial water level. Once these separations are made, the maximum storm surge height in each grid cell is utilized. The grids vary in resolution from tens of meters to over a kilometer. In this way, the MOM products represent an upper bound on storm surge potential by portraying the near-worst-case scenarios, and "no single hurricane will produce the flooding depicted in these products," [Zachry et al., 2015]. Near-worst-case scenarios are portrayed as opposed to strictly-worst-case scenarios due to limitations in the modeling. One such limitation is the exclusion of wave setup, which is one of the most significant determinants of storm surge. In simple terms, wave setup is the increase in the mean water level due to waves. Including this measure would increase water levels by 10 to 50 percent and subsequently increase flood depths. Once the products have been created, they are combined with elevation data to determine the extent of the flooding above ground.

Although it is not always the case, stronger storms have the potential to cause greater storm surges. Therefore, the MEOWs and MOMs associated with higher hurricane categories produce greater potential storm surges than those corresponding to lower hur-

ricane categories. However, it is quite possible for a category two hurricane to produce a greater storm surge than a category five hurricane. While a category five hurricane has the *potential* to produce a greater storm surge, that does not mean it actually will. It will ultimately depend on the numerous determining attributes of each individual hurricane.

Appendix B Construction of Sales Data Set

I restrict the sample to properties with land use codes 0101 which are classified as one-unit residential single-family property. Of these, I restrict the sales to those classified as "arms-length transactions" and included in the sales ratio analysis. In the data, these reflect qualified sales with qualification codes 1 and 2, or more plainly, sales determined to be arms-length transactions by documented evidence (code 2), examination of a deed (code 1), or examination of some other ownership-transferring instrument (code 1) [Florida Department of Revenue]. Arms-length transactions occur between unrelated individuals who presumably have equal bargaining power and do not face outside influence. Excluding non-arms-length transactions is customary in the hedonic literature as it omits cases where the observed sales price may be unequal to the true market value. This omits, for example, sales among relatives, which would be likely to contain some familial discount.

Further, by including only two of the six qualified sales codes, sales in which significant physical changes subsequently occurred and sales that involved multiple parcels are excluded. These sales accounted for 3.46% and 1.74%, respectively, of qualified one-unit residential single-family property sales from January 1, 2014, through August 31, 2017. This also omits sales in which significant legal changes subsequently occurred, such as a legal zoning change following the sale date, as well as sales of homes that cross county lines. However, neither of these sale types were present in the data for the relevant study period.

Sale prices are converted into 2014 U.S. dollars using the annual average from the Consumer Price Index for All Urban Consumers: All Items in U.S. City Average obtained from the Federal Reserve Economic Data (series CPIAUCSL).

Minimal trimming is done. I drop the lowest and highest percentile of inflation-adjusted prices. I then drop any remaining outliers, which include properties with zero bedrooms, bathrooms, or stories, properties whose lot square footage is listed as one, the number of stories is listed as 20101, or the year built listed as 9999. These outliers account for 0.16% of the sample. I create a variable for the age of the house at the time of sale by

subtracting the year built from the year of the sale. I drop properties whose age at the time of sale is less than zero, which accounts for 2.55% of the remaining sample.

I import this sample into ArcGIS Pro 2.9 and project the data using NAD 1983 (2011) StatePlane Florida East FIPS 0901 (Meters). I use the Clemson USA Geocoder to geocode the properties. 99.86% (40126) of observations were matched. I drop unmatched and tied properties so that only properties that match with a single address remain. I then spatially join numerous data sets to create variables of neighborhood and locational amenities specific to each property. Geodesic distances are calculated using the 'Near' tool.

Appendix C Functional Forms

I test the robustness of the main results to alternative specifications that include different transformations of the independent variables. Table A1 displays estimates from these alternative specifications. Column 1 is estimated from equation Equation 1.9 but omits the quadratic terms of the housing characteristics. Column 2 further uses distance measures rather than logged distance measures. Columns 3 (and 4) are the same as the model in column 2 but include quadratic housing and distance measures (and cubed housing and distance measures). The final model implements an alternative measure of coastal proximity that is shown in Figure A1. Again, the coefficients and their statistical significance remain consistent across models.

Figure A1: Illustration of Coastal Measures

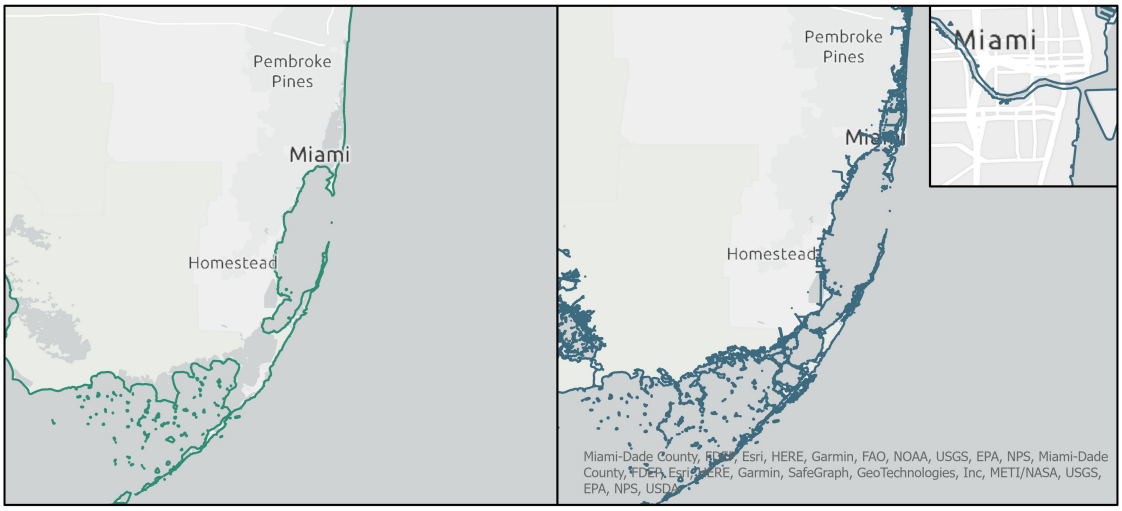

Notes: The left image shows the coastline used in the creation of the DIST_OCEAN variable. The image on the right shows the shoreline used in the creation of the DIST_WATER variable. As shown, the shoreline on the right includes outlines of inlets and waterways that can extend miles inland. Data on the left panel are from the U.S. Census Bureau's 2019 U.S. Coastline National Shapefile. Data on the right panel are from the National Oceanic and Atmospheric Administration's Office for Coastal Management's Composite Shoreline.

Table A1: Robustness: Transformation of Independent Variables

	(1) ln(P)	(2) ln(P)	(3) ln(P)	(4) ln(P)	(5) ln(P)
Panel A: Treated = Zone A					
ERIKA × EVACZONE_A	-0.124***	-0.131***	-0.126***	-0.130***	-0.121***
	(0.0320)	(0.0250)	(0.0235)	(0.0298)	(0.0242)
MATTHEW × EVACZONE_A	-0.0853***	-0.0830***	-0.0767***	-0.0787***	-0.0868***
	(0.0257)	(0.0230)	(0.0226)	(0.0230)	(0.0227)
N	10887	10887	10887	10887	10887
R^2	0.895	0.900	0.907	0.895	0.905
Panel B: Treated = Zone B					
ERIKA × EVACZONE_B	-0.0128	-0.0191	-0.0236	-0.0133	-0.0244
	(0.0243)	(0.0234)	(0.0235)	(0.0244)	(0.0239)
MATTHEW × EVACZONE_B	-0.0614***	-0.0500***	-0.0496**	-0.0578***	-0.0501**
	(0.0208)	(0.0192)	(0.0197)	(0.0203)	(0.0200)
N	14469	14469	14469	14469	14469
R^2	0.889	0.894	0.898	0.889	0.899
Panel C: Treated = Zone C					
ERIKA × EVACZONE_C	-0.0376**	-0.0394**	-0.0392**	-0.0392**	-0.0377**
	(0.0173)	(0.0172)	(0.0171)	(0.0170)	(0.0172)
MATTHEW × EVACZONE_C	-0.0559***	-0.0486***	-0.0516***	-0.0535***	-0.0532***
	(0.0179)	(0.0172)	(0.0172)	(0.0178)	(0.0172)
N	16001	16001	16001	16001	16001
R^2	0.883	0.890	0.892	0.884	0.893
Panel D: Treated = Zone D					
ERIKA × EVACZONE_D	-0.0374***	-0.0377***	-0.0367***	-0.0379***	-0.0368***
	(0.0142)	(0.0140)	(0.0138)	(0.0141)	(0.0140)
MATTHEW × EVACZONE_D	-0.0336**	-0.0338**	-0.0342**	-0.0341**	-0.0346**
	(0.0142)	(0.0134)	(0.0137)	(0.0140)	(0.0136)
N	21510	21510	21510	21510	21510
R^2	0.813	0.827	0.832	0.816	0.835
Panel E: Treated = Zone E					
ERIKA × EVACZONE_E	-0.0294*	-0.0259	-0.0271*	-0.0294*	-0.0293*
	(0.0162)	(0.0160)	(0.0160)	(0.0160)	(0.0159)
MATTHEW × EVACZONE_E	-0.0235	-0.0245	-0.0277	-0.0251	-0.0274
	(0.0180)	(0.0178)	(0.0180)	(0.0179)	(0.0178)
N	15979	15979	15979	15979	15979
R^2	0.830	0.842	0.848	0.833	0.849
All Covariates	✓	✓	✓	✓	✓
Year FE	✓	✓	✓	✓	✓
Quarter-of-Year FE	✓	✓	✓	✓	✓
Zip Code FE	✓	✓	✓	✓	✓

Notes: The dependent variable in all models is the natural logarithm of sale price in 2014 U.S. dollars. Model (1) is a log-linear model (there are no quadratic terms and distance measures are not transformed). Model (2) includes quadratic terms of distances and continuous housing variables. Model (3) includes quadratic and cubic terms for distance measures and continuous housing variables. Model (4) is Model (1) but uses logged distance measures. Model (5) is Model (3) but uses an alternative measure for coastal proximity. Standard errors are in parenthesis and clustered at the census tract level. There are 129, 181, 183, 235, and 201 clusters in panels A through E, respectively.
* p<0.10, ** p<0.05, *** p<0.010

Appendix D Spatial Fixed Effects

This section tests the robustness of the main results to the inclusion of differing scales of spatial fixed effects. Table A2 presents the results from models whose treated group is Zone A, B, C, D, and E, respectively. The third column of Table A2 presents the results from the main specification for comparison purposes. The first column omits time fixed effects (year and quarter-of-year). Columns 2 and 3 cumulatively add year and quarter-of-year fixed effects, respectively, to account for price changes over time common to all properties. Columns 4 through 7 show results from the main specification using census tract, three-, two-, and one-square-mile grid fixed effects rather than zip-code fixed effects. These more granular fixed effects capture heterogeneity at different spatial scales. The inclusion of square-mile grid fixed effects is inspired by Banzhaf [2021], who notes that there may be significant heterogeneity among census tracts that cover a larger geographical area, which can be accounted for with increasingly small overlaid grids. The estimates are similar in magnitude and significance across specifications.

Table A2: Robustness: Additional Fixed Effects

	(1) ln(P)	(2) ln(P)	(3) ln(P)	(4) ln(P)	(5) ln(P)	(6) ln(P)	(7) ln(P)
Panel A: Treated = Zone A							
ERIKA × EVACZONE_A	-0.124***	-0.120***	-0.122***		-0.128***		
	(0.0276)	(0.0261)	(0.0263)		(0.0280)		
MATTHEW × EVACZONE_A	-0.0794***	-0.0845***	-0.0854***		-0.0865***		
	(0.0224)	(0.0208)	(0.0207)		(0.0227)		
N	10887	10887	10887		10887		
R^2	0.893	0.898	0.898		0.891		
Panel B: Treated = Zone B							
ERIKA EVACZONE_B	-0.0130	-0.0156	-0.0158		-0.0212	-0.0200	-0.0278
	(0.0237)	(0.0240)	(0.0242)		(0.0238)	(0.0223)	(0.0215)
MATTHEW × EVACZONE_B	-0.0460**	-0.0497**	-0.0514***		-0.0642***	-0.0621***	-0.0621***
	(0.0209)	(0.0196)	(0.0193)		(0.0190)	(0.0182)	(0.0175)
N	14469	14469	14469		14469	14469	14469
R^2	0.887	0.892	0.893		0.884	0.901	0.914
Panel C: Treated = Zone C							
ERIKA × EVACZONE_C	-0.0391**	-0.0404**	-0.0416**	-0.0432**	-0.0469***	-0.0488***	-0.0497***
	(0.0166)	(0.0168)	(0.0170)	(0.0174)	(0.0166)	(0.0168)	(0.0164)
MATTHEW × EVACZONE_C	-0.0451**	-0.0472***	-0.0479***	-0.0504***	-0.0500***	-0.0516***	-0.0583***
	(0.0183)	(0.0175)	(0.0172)	(0.0171)	(0.0174)	(0.0165)	(0.0165)
N	16001	16001	16001	16001	16001	16001	16001
R^2	0.884	0.889	0.890	0.918	0.880	0.892	0.907
Panel D: Treated = Zone D							
ERIKA × EVACZONE_D	-0.0394***	-0.0360**	-0.0356**	-0.0398***	-0.0353**	-0.0369***	-0.0373***
	(0.0136)	(0.0139)	(0.0140)	(0.0145)	(0.0137)	(0.0132)	(0.0131)
MATTHEW × EVACZONE_D	-0.0291*	-0.0324**	-0.0333**	-0.0340**	-0.0337**	-0.0376***	-0.0418***
	(0.0151)	(0.0139)	(0.0136)	(0.0138)	(0.0137)	(0.0127)	(0.0128)
N	21510	21510	21510	21510	21510	21510	21510
R^2	0.815	0.822	0.823	0.876	0.818	0.837	0.865
Panel E: Treated = Zone E							
ERIKA × EVACZONE_E	-0.0361**	-0.0296*	-0.0282*	-0.0356**	-0.0364**	-0.0353**	-0.0337**
	(0.0160)	(0.0157)	(0.0158)	(0.0163)	(0.0155)	(0.0157)	(0.0154)
MATTHEW × EVACZONE_E	-0.0206	-0.0232	-0.0249	-0.0247	-0.0257	-0.0285*	-0.0292*
	(0.0191)	(0.0180)	(0.0178)	(0.0175)	(0.0177)	(0.0163)	(0.0172)
N	15979	15979	15979	15979	15979	15979	15979
R^2	0.830	0.838	0.839	0.879	0.826	0.843	0.864
All Covariates	✓	✓	✓	✓	✓	✓	✓
Year FE		✓	✓	✓	✓	✓	✓
Quarter-of-Year FE			✓	✓	✓	✓	✓
Zip Code FE	✓	✓	✓				
Census Tract FE				✓			
3-Square-Mile Grid FE					✓		
2-Square-Mile Grid FE						✓	
1-Square-Mile Grid FE							✓

Notes: The estimating equation is Equation 1.9 with differing fixed effects across models. Missing coefficients indicate that the model suffers from multicollinearity. The dependent variable in all models is the natural logarithm of sale price in 2014 U.S. dollars. Standard errors are in parentheses and are clustered at the census tract level. There are 129, 181, 183, 235, and 201 clusters in panels A through E, respectively.

* p<0.10, ** p<0.05, *** p<0.010

Appendix E Heterogeneity by Federal Flood Zones

This section presents descriptive plots of the subsamples comprising SFHA and non-SFHA properties as well as event study plots that provide evidence of the parallel trends assumption necessary to interpret estimates from Table 1.7 and Table 1.8 as causal. Figure A2 displays log sale prices and transactions by quarter for sales inside and outside HEZs by subsample. The growth rate in sale prices after TS Erika increases in non-HEZs inside and outside SFHAs. While this is suggestive of a negative price effect on HEZs, these prices do not hold other factors fixed. Figure A3 and Figure A5 present the event study plots for the aggregate treated group comprising all HEZs for sales outside and inside SFHAs, respectively. Figure A4 and Figure A6 present the event study plots for the disaggregate treated groups for sales outside and inside SFHAs, respectively.

Figure A2: Quarterly Sale Price and Transaction Volumes By Special Flood Hazard Area

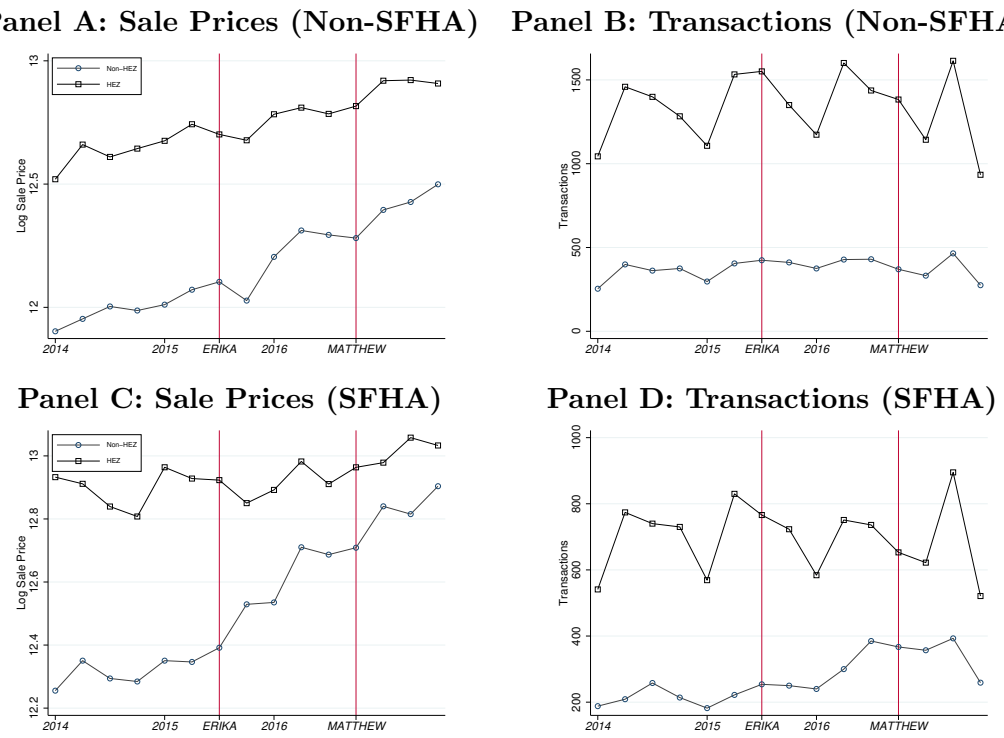

Notes: This figure displays the mean log sale price and the number of sale transactions by quarter for sales inside and outside hurricane evacuation zones, by special flood hazard area.

Figure A3: Effect of Near-Miss Hurricane on Sale Prices in Hurricane Evacuation Zone (Restricted Sample: Outside Special Flood Hazard Area)

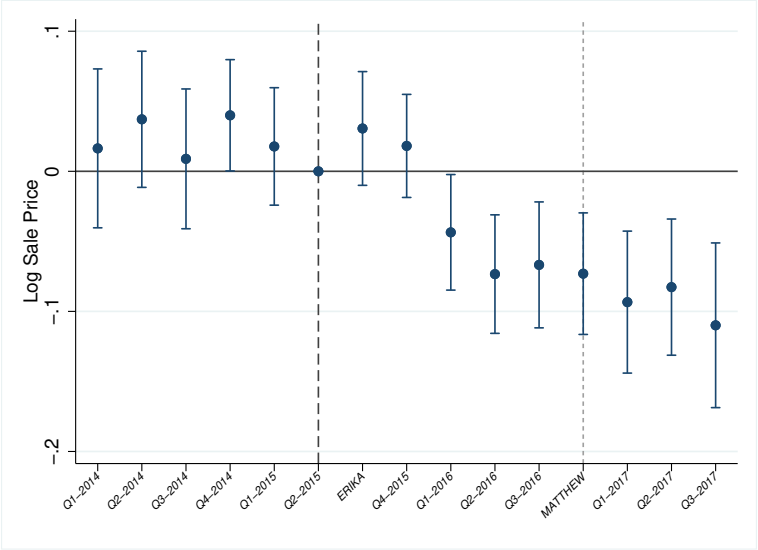

Notes: Average treatment effect on the treated of near-miss on log sale prices for the restricted sample of sales outside special flood hazard areas. The treated group comprises all sales occurring within a hurricane evacuation zone. The dependent variable is the log sale price in 2014 U.S. dollars. Point estimates correspond to the γ_τ's in Equation 1.8 for the restricted sample. Estimates are relative to the quarter prior to Tropical Storm Erika's occurrence (Q2-2015). Error bars represent the 95% confidence interval with standard errors clustered at the census tract level.

Figure A4: Effect of Near-Miss Hurricane on Sale Prices In Hurricane Evacuation Zone (Restricted Sample: Outside Special Flood Hazard Area

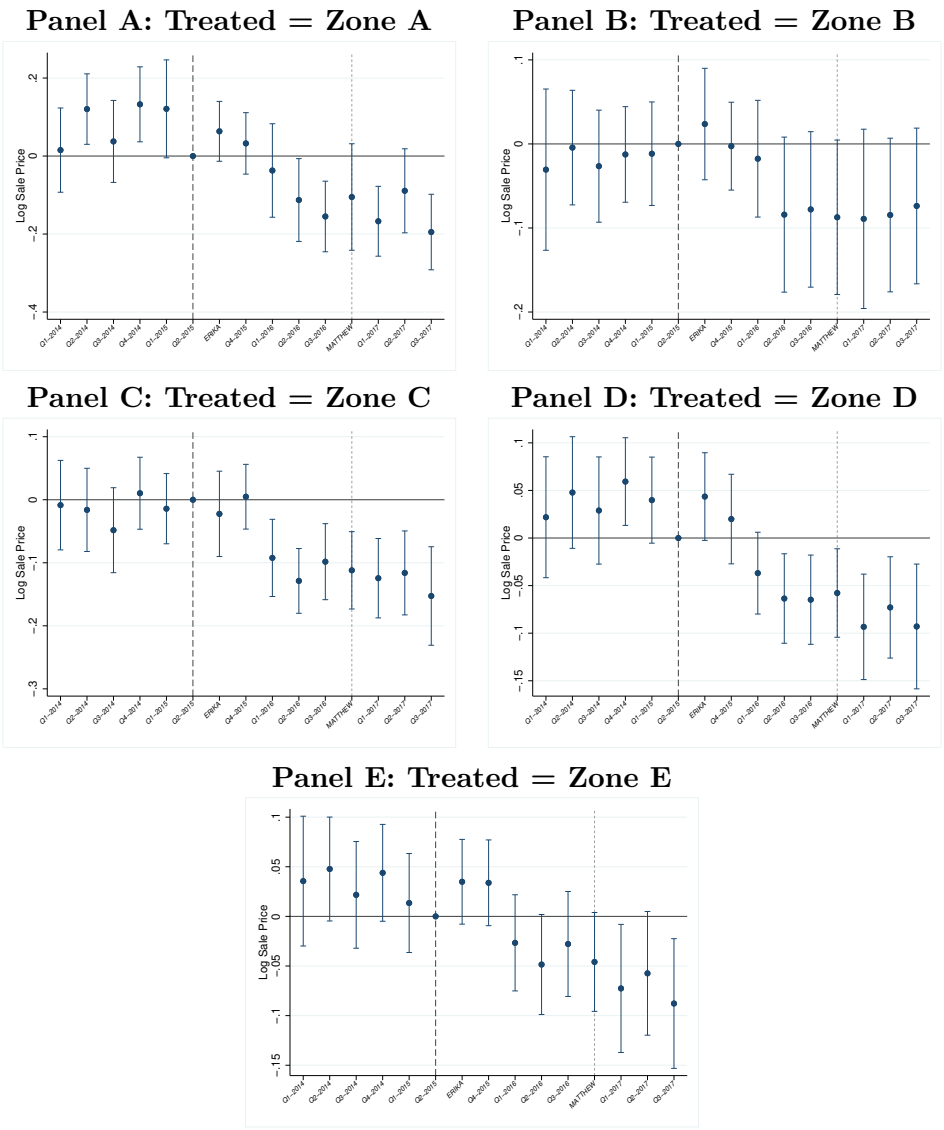

Notes: Average treatment effect on the treated of near-miss on log sale prices for the restricted sample of sales outside special flood hazard areas. The treated group consists of properties in Zones A through E for panels A through E, respectively. The control group in all panels comprises all sales outside hurricane evacuation zones. The dependent variable is the log sale price in 2014 U.S. dollars. Point estimates correspond to the γ_τ's in Equation 1.8 for the restricted sample. Estimates are relative to the quarter prior to Tropical Storm Erika's occurrence (Q2-2015), denoted by the thicker dashed line. The thinner dashed line indicates the occurrence of Hurricane Matthew. Error bars represent the 95% confidence interval with standard errors clustered at the census tract level.

Figure A5: Effect of Near-Miss Hurricane on Sale Prices In Hurricane Evacuation Zones (Restricted Sample: Inside Special Flood Hazard Area)

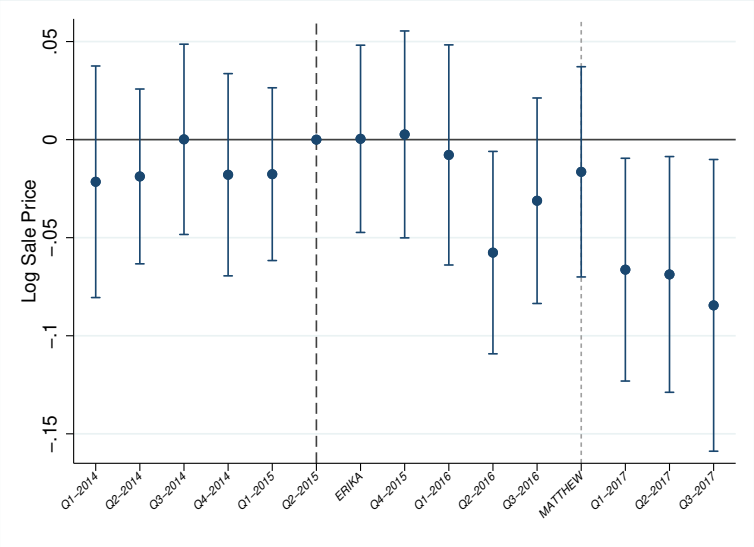

Notes: Average treatment effect on the treated of near-miss on log sale prices for the restricted sample of sales inside a special flood hazard area. The treated group comprises all sales in a hurricane evacuation zone. The dependent variable is the log sale price in 2014 U.S. dollars. Point estimates correspond to the γ_τ's in Equation 1.8 for the restricted sample. Estimates are relative to the quarter prior to Tropical Storm Erika's occurrence (Q2-2015), denoted by the thicker dashed line. The thinner dashed line indicates the occurrence of Hurricane Matthew. Error bars represent the 95% confidence interval with standard errors clustered at the census tract level.

Figure A6: Effect of Near-Miss Hurricane on Sale Prices In Hurricane Evacuation Zone (Restricted Sample: Inside Special Flood Hazard Area)

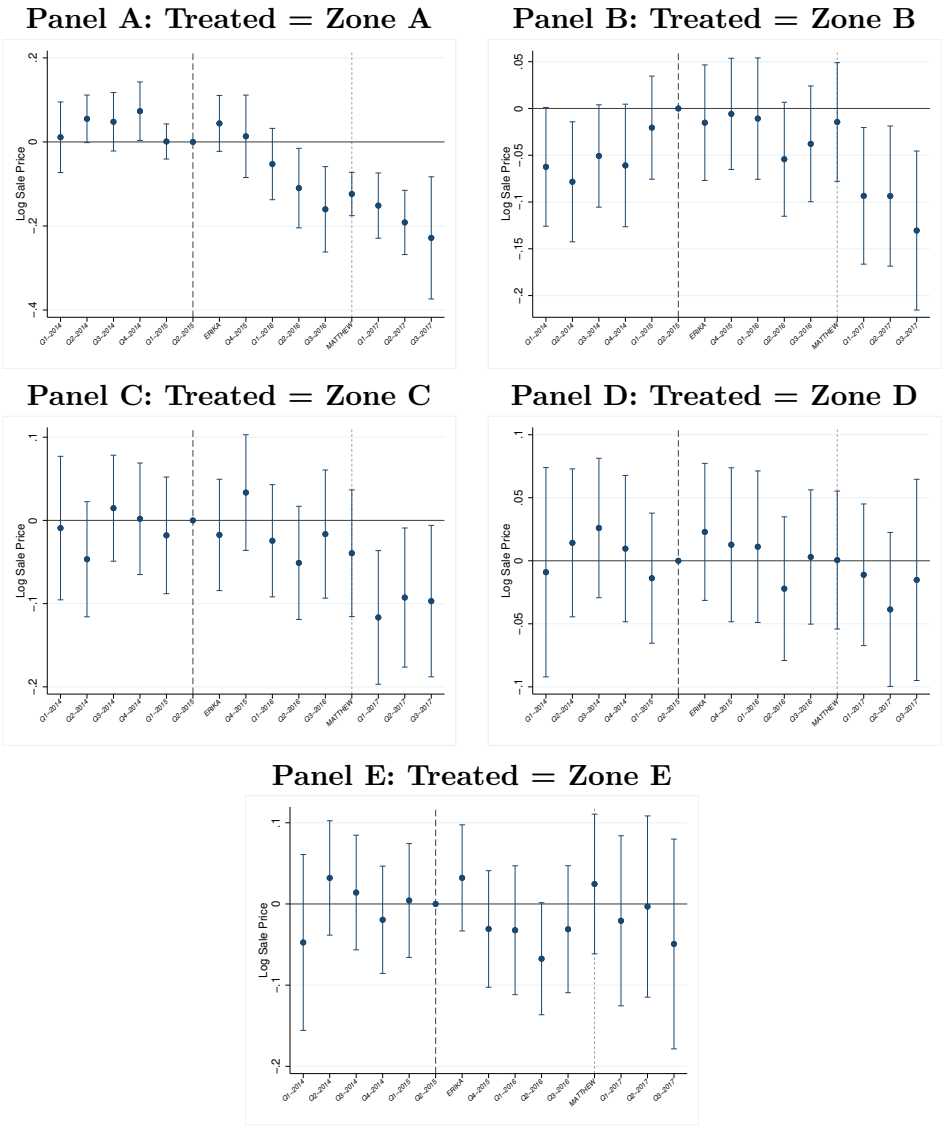

Notes: Average treatment effect on the treated of near-miss on log sale prices for the restricted sample of sales inside a special flood hazard area. The treated group consists of properties in Zones A through E for panels A through E, respectively. The control group in all panels comprises all sales outside hurricane evacuation zones. The dependent variable is the log sale price in 2014 U.S. dollars. Point estimates correspond to the γ_τ's in Equation 1.8, for the restricted sample. Estimates are relative to the quarter prior to Tropical Storm Erika's occurrence (Q2-2015), denoted by the thicker dashed line. The thinner dashed line indicates the occurrence of Hurricane Matthew. Error bars represent the 95% confidence interval with standard errors clustered at the census tract level.

Appendix F Derivation of First Order Conditions from Utility Maximization Problem

Equation 1.3 shows that consumers maximize expected utility given by

$$EU = \rho(g)U_H(X_H, \mathbf{Z}, g) + (1 - \rho(g))U_{NH}(X_{NH}, \mathbf{Z}, g)$$

Substitution gives:

$$EU = \rho(g)U_H[Y - P(\rho(g), Z, r) - L(g, Z, r), Z, g] + (1 - \rho(g))U_{NH}[Y - P(\rho(g), Z, r), Z, g].$$

Rewriting

$$X = Y - P(\rho(g), Z, r)$$

gives the following first order condition:

$$\frac{\partial EU}{\partial g} = \rho_g U_H + \rho\left[\frac{\partial U_H}{\partial X}\frac{\partial X}{\partial g} - \frac{\partial L}{\partial g} + \frac{\partial U_H}{\partial g}\right] + U_{NH}\frac{\partial(1-\rho(g))}{\partial g} + (1-\rho)\left[\frac{\partial U_{NH}}{\partial X}\frac{\partial X}{\partial g} + \frac{\partial U_{NH}}{\partial g}\right] = 0.$$

Since

$$\frac{\partial X}{\partial g} = \frac{-\partial P}{\partial g},$$

the first order condition becomes:

$$\rho\frac{\partial U_H}{\partial X}\frac{\partial P}{\partial g} + (1-\rho(g))\left[\frac{\partial U_{NH}}{\partial X}\frac{\partial P}{\partial g}\right] = \rho_g U_H + \rho\frac{\partial U_H}{\partial g} - \rho\frac{\partial L}{\partial g} + U_{NH}\frac{\partial(1-\rho(g))}{\partial g} + (1-\rho)\frac{\partial U_{NH}}{\partial g}.$$

Rearranging the first order condition results in:

$$\frac{\partial P}{\partial g} = \frac{\frac{\partial \rho}{\partial g}(U_H - U_{NH})}{\rho\frac{\partial U_H}{\partial X_H} + (1-\rho)\frac{\partial U_{NH}}{\partial X_{NH}}} - \frac{\rho\frac{\partial L}{\partial g}}{\rho\frac{\partial U_H}{\partial X_H} + (1-\rho)\frac{\partial U_{NH}}{\partial X_{NH}}} + \frac{\rho\frac{\partial U_H}{\partial g} + (1-\rho)\frac{\partial U_{NH}}{\partial g}}{\rho\frac{\partial U_H}{\partial X_H} + (1-\rho)\frac{\partial U_{NH}}{\partial X_{NH}}}.$$

Appendix G Results from Pooled Sample

Table A3: Impact of Near-Miss on Sale Prices in Hurricane Evacuation Zones

	(1) ln(P)
ERIKA × EVACZONE_A	-0.127***
	(0.0334)
ERIKA × EVACZONE_B	-0.0260
	(0.0235)
ERIKA × EVACZONE_C	-0.0404**
	(0.0178)
ERIKA × EVACZONE_D	-0.0396***
	(0.0142)
ERIKA × EVACZONE_E	-0.0297*
	(0.0168)
MATTHEW × EVACZONE_A	-0.0884***
	(0.0237)
MATTHEW × EVACZONE_B	-0.0539***
	(0.0194)
MATTHEW × EVACZONE_C	-0.0421**
	(0.0179)
MATTHEW × EVACZONE_D	-0.0339**
	(0.0146)
MATTHEW × EVACZONE_E	-0.0225
	(0.0186)
All Covariates	✓
Year FE	✓
Quarter-of-Year FE	✓
Zip Code FE	✓
N	40126
R^2	0.873

Notes: This table displays the estimates from Equation 1.9, using the pooled sample. The reference group comprises sales outside hurricane evacuation zones. The dependent variable is the natural logarithm of the sale price in 2014 U.S. dollars. Standard errors are in parentheses and clustered at the census tract. There are 412 clusters.

* p<0.10, ** p<0.05, *** p<0.010

Appendix H Results from Event Studies

Table A4: Time-Varying Coefficients By Quarter (Aggregate Treated Group: All Evacuation Zones)

	(1) ln(P)
T × Q1	-0.00360
	(0.0213)
T × Q2	0.0136
	(0.0182)
T × Q3	0.00170
	(0.0186)
T × Q4	0.0142
	(0.0166)
T × Q5	0.000469
	(0.0162)
T × Q7	0.0149
	(0.0160)
T × Q8	0.00776
	(0.0159)
T × Q9	-0.0297*
	(0.0179)
T × Q10	-0.0696***
	(0.0183)
T × Q11	-0.0489**
	(0.0191)
T × Q12	-0.0478**
	(0.0195)
T × Q13	-0.0761***
	(0.0220)
T × Q14	-0.0741***
	(0.0208)
T × Q15	-0.0966***
	(0.0254)
All Covariates	✓
Year FE	✓
Quarter-of-Year FE	✓
Zip Code FE	✓
N	40126
R^2	0.872

Notes: This table displays the coefficients corresponding to the event study plot in Figure 1.10 and the γ_τ's in Equation 1.8. Estimates are relative to the quarter prior to Tropical Storm Erika's occurrence (Q6). T denotes the treatment group and comprises all sales that occurred within hurricane evacuation zones. The dependent variable is the natural logarithm of the sale price in 2014 U.S. dollars. Standard errors are in parentheses and clustered at the census tract. There are 412 clusters.
* p<0.10, ** p<0.05, *** p<0.010

Table A5: Time-Varying Coefficients By Quarter (Disaggregate Treated Group)

	(1) Treated= Zone A	(2) Treated= Zone B	(3) Treated= Zone C	(4) Treated= Zone D	(5) Treated= Zone E
T × Q1	0.0372	-0.0331	-0.0196	-0.00533	-0.00744
	(0.0392)	(0.0299)	(0.0267)	(0.0253)	(0.0259)
T × Q2	0.120***	-0.0351	-0.0335	0.0256	0.0348*
	(0.0266)	(0.0244)	(0.0260)	(0.0229)	(0.0206)
T × Q3	0.0443*	-0.0426*	-0.0293	0.0177	0.0106
	(0.0255)	(0.0225)	(0.0240)	(0.0214)	(0.0219)
T × Q4	0.108***	-0.0280	0.00807	0.0319*	0.0185
	(0.0298)	(0.0239)	(0.0222)	(0.0192)	(0.0211)
T × Q5	0.0493	-0.00950	-0.0227	0.0108	-0.00518
	(0.0349)	(0.0230)	(0.0224)	(0.0184)	(0.0204)
T × Q7	0.0535**	0.00412	-0.0253	0.0256	0.0215
	(0.0260)	(0.0235)	(0.0267)	(0.0178)	(0.0185)
T × Q8	0.0112	0.0126	0.00887	0.0116	0.0102
	(0.0277)	(0.0211)	(0.0223)	(0.0193)	(0.0201)
T × Q9	-0.0306	-0.0151	-0.0632***	-0.0199	-0.0182
	(0.0356)	(0.0261)	(0.0237)	(0.0187)	(0.0221)
T × Q10	-0.117***	-0.0732**	-0.102***	-0.0508**	-0.0545**
	(0.0374)	(0.0290)	(0.0220)	(0.0198)	(0.0223)
T × Q11	-0.161***	-0.0564*	-0.0646***	-0.0385*	-0.0207
	(0.0395)	(0.0317)	(0.0244)	(0.0197)	(0.0217)
T × Q12	-0.113***	-0.0477	-0.0808***	-0.0339*	-0.0262
	(0.0428)	(0.0318)	(0.0257)	(0.0197)	(0.0228)
T × Q13	-0.151***	-0.0976***	-0.114***	-0.0627***	-0.0460
	(0.0298)	(0.0351)	(0.0267)	(0.0226)	(0.0287)
T × Q14	-0.140***	-0.0928***	-0.104***	-0.0577***	-0.0412
	(0.0412)	(0.0326)	(0.0277)	(0.0219)	(0.0288)
T × Q15	-0.206***	-0.116***	-0.129***	-0.0649**	-0.0657**
	(0.0501)	(0.0382)	(0.0328)	(0.0280)	(0.0300)
All Covariates	✓	✓	✓	✓	✓
Year FE	✓	✓	✓	✓	✓
Quarter-of-Year FE	✓	✓	✓	✓	✓
Zip Code FE	✓	✓	✓	✓	✓
N	10887	14469	16001	21510	15979
R^2	0.899	0.893	0.890	0.824	0.839

Notes: This table displays the coefficients corresponding to the event study plot in Figure 1.11 and the γ_τ's in Equation 1.8. Estimates are relative to the quarter prior to Tropical Storm Erika's occurrence (Q6). T denotes the treatment group and comprises all sales that occurred Zone A, B, C, D, and E for models (1), (2), (3), (4), and (5), respectively. The dependent variable is the natural logarithm of the sale price in 2014 U.S. dollars. Standard errors are in parentheses and clustered at the census tract. There are 129, 181, 183, 235, and 201 clusters in models (1) through (5), respectively.

* p<0.10, ** p<0.05, *** p<0.010

Appendix I Restricted Sample of Non-Coastal Properties

Table A6: Impact of Near-Miss on Properties More Than 5 Miles from the Coast
(Aggregate Treatment Group: All Hurricane Evacuation Zones)

	(1) ln(P)	(2) ln(P)	(3) ln(P)	(4) ln(P)	(5) ln(P)
ERIKA × EVACZONE	-0.0206	-0.0251**	-0.0252**	-0.0277**	-0.0281**
	(0.0127)	(0.0124)	(0.0126)	(0.0121)	(0.0116)
MATTHEW × EVACZONE	-0.0255*	-0.0243	-0.0312**	-0.0272**	-0.0283**
	(0.0143)	(0.0147)	(0.0144)	(0.0134)	(0.0136)
EVACZONE	0.0222	0.0905**	0.105**	0.0673	0.0586**
	(0.0403)	(0.0415)	(0.0481)	(0.0443)	(0.0262)
ERIKA	0.0211*	0.0229**	0.0253**	0.0242**	0.0255**
	(0.0121)	(0.0114)	(0.0121)	(0.0118)	(0.0113)
MATTHEW	0.0392***	0.0347**	0.0424***	0.0393***	0.0405***
	(0.0135)	(0.0134)	(0.0134)	(0.0126)	(0.0121)
Constant	11.42***	11.59***	11.35***	11.79***	11.24***
	(0.172)	(0.186)	(0.249)	(0.327)	(0.276)
All Covariates	✓	✓	✓	✓	✓
Year FE	✓	✓	✓	✓	✓
Quarter-of-Year FE	✓	✓	✓	✓	✓
Zip Code FE	✓				
Census Tract FE		✓			
3-Square-Mile Grid FE			✓		
2-Square-Mile Grid FE				✓	
1-Square-Mile Grid FE					✓
N	20808	20808	20808	20808	20808
R^2	0.850	0.879	0.838	0.851	0.873

Notes: This table displays the coefficients corresponding to Equation 1.9 for the subsample of properties more than five miles from the coastline. In all models, the treatment group comprises all properties in hurricane evacuation zones. The control group consists of properties outside hurricane evacuation zones. These models omit the waterfront dummy variable. The dependent variable is the natural logarithm of the sale price in 2014 U.S. dollars. Standard errors are in parentheses and clustered at the census tract. There are 232 clusters.

* p<0.10, ** p<0.05, *** p<0.010

Table A7: Impact of Near-Miss on Properties More Than 5 Miles from the Coast

	(2) Treated= Zone B	(3) Treated= Zone C	(4) Treated= Zone D	(5) Treated= Zone E
ERIKA × EVACZONE	0.421***	0.0933***	-0.0336***	-0.0362**
	(0.135)	(0.0258)	(0.0119)	(0.0155)
MATTHEW × EVACZONE	-0.0266	-0.00415	-0.0355***	-0.0228
	(0.0378)	(0.0302)	(0.0135)	(0.0214)
EVACZONE	-0.522***	-0.108	0.0911*	-0.0178
	(0.145)	(0.114)	(0.0519)	(0.0408)
ERIKA	0.00493	-0.00818	0.0195	0.0207*
	(0.0144)	(0.0151)	(0.0118)	(0.0114)
MATTHEW	-0.0000638	-0.00109	0.0353***	0.0375***
	(0.0163)	(0.0169)	(0.0129)	(0.0122)
Constant	10.28***	10.27***	11.35***	11.01***
	(0.219)	(0.233)	(0.270)	(0.383)
All Covariates	✓	✓	✓	✓
Year FE	✓	✓	✓	✓
Quarter-of-Year FE	✓	✓	✓	✓
Zip Code FE			✓	✓
N	9158	9906	16456	11853
R^2	0.821	0.806	0.849	0.873

Notes: This table displays the coefficients corresponding to Equation 1.9 for the subsample of properties more than five miles from the coastline. There is no model with a treatment group comprising sales in Zone A because all properties in Zone A are within five miles of the coast. Models (2) and (3) omit zip code fixed effects due to multicollinearity. All models omit the waterfront dummy variable. The dependent variable is the natural logarithm of the sale price in 2014 U.S. dollars. Standard errors are in parentheses and clustered at the census tract. There are 232, 104, 116, 185, and 145 clusters in models (1) through (5), respectively.

* p<0.10, ** p<0.05, *** p<0.010

Appendix J Sale Prices Deflated With Local Consumer Price Index

Sale prices in this section are deflated to 2014 U.S. dollars using the annual average of the Consumer Price Index for All Urban Consumers: All Items in Miami-Fort Lauderdale-West Palm Beach, FL from the Federal Reserve Economic Data (series CUURA320SA0).

Table A8: Impact of Near-Miss on Sale Prices Deflated Using a Local Consumer Price Index (Aggregate Treatment Group: All Hurricane Evacuation Zones)

	(1) ln(P)	(2) ln(P)	(3) ln(P)	(4) ln(P)	(5) ln(P)
ERIKA × EVACZONE	-0.176***	-0.0769***	-0.0746***	-0.0747***	-0.0386***
	(0.0562)	(0.0197)	(0.0196)	(0.0195)	(0.0136)
MATTHEW × EVACZONE	-0.103***	-0.0612***	-0.0636***	-0.0645***	-0.0390***
	(0.0293)	(0.0169)	(0.0169)	(0.0169)	(0.0144)
EVACZONE	0.613***	0.0478	0.0471	0.0470	0.0398
	(0.0750)	(0.0450)	(0.0452)	(0.0452)	(0.0446)
ERIKA	0.258***	0.208***	0.0731***	0.0465**	0.0240*
	(0.0540)	(0.0172)	(0.0175)	(0.0186)	(0.0127)
MATTHEW	0.229***	0.168***	0.0789***	0.0531***	0.0292*
	(0.0271)	(0.0150)	(0.0153)	(0.0190)	(0.0150)
Constant	12.13***	11.59***	11.54***	11.51***	11.99***
	(0.0552)	(0.131)	(0.131)	(0.131)	(0.110)
All Covariates		✓	✓	✓	✓
Year FE			✓	✓	✓
Quarter-of-Year FE				✓	✓
Zip Code FE					✓
N	40126	40126	40126	40126	40126
R^2	0.107	0.739	0.743	0.744	0.872

Notes: This table displays the coefficients corresponding to Equation 1.9 using a local Consumer Price Index to deflate sale prices. In all models, the treatment group comprises all properties in hurricane evacuation zones. The control group in each model contains sales outside hurricane evacuation zones. The dependent variable is the natural logarithm of the sale price in 2014 U.S. dollars. Standard errors are in parentheses and clustered at the census tract. There are 412 clusters.
* p<0.10, ** p<0.05, *** p<0.010

Table A9: Impact of Near-Miss on Sale Prices in Hurricane Evacuation Zones Deflated Using a Local Consumer Price Index

	(1) Treated= Zone A	(2) Treated= Zone B	(3) Treated= Zone C	(4) Treated= Zone D	(5) Treated= Zone E
ERIKA × EVACZONE	-0.122***	-0.0158	-0.0416**	-0.0356**	-0.0282*
	(0.0263)	(0.0242)	(0.0170)	(0.0140)	(0.0158)
MATTHEW × EVACZONE	-0.0854***	-0.0514***	-0.0479***	-0.0333**	-0.0249
	(0.0207)	(0.0193)	(0.0172)	(0.0136)	(0.0178)
EVACZONE	0.0725	0.380	0.141	0.0716	-0.0613
	(0.0630)	(0.279)	(0.107)	(0.0624)	(0.0517)
ERIKA	0.0110	-0.00490	-0.00162	0.0172	0.0146
	(0.0129)	(0.0129)	(0.0132)	(0.0118)	(0.0115)
MATTHEW	0.0200	0.0143	0.00384	0.0254*	0.0266*
	(0.0156)	(0.0164)	(0.0159)	(0.0144)	(0.0145)
Constant	12.05***	11.98***	12.19***	11.91***	12.46***
	(0.184)	(0.189)	(0.144)	(0.170)	(0.265)
All Covariates	✓	✓	✓	✓	✓
Year FE	✓	✓	✓	✓	✓
Quarter-of-Year FE	✓	✓	✓	✓	✓
N	10887	14469	16001	21510	15979
R^2	0.899	0.893	0.890	0.824	0.840

Notes: This table displays the coefficients corresponding to Equation 1.9 using a local Consumer Price Index to deflate sale prices. Models (1) through (5) have treatment groups comprising sales in Zones A through E, respectively. The control group in each model contains sales outside hurricane evacuation zones. The dependent variable is the natural logarithm of the sale price in 2014 U.S. dollars. Standard errors are in parentheses and clustered at the census tract. There are 129, 181, 183, 235, and 201 clusters.
* p<0.10, ** p<0.05, *** p<0.010

Appendix K Construction of Irrigation Dataset

This section describes the construction of the main sample (n=7,081) used in the analysis. In total, there are 15,296 observations with well capacity. However, some wells are tested more than once in a year. There are 2,651 observations associated with multiple tests in a year. In order to merge this with our annual water use and crop data, we retain the well test value that is closest to the well's long-term average yield. To do this, we first create a variable DUPLICATE that is equal to one for each well-by-year observation that has more than one test value for that year. In other words, if a well was tested twice in 2014 and only once in 2016, the indicator DUPLICATE would be equal to one for both of the well observations in 2014, and equal to zero for the well observation in 2016. We construct a long-term average well test by calculating the average for each well, using only observations where DUPLICATE=0. We then drop 56 observations with no long-term average. These reflect wells whose observations only contain duplicate annual test values. We also drop duplicate observations (23 obs) where the well test value is identical, as these are redundant and we only need to retain one of each observation (the observation retained is automated by R and may have occurred in a different month than the corresponding identical observation). For the remaining observations whose DUPLICATE=1, we retain the well test value that is closest to the well's long-term average test value. The resulting data set has 13,901 observations.

Next, we import groundwater usage data. Some wells also report multiple groundwater usage values for a given year. 222 out of 36,488 groundwater use observations are classified as DUPLICATE=1. Again, we retain the value which is closest to the long-term value of groundwater use for the individual well. We drop 26 observations with no long-term average representing wells that only contain duplicate annual groundwater use values. We drop 13 observations where the duplicate values in a year are identical. We then merge the groundwater use data set with the well test data set based on the wells' unique identification number. We drop seven observations that reported zero annual water use. For observations

with missing well test values, we impute the most recent well test value if that test was conducted within the last three years, as this is the maximum length of time a well test is valid for. (Note: the water pump data is an annual measurement whereas the well pump tests have a specific date). We drop any remaining observations that contain missing values, resulting in a data set with 29,434 observations.

Next, we import weather data and data on depth to water. Where there is more than one depth to water estimate for a given well in a given year, we retain the value closest to the well's long-term depth to water average using the method described above. PRISM data were extracted at the well level and merged to this data set along with marginal cost data and irrigation data.

Irrigation data originally contain 45,952 parcel-year entries. We drop 16 observations in which parcels were irrigated with surface water. We drop 1,363 observations with receipt numbers recorded rather than well identifier numbers, as these observations cannot be matched to the well test data. Irrigation data are matched over time by their MASTERID. A MASTERID may contain one or many parcels per year. Each parcel-year observation corresponds to one type of crop and its associated acreage. Each land parcel is also associated with the well (or wells) from which it received water that year.

Appendix L Interpolating Well-Level Depth to Water: Data and Methods

We construct our depth to water variable relying on the following sources compatible with Arcmap: Flynn et al. [2009], McGuire et al. [2012a,b], McGuire [2017b], Division [2014], McGuire [2009], McGuire and Strauch [2022], Stanton [2015], McGuire [2014, 2012].

We first calculate depth to water (DTW) in 2000, 2005, and 2009 at the well-level by extracting raster values to well locations. We calculate this using DTW in 2000, water level changes from 2000 to 2005, and water level changes from 2005 to 2009. We calculate DTW in 2011, 2013, and 2017 by subtracting the changes in DTW from predevelopment to each of these years from predevelopment DTW, again extracting raster values to well locations. Predevelopment DTW is calculated by extracting the aquifer elevation at the top of the aquifer and the surface elevation to well locations. Surface elevation is recalculated in feet. The elevation of the top of the aquifer is subtracted from the surface elevation to produce predevelopment DTW. We extract raster values for the change in DTW from 2015 to 2017 to well locations to calculate 2015 DTW by subtracting the change from 2017 DTW. We now have well-level DTW measures for 2000, 2005, 2009, 2011, 2013, 2015, and 2017. Negative depth to water values are dropped, indicating the top of the aquifer is above the surface elevation. Spline interpolation is used to impute depth to water values for missing years.

Bibliography

J. D. Angrist and J.-S. Pischke. Mostly harmless econometrics: An empiricist's companion. Princeton university press, 2009.

T. Armstrong. Hurricane Matthew in the Carolinas: October 8, 2016. `https://www.weather.gov/ilm/Matthew`, 2015.

A. Atreya and S. Ferreira. Seeing is believing? Evidence from property prices in inundated areas. Risk Analysis, 35(5):828–848, 2015.

A. Atreya, S. Ferreira, and W. Kriesel. Forgetting the flood? An analysis of the flood risk discount over time. Land Economics, 89(4):577–596, 2013.

L. A. Bakkensen, X. Ding, and L. Ma. Flood risk and salience: New evidence from the sunshine state. Southern Economic Journal, 85(4):1132–1158, 2019.

H. S. Banzhaf. Difference-in-differences hedonics. Journal of Political Economy, 129(8): 2385–2414, 2021.

R. Barta, I. Broner, J. Schneekloth, and R. Waskom. Colorado high plains irrigation practices guide. Colorado Water Resources Research Institute Special Report, 14, 2004.

T. A. Bauder. Center Pivot Irrigation in Colorado as Mapped by Landsat Imagery. Colorado State University, Agriculture Experiment Station, Department of . . . , 2004.

R. Baumhardt, S. Staggenborg, P. Gowda, P. Colaizzi, and T. Howell. Modeling irrigation management strategies to maximize cotton lint yield and water use efficiency. Agronomy journal, 101(3):460–468, 2009.

A. Beltrán, D. Maddison, and R. J. Elliott. Is flood risk capitalised into property values? Ecological Economics, 146:668–685, 2018.

R. Bentall. Methods of determining permeability, transmissibility and drawdown. Technical report, USGPO,, 1964.

R. Berg. Hurricane Hermine. National Oceanic and Atmospheric Administration, National Hurricane Center, 2017.

M. Bertrand, E. Duflo, and S. Mullainathan. How much should we trust differences-in-differences estimates? The Quarterly journal of economics, 119(1):249–275, 2004.

O. Bin and C. E. Landry. Changes in implicit flood risk premiums: Empirical evidence from the housing market. Journal of Environmental Economics and management, 65(3): 361–376, 2013.

O. Bin and S. Polasky. Effects of flood hazards on property values: evidence before and after hurricane floyd. Land Economics, 80(4):490–500, 2004.

O. Bin, T. W. Crawford, J. B. Kruse, and C. E. Landry. Viewscapes and flood hazard: Coastal housing market response to amenities and risk. Land economics, 84(3):434–448, 2008a.

O. Bin, J. B. Kruse, and C. E. Landry. Flood hazards, insurance rates, and amenities: Evidence from the coastal housing market. Journal of Risk and Insurance, 75(1):63–82, 2008b.

K. C. Bishop, N. V. Kuminoff, H. S. Banzhaf, K. J. Boyle, K. von Gravenitz, J. C. Pope, V. K. Smith, and C. D. Timmins. Best practices for using hedonic property value models to measure willingness to pay for environmental quality. Review of Environmental Economics and Policy, 2020.

A. Brookfield. Minimum saturated thickness calculator. Kansas Geological Survey Open-File Report, 3, 2016.

D. S. Brookshire, M. A. Thayer, J. Tschirhart, and W. D. Schulze. A test of the expected utility model: Evidence from earthquake risks. Journal of political economy, 93(2):369–389, 1985.

R. Buchanan, R. W. Buddemeier, and B. B. Wilson. The high plains aquifer. Kansas Geological Survey Lawrence, KS, 2001.

R. Buddemeier. Water table drawdown and wll pumping, 2000.

L. A. S. Cangialosi, John P. and R. Berg. Hurricane Irma. National Oceanic and Atmospheric Administration, National Hurricane Center, 2021.

J. C. Carbone, D. G. Hallstrom, and V. K. Smith. Can natural experiments measure behavioral responses to environmental risks? Environmental and Resource Economics, 33:273–297, 2006.

E. Chuck. Tropical Storm Erika kills at least 20 in Caribbean, Florida governor declares emergency. https://www.nbcnews.com/news/weather/tropical-storm-erika-kills-least-dozen-caribbean-n417611, 2015.

J. P. Cohen, J. Barr, and E. Kim. Storm surges, informational shocks, and the price of urban real estate: An application to the case of hurricane sandy. Regional Science and Urban Economics, 90:103694, 2021.

J. Colvin. Fema redrawing city's flood zone after superstorm sandy, 2012. URL https://www.dnainfo.com/new-york/20121206/new-york-city/fema-redrawing-citys-flood-zone-after-superstorm-sandy/#:~:text=LOWER%

20MANHATTAN%20%E2%80%94%20FEMA%20is%20dramatically,far%20outside%20the%20current%20lines.

CoreLogic. Hurricane risk report 2023. 2023.

S. Cunningham. Causal inference: The mixtape. Yale university press, 2021.

T. Davie and N. W. Quinn. Fundamentals of hydrology. Routledge, 2019.

R. L. Dillon, C. H. Tinsley, and M. Cronin. Why near-miss events can decrease an individual's protective response to hurricanes. Risk Analysis: An International Journal, 31(3): 440–449, 2011.

E. S. P. Division. Groundwater depletion in the united states (1900-2008): U.s. geological survey data release. https://doi.org/10.5066/P9QFHC25, 2014.

J. Douris and G. Kim. The atlas of mortality and economic losses from weather, climate and water extremes (1970-2019). 2021.

R. E. Dumm, G. S. Sirmans, and G. Smersh. The capitalization of building codes in house prices. The Journal of Real Estate Finance and Economics, 42:30–50, 2011.

J. S. Famiglietti. The global groundwater crisis. Nature Climate Change, 4(11):945–948, 2014.

Federal Emergency Management Agency. Flood insurance manuals archive: 2005-2021. https://www.fema.gov/flood-insurance/work-with-nfip/manuals/archive, 2022.

E. P. Fenichel, J. K. Abbott, J. Bayham, W. Boone, E. M. Haacker, and L. Pfeiffer. Measuring the value of groundwater and other forms of natural capital. Proceedings of the National Academy of Sciences, 113(9):2382–2387, 2016.

C. W. Fetter. Applied hydrogeology. Waveland Press, 2018.

C. Field, V. Barros, T. Stocker, Q. Dahe, D. Dokken, K. Ebi, M. Mastrandrea, K. Mach, G. Plattner, S. Allen, M. Tignor, and P. Midgley. Managing the risks of extreme events and disasters to advance climate change adaptation: special report of the intergovernmental panel on climate change. Cambridge University Press, 2012.

Florida Department of Revenue. Real Property Transfer Qualification Codes for DOR & Property Appraisers to Use Beginning January 1, 2015. https://floridarevenue.com/property/Documents/salequalcodes_bef01012016.pdf.

Florida Office of Insurance Regulation. Hurricane Matthew claims data. https://www.floir.com/Office/HurricaneSeason/HurricaneMatthewClaimsData.aspx, 2017.

J. Flynn, R. Arnold, and S. Paschke. Depth to water in the high plains aquifer in colorado, 2000, us geologic survey, data series 472. https://doi.org/10.5066/P9JCZM9C, 2009.

T. Foster, N. Brozović, and A. P. Butler. Modeling irrigation behavior in groundwater systems. Water resources research, 50(8):6370–6389, 2014.

T. Foster, N. Brozović, and A. Butler. Why well yield matters for managing agricultural drought risk. Weather and Climate Extremes, 10:11–19, 2015a.

T. Foster, N. Brozović, and A. P. Butler. Analysis of the impacts of well yield and groundwater depth on irrigated agriculture. Journal of Hydrology, 523:86–96, 2015b.

T. Foster, N. Brozović, and C. Speir. The buffer value of groundwater when well yield is limited. Journal of hydrology, 547:638–649, 2017.

A. M. Freeman III, J. A. Herriges, and C. L. Kling. The Measurement of Environmental and Resource Values: Theory and Methods. Routledge, 2014.

F. García Suárez, L. E. Fulginiti, and R. K. Perrin. What is the use value of irrigation water from the high plains aquifer? American Journal of Agricultural Economics, 101 (2):455–466, 2019.

S. Gibbons, S. Heblich, and C. Timmins. Market tremors: Shale gas exploration, earthquakes, and their impact on house prices. Journal of Urban Economics, 122:103313, 2021.

Y. Gonzalez-Alvarez, A. G. Keeler, and J. D. Mullen. Farm-level irrigation and the marginal cost of water use: Evidence from georgia. Journal of environmental management, 80(4): 311–317, 2006.

T. Guilfoos, A. D. Pape, N. Khanna, and K. Salvage. Groundwater management: The effect of water flows on welfare gains. Ecological Economics, 95:31–40, 2013.

E. Haacker, A. D. Kendall, and D. W. Hyndman. High Plains/Ogallala water table elevations annual estimates. `http://www.hydroshare.org/resource/7d925c7944244032af98c9ed20c22db6`, 2023.

K. Hall. Expected costs of damage from hurricane winds and storm-related flooding. Congressional Budget Office, Washington, DC, USA, pages 1–48, 2019.

D. G. Hallstrom and V. K. Smith. Market responses to hurricanes. Journal of Environmental Economics and Management, 50(3):541–561, 2005.

D. Harrison, G. T. Smersh, and A. Schwartz. Environmental determinants of housing prices: The impact of flood zone status. Journal of Real Estate Research, 21(1-2):3–20, 2001.

G. Hecox, P. Macfarlane, and B. Wilson. Calculation of yield for high plains wells: Relationship between saturated thickness and well yield. Technical report, Kansas Geological Survey, 2002.

N. P. Hendricks and J. M. Peterson. Fixed effects estimation of the intensive and extensive margins of irrigation water demand. Journal of Agricultural and Resource Economics, pages 1–19, 2012.

H. Hennighausen and J. F. Suter. Flood risk perception in the housing market and the impact of a major flood event. Land economics, 96(3):366–383, 2020.

R. Hornbeck and P. Keskin. The historically evolving impact of the ogallala aquifer: Agricultural adaptation to groundwater and drought. American Economic Journal: Applied Economics, 6(1):190–219, 2014.

R. A. Hrozencik, D. T. Manning, J. F. Suter, C. Goemans, and R. T. Bailey. The heterogeneous impacts of groundwater management policies in the republican river basin of colorado. Water Resources Research, 53(12):10757–10778, 2017.

R. A. Hrozencik, D. T. Manning, J. F. Suter, and C. Goemans. Impacts of block-rate energy pricing on groundwater demand in irrigated agriculture. American Journal of Agricultural Economics, 104(1):404–427, 2022.

S. K. Kim and J. K. Hammitt. Hurricane risk perceptions and housing market responses: the pricing effects of risk-perception factors and hurricane characteristics. Natural Hazards, 114(3):3743–3761, 2022.

C. Kousky. Learning from extreme events: Risk perceptions after the flood. Land Economics, 86(3):395–422, 2010.

C. Kousky, H. Kunreuther, B. Lingle, and L. Shabman. The emerging private residential flood insurance market in the United States. Wharton Risk Management and Decision Processes Center, 2018.

P. Kreins, M. Henseler, J. Anter, F. Herrmann, and F. Wendland. Quantification of climate change impact on regional agricultural irrigation and groundwater demand. Water resources management, 29:3585–3600, 2015.

R. Kristine Uhlman and J. F. Artiola. Arizona wells: Low yielding domestic water wells. Arizona Cooperative Extension, 2011.

F. Lamm, L. Stone, and D. O'brien. Crop production and economics in northwest kansas as related to irrigation capacity. Applied Engineering in Agriculture, 23(6):737–745, 2007.

H. Lee, K. Calvin, D. Dasgupta, G. Krinner, A. Mukherji, P. Thorne, C. Trisos, J. Romero, P. Aldunce, K. Barrett, et al. Climate change 2023: synthesis report. Contribution of working groups I, II and III to the sixth assessment report of the intergovernmental panel on climate change. The Australian National University, 2023.

J. Loomis. Do nearby forest fires cause a reduction in residential property values? Journal of forest economics, 10(3):149–157, 2004.

L. Martinez-Diaz and J. M. Keenan. Managing Climate Risk in the U.S. Financial System. US Commodity Futures Trading Commission, 2020.

V. Masson-Delmotte, P. Zhai, A. Pirani, S. L. Connors, C. Péan, S. Berger, N. Caud, Y. Chen, L. Goldfarb, M. Gomis, et al. Climate change 2021: the physical science basis. Contribution of working group I to the sixth assessment report of the intergovernmental panel on climate change, 2(1):2391, 2021.

M. A. Maupin and N. L. Barber. Estimated withdrawals from principal aquifers in the United States, 2000, volume 1279. US Department of the Interior, US Geological Survey, 2005.

V. McGuire. Digital map of water-level changes in the high plains aquifer in parts of colorado, kansas, nebraska, new mexico, oklahoma, south dakota, texas, and wyoming, predevelopment (about 1950) to 2007: U.s. geological survey data release. https://doi.org/10.5066/P94BH585, 2009.

V. McGuire. Digital map of water-level changes in the high plains aquifer in parts of colorado, kansas, nebraska, new mexico, oklahoma, south dakota, texas, and wyoming, predevelopment (about 1950) to 2011: U.s. geological survey data release. https://doi.org/10.5066/P98J54XL, 2012.

V. McGuire. Digital map of water-level changes in the high plains aquifer in parts of colorado, kansas, nebraska, new mexico, oklahoma, south dakota, texas, and wyoming, predevelopment (about 1950) to 2013: U.s. geological survey data release. https://doi.org/10.5066/P9091BCO, 2014.

V. McGuire. Water-level changes in the high plains aquifer, republican river basin in colorado, kansas, and nebraska, 2002 to 2015. US Geological Survey, Scientific Investigations Map, 3373, 2017a.

V. McGuire. Data used to map water-level changes in the high plains aquifer, predevelopment (about 1950) to 2015 and 2013 to 2015: U.s. geological survey data release. https://doi.org/10.5066/F7SB43WM, 2017b.

V. McGuire and K. Strauch. Data from maps of water-level changes in the high plains aquifer in parts of colorado, kansas, nebraska, new mexico, oklahoma, south dakota, texas, and wyoming, predevelopment (about 1950) to 2017 and 2015–17: U.s. geological survey data release. https://doi.org/10.5066/P9YN7PY3, 2022.

V. McGuire, K. Lund, and B. Densmore. Water-level change, high plains aquifer, 2000 to 2005, us geological survey data release. https://doi.org/10.5066/P91B856T, 2012a.

V. McGuire, K. Lund, and B. Densmore. Water-level change, high plains aquifer, 2005 to 2009: U.s. geological survey data release. https://doi.org/10.5066/P90Q1CG1, 2012b.

V. L. McGuire, K. D. Lund, and B. K. Densmore. Saturated thickness and water in storage in the High Plains aquifer, 2009, and water-level changes and changes in water in storage in the High Plains aquifer, 1980 to 1995, 1995 to 2000, 2000 to 2005, and 2005 to 2009, volume 2012. US Department of the Interior, US Geological Survey, 2012c.

Miami-Dade County. Property sale disclosure. https://www.miamidade.gov/environment/flood-disclosure.asp, 2015.

Miami-Dade County. Local mitigation strategy whole community hazard mitigation part I: The strategy. https://www.miamibeachfl.gov/wp-content/uploads/2017/12/local-mitigation-strategy-part-1-strategy.pdf, 2017.

T. Mieno, M. R. Rad, J. F. Suter, and R. A. Hrozencik. The importance of well yield in groundwater demand specifications. Land Economics, 97(3):672–687, 2021.

T. Mieno, T. Foster, S. Kakimoto, and N. Brozović. Aquifer depletion exacerbates agricultural drought losses in the US High Plains. Nature Water, pages 1–11, 2024.

M. R. Moore, N. R. Gollehon, and M. B. Carey. Multicrop production decisions in western irrigated agriculture: the role of water price. American Journal of Agricultural Economics, 76(4):859–874, 1994.

J. D. Morgan, T. Douthat, and L.-H. Lin. On the geographic balance of risk and amenity: Changes in evacuation zones and their ripples in housing prices in pinellas county, FL. Papers in Applied Geography, 9(1):49–69, 2023.

J. Mueller, J. Loomis, and A. González-Cabán. Do repeated wildfires change homebuyers' demand for homes in high-risk areas? a hedonic analysis of the short and long-term effects of repeated wildfires on house prices in southern California. The Journal of Real Estate Finance and Economics, 38:155–172, 2009.

M. Naoi, M. Seko, and K. Sumita. Earthquake risk and housing prices in Japan: Evidence before and after massive earthquakes. Regional Science and Urban Economics, 39(6): 658–669, 2009.

National Oceanic and Atmospheric Administration. Historical hurricane tracks. https://coast.noaa.gov/hurricanes/#map=4/32/-80, n.d.a.

National Oceanic and Atmospheric Administration. The hurricane weather research forecast model. https://www.aoml.noaa.gov/hurricane-weather-research-forecast-model/#:~:text=HWRF%20is%20the%20driving%20dynamical,at%20the%20National%20Weather%20Service., n.d.b.

National Oceanic and Atmospheric Administration. Storm surge overview. https://www.nhc.noaa.gov/surge/, n.d.c.

J. Nott, C. Green, I. Townsend, and J. Callaghan. The world record storm surge and the most intense southern hemisphere tropical cyclone: New evidence and modeling. Bulletin of the American Meteorological Society, 95(5):757–765, 2014.

C. W. Ogg and N. R. Gollehon. Western irrigation response to pumping costs: a water demand analysis using climatic regions. Water Resources Research, 25(5):767–773, 1989.

F. Ortega and S. Taşpınar. Rising sea levels and sinking property values: Hurricane Sandy and New York's housing market. Journal of Urban Economics, 106:81–100, 2018.

D. O'brien, F. Lamm, L. Stone, and D. Rogers. Corn yields and profitability for low–capacity irrigation systems. Applied Engineering in Agriculture, 17(3):315, 2001.

R. B. Palmquist. Property value models. Handbook of environmental economics, 2:763–819, 2005.

C. F. Parmeter and J. C. Pope. Quasi-experiments and hedonic property value methods. In Handbook on Experimental Economics and the Environment, 2013.

R. J. Pasch and A. B. Penny. Tropical Storm Erika. National Oceanic and Atmospheric Administration, National Hurricane Center, 2016.

G. Perez-Quesada, N. P. Hendricks, and D. R. Steward. The economic cost of groundwater depletion in the high plains aquifer. Journal of the Association of Environmental and Resource Economists, 11(2):253–285, 2024.

L. Pfeiffer and C.-Y. C. Lin. Does efficient irrigation technology lead to reduced groundwater extraction? Empirical evidence. Journal of Environmental Economics and Management, 67(2):189–208, 2014.

M. R. Rad, N. Brozović, T. Foster, and T. Mieno. Effects of instantaneous groundwater availability on irrigated agriculture and implications for aquifer management. Resource and Energy Economics, 59:101129, 2020.

E. N. Rappaport. Fatalities in the United States from Atlantic tropical cyclones: New data and interpretation. Bulletin of the American Meteorological Society, 95(3):341–346, 2014.

R. Rebecca, L. E. Beckley, and M. Tull. The economic value of cyclonic storm-surge risks: A hedonic case study of residential property in exmouth, western australia. Climate change in the Asia-Pacific region, pages 143–156, 2015.

S. G. Robson and E. R. Banta. Ground water atlas of the united states: Segment 2, arizona, colorado, new mexico, utah. Technical report, US Geological Survey, 1995.

S. Rosen. Hedonic prices and implicit markets: Product differentiation in pure competition. Journal of political economy, 82(1):34–55, 1974.

G. S. Sampson, N. P. Hendricks, and M. R. Taylor. Land market valuation of groundwater. Resource and Energy Economics, 58:101120, 2019.

S. M. Scheierling, J. B. Loomis, and R. A. Young. Irrigation water demand: A meta-analysis of price elasticities. Water resources research, 42(1), 2006.

J. Schneekloth and A. Andales. Seasonal water needs and opportunities for limited irrigation for colorado crops. Colorado State University Extension Fact Sheet, 4(4.718), 2017.

S. Siebert, J. Burke, J.-M. Faures, K. Frenken, J. Hoogeveen, P. Döll, and F. T. Portmann. Groundwater use for irrigation–a global inventory. Hydrology and earth system sciences, 14(10):1863–1880, 2010.

A. B. Smith. 2022 U.S. billion-dollar weather and climate disasters in historical context. https://www.climate.gov/news-features/blogs/beyond-data/2022-us-billion-dollar-weather-and-climate-disasters-historical, 2023.

J. Stanton. Geodatabase of the datasets used to represent the high plains aquifer, colorado, kansas, nebraska, new mexico, oklahoma, south dakota, texas, and wyoming: U.s. geological survey data release. https://doi.org/10.5066/P9PK3K87, 2015.

S. R. Stewart. Hurricane Matthew. National Oceanic and Atmospheric Adminstration, National Hurricane Center, 2017.

H. T. Taylor, B. Ward, M. Willis, and W. Zaleski. The Saffir-Simpson hurricane wind scale. Atmospheric Administration: Washington, DC, USA, 2010.

L. Taylor. The hedonic method. A Primer on Nonmarket Valuation, 2013.

J. Thorvaldson, J. Pritchett, et al. Profile of the republican river basin. 2005.

J. Thorvaldson, J. G. Pritchett, et al. Economic impact analysis of reduced irrigated acreage in four river basins in Colorado. Number 207. Colorado Water Resources Research Institute Colorado, 2006.

J. M. Wooldridge. Fixed-effects and related estimators for correlated random-coefficient and treatment-effect panel data models. Review of Economics and Statistics, 87(2):385–390, 2005.

B. C. Zachry, W. J. Booth, J. R. Rhome, and T. M. Sharon. A national view of storm surge risk and inundation. Weather, climate, and society, 7(2):109–117, 2015.

J. G. Zivin, Y. Liao, and Y. Panassie. How hurricanes sweep up housing markets: Evidence from Florida. Journal of Environmental Economics and Management, 118:102770, 2023.